Supporting Information

Dynamic N→B Coordination and Anion-selective Turn-On Fluorescence in Oxadiazole-functionalized Organoboranes

Jonas Schepper, Andreas Orthaber, Frank Pammer*

Contents

1. Experimental Section

1.1. Materials and Instrumentation

All reactions and manipulations of sensitive compounds were carried out under an atmosphere of pre-purified argon using either Schlenk techniques or an inert-atmosphere glovebox (MBraun Labmaster). Toluene, Et_2O, THF, DMF and dichloromethane were purified using a solvent purification system (MBraun; alumina / copper columns for hydrocarbon solvents). Hexane, and benzene were dried by distillation from CaH_2 under argon atmosphere prior to use. Mes_2BF,[1] 2-(dimesitylboryl)benzonitrile[2] (**1**) and 5-(2-(dimesitylboryl)phenyl)-1*H*-tetrazol (**2H**)[3] were synthesized according to reported methods. Other reagents were commercially available (Aldrich, ABCR, Alfa Aesar) and were either used as obtained or purified by standard procedures.[4]

^1H, ^{13}C, and ^{11}B NMR spectra were recorded at 293 K on a Bruker Avance DRX 400 (400 MHz) spectrometer or a Bruker Avance 500 AMX (500 MHz). Solution ^1H-and ^{13}C-NMR spectra were referenced internally to the solvent residual signals.[5] Solution ^{11}B-NMR spectra were referenced externally to $BF_3 \bullet Et_2O$ (10% in $CHCl_3$). ^{19}F NMR spectra were referenced externally to the chemical shift of C_6F_5 at 162.50 ppm.[6] Individual signals are referred to as singlet (s), doublet (d), triplet (t), (q) quartet, (dd) doublet of doublets, multiplet (m) and broadened (br). High resolution mass spectrometry measurements were performed on a Bruker SolariX FTMS using MALDI (Matrix Assisted Laser Desorption Ionization). Trans-2-[3-(4-tert-butylphenyl)-2-methyl-2-propenylidene]malononitrile (DCTB) was used as matrix in MALDI measurements. UV-visible absorption spectra and photoluminescence spectra were acquired on a Perkin Elmer Lambda 19 UV-vis/NIR spectrometer and a Perkin Elmer LS 55 fluorescence spectrometer, respectively. Electrochemical analyses were performed both in cyclic voltammetry- and square-wave voltammetry-mode with an Autolab Potentiostat Galvanostat with a three-electrode system, consisting of a Pt working electrode (0.785 mm^2), a Pt-counter electrode, and an Ag/AgCl reference electrode. The measurements were carried out in THF with $[N(n\text{-}Bu)_4][PF_6]$ (0.1 M) as supporting electrolyte, and were internally referenced against the ferrocene/ ferrocenium redox-couple.

Crystallography: X-ray diffraction intensities were collected either on an Agilent Technologies SuperNova single-crystal X-ray diffractometer, or on a Bruker D8 Quest diffractometer. Data collection was performed at 150 K using either Cu- or Mo-Kα radiation, and the structures were solved using direct methods (SIR92[7] or Shelxs-2014[8]), completed by subsequent difference Fourier syntheses, and refined by full-matrix least-squares procedures. Semi-empirical absorption corrections from equivalents (Multiscan) were carried out.

Computational Details: Quantum chemical calculations were performed on the bwForCluster JUSTUS at the University of Ulm, using release C.01 of the Gaussian16 program package.[9] Geometry optimizations were performed at the M06-2X/TZVP-level. The converged structures were found to be local energetic minima, as established by frequency calculations. The converged structures were found to be local energetic minima, as established by frequency calculations. Time-dependent DFT calculations on the optimized structures were performed using at the M06-2X/def2-TZVP level in combination with the polarized continuum solvent model (PCM) with dichloromethane as solvent.

1.2. Chemical Synthesis

1.2.1. Synthesis of 1,3,4-Oxadiazoles – General Method

Tetrazole **2H**[3] (1 eq) and K_2CO_3 (7 eq) were suspended (1.6 mM) in dry toluene (**4a**-**4g**) or DCM (**4h**). The corresponding acid chloride or anhydride (1.3 eq.) was added to the cloudy suspension at room temperature and the immediately resulting intense yellow reaction mixture was stirred at room temperature until a clear solution was formed (5-60 min). The solution was then heated to 110 °C for 1.5 h (**4a**-**4g**) or stirred at room temperature (**4h**). The solvent was removed *in vacuo* and the crude product was adsorbed on silica and subjected to SiO_2 column chromatography using PE/EA mixtures as eluents.

1.2.2. Synthesis of 2-(2-(Dimesitylboryl)phenyl)-5-(p-tolyl)-1,3,4-oxadiazol (4a)

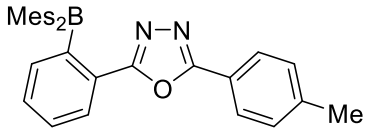

Compound **4a** was synthesized by the general method using 0.13 mmol **2H**[3], 0.93 mmol K_2CO_3, and 0.17 mmol 4-methylbenzoyl chloride. After purification by column chromatography (PE/EA 8/1), the product could be isolated as a colorless solid (62 mg, 0.127 mmol, 95%). Single crystals that were suitable for X-ray crystallographic structure determinations could be obtained by slow diffusion of n-pentane into a saturated THF solution of the oxadiazole.

^{1}H NMR (400 MHz, THF): δ = 8.02 – 7.98 (m, 2H), 7.88 – 7.84 (m, 1H), 7.77 – 7.73 (m, 1H), 7.45 – 7.33 (m, 4H), 6.55 (s, 4H, *Mes-H*), 2.43 (s, 3H, Ph-CH_3), 2.11 (s, 6H, *p-Mes-CH₃*), 1.90 (s, 12H, *o-Mes-CH₃*) ppm.

^{13}C NMR (126 MHz, THF): δ = 168.63(*N-C-O*), 167.36(*N-C-O*), 144.84, 141.32, 134.53, 134.47, 133.18, 130.95, 130.23, 127.98, 127.13, 122.92, 122.51, 121.24, 21.81, 21.10 ppm.

^{11}B NMR (128 MHz, THF): δ = 3.7 (br s) ppm.

MS (MALDI pos, Matrix: DCTB): m/z calcd. for $C_{33}H_{33}BN_2O$: 484.26859 Da; experim.: m/z = 484.26719 Da $[M]^+$, 469.24364 Da $[M\text{-}CH_3]^+$, 365.18127 Da [M-Mes]$^+$, 734.41391 Da [M+Matrix]$^+$, 614.32020 Da [M-Mes-H+Matrix]$^+$.

Smp.: 213.7-214.7 °C.

1.2.3. Synthesis of 2-(4-Chlorophenyl)-5-(2-(dimesitylboryl)phenyl)-1,3,4-oxadiazol (4b)

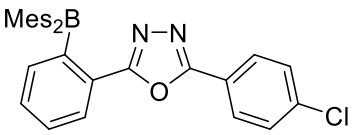

Compound **4b** was synthesized by the general method using 0.11 mmol **2H**[3], 0.80 mmol K_2CO_3, and 0.15 mmol 4-chlorobenzoyl chloride. After purification by column chromatography (PE/EA 10/1 → 8/1), the product could be isolated as a colorless solid (57 mg, 0.11 mmol, 100%). Single crystals that were suitable for X-ray crystallographic structure determinations could be obtained by slowly evaporating a THF solution.

^{1}H NMR (400 MHz, $CDCl_3$): δ = 8.03 – 7.95 (m, 2H), 7.84 – 7.75 (m, 2H), 7.54 – 7.50 (m, 2H), 7.50 – 7.45 (m, 1H), 7.39 (td, *J* = 7.5, 0.9 Hz, 1H), 6.67 (s, 4H, *Mes-H*), 2.19 (d, *J* = 7.9 Hz, 6H, *p-Mes-CH₃*), 1.93 (s, 12H, *o-Mes-CH₃*) ppm.

^{1}H NMR (400 MHz, THF): δ = 8.11 – 8.07 (m, 2H), 7.89 – 7.85 (m, 1H), 7.75 (dd, *J* = 7.4, 0.9 Hz, 1H), 7.64 – 7.60 (m, 2H), 7.45 (td, *J* = 7.4, 1.3 Hz, 1H), 7.38 (td, *J* = 7.5, 1.1 Hz, 1H), 6.55 (s, 4H), 2.11 (s, 6H), 1.90 (s, 12H) ppm.

^{11}B NMR: (128 MHz, THF) δ 6.8 (br s) ppm.

^{11}B NMR (128 MHz, $CDCl_3$): δ = 14.0 (br s) ppm.

^{13}C NMR (126 MHz, $CDCl_3$): δ = 167.63(*N-C-O*), 165.00(*N-C-O*), 140.91, 139.19, 135.25, 133.92, 132.87, 129.74, 129.37, 128.49, 127.02, 122.87, 122.26, 121.51, 24.77 (*Mes-CH₃*), 20.96 (*Mes-CH₃*) ppm.

MS (MALDI pos, Matrix: DCTB): m/z calcd. for $C_{32}H_{30}BClN_2O$: 504.21397 Da; experim.: m/z = 504.21283 Da $[M]^+$, 489.18940 Da $[M\text{-}CH_3]^+$, 385.12702 Da [M-Mes]$^+$, 754.35908 Da [M+Matrix]$^+$, 634.26561 Da [M-Mes-H+Matrix]$^+$.

Smp.: 201.8 °C.

1.2.4. Synthesis of 2-(2-(*D*imesitylboryl)phenyl)-5-(4-methoxyphenyl)-1,3,4-oxadiazol (4c)

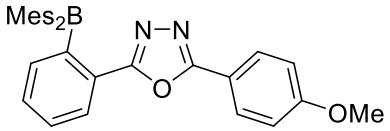

Compound **4c** was synthesized by the general method using 0.10 mmol **2H**[3], 0.67 mmol K_2CO_3, and 0.12 mmol 4-methoxybenzoyl chloride. After purification by column chromatography (PE/EA 4/1), the product could be isolated as a colorless solid (42 mg, 0.08 mmol, 84%). Single crystals that were suitable for X-ray crystallographic structure determinations could be obtained by slow diffusion of n-pentane into a saturated THF solution of the oxadiazole.

^{1}H NMR (400 MHz, THF): δ = 8.09 – 8.00 (m, 2H), 7.85 (d, *J* = 7.5 Hz, 1H), 7.75 (d, *J* = 7.5 Hz, 1H), 7.41 (td, *J* = 7.4, 1.2 Hz, 1H), 7.35 (td, *J* = 7.5, 1.0 Hz, 1H), 7.15 – 7.05 (m, 2H), 6.55 (s, 4H, *Mes-H*), 3.88 (s, 3H, *-Ph-CH₃*), 2.11 (s, 6H, *p-Mes-CH₃*), 1.90 (s, 12H, *o-Mes-CH₃*) ppm.
^{11}B NMR (128 MHz, THF): δ = 3.2 (br s) ppm.

^{13}C NMR (101 MHz, THF): δ = 168.41(*N-C-O*), 167.30(*N-C-O*), 164.72(*C-OMe*), 141.32, 134.43, 133.06, 130.23, 129.91, 127.02, 122.93, 122.31, 116.04, 115.77, 56.10 (*O-CH₃*), 21.11 (*Mes-CH₃*) ppm.

MS (MALDI pos, Matrix: DCTB): m/z calcd. for $C_{33}H_{33}BN_2O_2$: 500.26351 Da; experim.: m/z = 500.26257 Da $[M]^+$, 485.23912 Da $[M\text{-}CH_3]^+$, 381.17661 Da [M-Mes]$^+$, 750.40914 Da [M+Matrix]$^+$, 630.31551 Da [M-Mes-H+Matrix]$^+$.

Smp.: 204.8-205.7 °C.

1.2.5. Synthesis of 2-(2-(Dimesitylboryl)phenyl)-5-(4-nitrophenyl)-1,3,4-oxadiazol (4d)

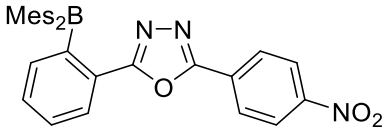

Compound **4d** was synthesized by the general method using 0.095 mmol **2H**[3], 0.666 mmol K_2CO_3, and 0.124 mmol 4-nitrobenzoyl chloride. After purification by column chromatography (PE/EA 6/1), the product could be isolated as a yellow solid (48 mg, 0.093 mmol, 98%).

^{1}H NMR (400 MHz, THF): δ = 8.46 – 8.40 (m, 2H), 8.36 – 8.29 (m, 2H), 7.94 – 7.89 (m, 1H), 7.78 – 7.72 (m, 1H), 7.48 (td, *J* = 7.4, 1.3 Hz, 1H), 7.43 (td, *J* = 7.4, 1.1 Hz, 1H), 6.57 (br s, 4H, *Mes-H*), 2.10 (br s, 6H, *p-Mes-CH₃*), 1.91 (br s, 12H, *o-Mes-CH₃*) ppm.

^{11}B NMR (128 MHz, THF): δ = 11.8 (br s) ppm.

^{13}C NMR (101 MHz, THF): δ = 169.26(*N-C-O*), 165.58(*N-C-O*), 151.34, 141.38, 135.34, 134.71, 133.54, 130.18, 129.58, 129.15, 127.91, 125.32, 123.69, 123.30, 21.11 ppm.

MS (MALDI pos, Matrix: DCTB): m/z calcd. for $C_{32}H_{30}BN_3O_3$: 515.23802 Da; experim.: m/z = 514.22931 Da [M-H]$^+$, 500.21337 Da [M-CH_3]$^+$, 396.15094 Da [M-Mes]$^+$, 645.29014 Da [M-Mes-H+Matrix]$^+$, 764.37671 Da [M-H+Matrix]$^+$.

Smp.: 151.1-152.0 °C.

1.2.6. Synthesis of 2-(3,5-Bis(trifluoromethyl)phenyl)-5-(2-(dimesitylboryl)phenyl)-1,3,4-oxadiazol (4e)

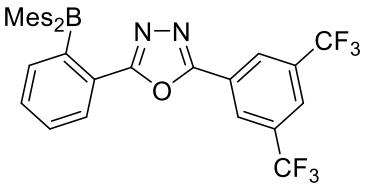

Compound **4e** was synthesized by the general method using 0.097 mmol **2H**[3], 0.666 mmol K_2CO_3, and 0.123 mmol 3,5-bis(trifluoromethyl)benzoyl chloride. After purification by column chromatography (PE/EA 8/1), the product could be isolated as a light yellow solid (55 mg, 0.091 mmol, 93%).

^{1}H NMR (400 MHz, THF): δ = 8.58 (s, 2H, *CF₃-Ph-H*), 8.34 (s, 1H, *CF₃-Ph-H*), 7.95 (dd, *J* = 6.7, 1.1 Hz, 1H), 7.75 – 7.68 (m, 1H), 7.51 (td, *J* = 7.4, 1.5 Hz, 1H), 7.46 (td, *J* = 7.4, 1.3 Hz, 1H), 6.57 (br s, 4H, Mes-H), 2.10 (br s, 6H, *p-Mes-CH₃*), 1.91 (br s, 12H, *o-Mes-CH₃*) ppm.

^{11}B NMR (128 MHz, THF): δ = 18.6 (br s) ppm.

^{19}F NMR (376 MHz, THF): δ = -63.80 (s) ppm.

^{13}C NMR (126 MHz, THF): δ = 169.05(*N-C-O*), 164.58(*N-C-O*), 141.47, 136.03, 134.86, 133.58 (q, *J* = 34.1 Hz), 133.46, 130.77 – 129.57 (m), 128.49, 128.25 (d, *J* = 3.0 Hz), 127.04, 126.86 – 126.65 (m), 124.64, 124.15 (q, *J* = 272.8 Hz), 124.01, 25.10, 21.12 ppm.

MS (MALDI pos, Matrix: DCTB): m/z calcd. for $C_{34}H_{29}BF_6N_2O$: 606.22771 Da; experim.: m/z = 606.22714 Da [M]$^+$, 591.20370 Da [M-CH_3]$^+$, 487.14108 Da [M-Mes]$^+$, 736.28024 Da [M-Mes-H+Matrix]$^+$.

Smp.: 76.2-77.0 °C.

1.2.7. Synthesis of 2-([1,1'-Biphenyl]-4-yl)-5-(2-(dimesitylboryl)phenyl)-1,3,4-oxadiazol (4f)

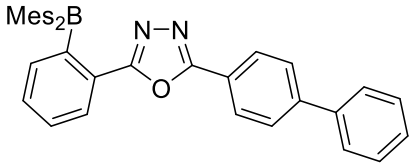

Compound **4f** was synthesized by the general method using 0.095 mmol **2H**[3], 0.666 mmol K_2CO_3, and 0.180 mmol [1,1'-biphenyl]-4-carbonyl chloride. After purification by column chromatography (PE/EA 6/1), the product could be isolated as a colorless solid (48 mg, 0.091 mmol, 92%). Single crystals that were suitable for X-ray crystallographic structure determinations could *be* obtained by slow diffusion of n-pentane into a saturated THF solution of the oxadiazole.

^{1}H NMR (400 MHz, THF): δ = 8.21 – 8.15 (m, 2H), 7.92 – 7.85 (m, 3H), 7.79 – 7.75 (m, 1H), 7.75 – 7.70 (m, 2H), 7.50 – 7.35 (m, 5H), 6.57 (s, 4H, *Mes-H*), 2.11 (s, 6H, *p-Mes-CH₃*), 1.92 (s, 12H, *o-Mes-CH₃*) ppm.

^{11}B NMR (128 MHz, THF): δ = 6.5 (br s) ppm.

^{13}C NMR (101 MHz, THF): δ = 168.81(*N-C-O*), 167.15(*N-C-O*), 146.52, 141.33, 140.45, 134.60, 134.51, 133.26, 130.25, 129.99, 129.42, 128.66, 128.54, 128.09, 127.21, 122.93, 122.71, 122.65, 21.11 ppm.

MS (MALDI pos, Matrix: DCTB): m/z calcd. for $C_{38}H_{35}BN_2O$: 546.28424 Da; experim.: m/z = 546.28371 Da $[M]^+$, 531.26025 Da $[M\text{-}CH_3]^+$, 427.19766 Da [M-Mes]$^+$, 676.33696 Da [M-Mes-H+Matrix]$^+$, 796.43085 Da [M+Matrix]$^+$.

Smp.: 195.6-196.6 °C.

1.2.8. Synthesis of 1,4-Bis(5-(2-(dimesitylboryl)phenyl)-1,3,4-oxadiazol-2-yl)benzol (4g)

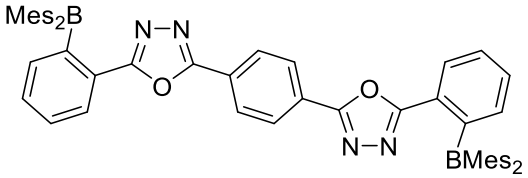

Compound **4g** was synthesized according to the general method, using 0.099 mmol **2H**[3], 0.666 mmol K_2CO_3, but deviating from 6.2.16 only 0.054 mmol terephthaloyl dichloride was used. After purification by column chromatography (PE/EA 3/1), the product could be isolated as a yellow solid (17 mg, 0.020 mmol, 36%).

^{1}H NMR (400 MHz, CD_2Cl_2): δ = 8.27 (br s, 4H), 7.90 (d, *J* = 7.4 Hz, 2H), 7.76 (d, *J* = 7.5 Hz, 2H), 7.52 (td, *J* = 7.5, 1.2 Hz, 2H), 7.45 (td, *J* = 7.5, 1.0 Hz, 2H), 6.65 (br s, 8H, *Mes-H*), 2.16 (br s, 12H, *p-Mes-CH₃*), 1.92 (br s, 24H, *o-Mes-CH₃*) ppm.

^{11}B NMR (128 MHz, CD_2Cl_2): δ = 13.1 (br s) ppm.

^{13}C NMR (126 MHz, CD_2Cl_2): δ = 168.62(*N-C-O*), 165.46(*N-C-O*), 141.22, 135.62, 133.95, 133.37, 129.80, 128.30, 127.57, 126.93, 123.64, 122.52, 25.02, 21.03 ppm.

MS (MALDI pos, Matrix: DCTB): m/z calcd. for $C_{58}H_{56}B_2N_4O_2$: 862.45894 Da; experim.: m/z = 862.45687 Da $[M]^+$, 847.43348 Da $[M\text{-}CH_3]^+$, 743.37162 Da [M-Mes]$^+$, 992.50898 Da [M-Mes-H+Matrix]$^+$, 1112.60304 Da [M+Matrix]$^+$.

Smp.: decomposition above 274.0 °C.

1.2.9. Synthesis of 2-(2-(Dimesitylboryl)phenyl)-5-(trifluormethyl)-1,3,4-oxadiazole (4h)

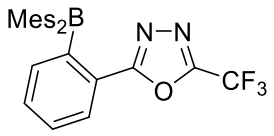

Compound **4h** was synthesized by the general method in DCM as solvent and at room temperature using 0.11 mmol **2H**[3], 0.796 mmol K_2CO_3, and 0.148 mmol trifluoroacetic anhydride. After purification by column chromatography (PE/EA 4/1), the product could be isolated as a colorless solid (12 mg, 0.026 mmol, 23%).

^{1}H NMR (400 MHz, $CDCl_3$): δ = 7.89 – 7.72 (m, 1H), 7.64 – 7.56 (m, 2H), 7.55 – 7.50 (m, 1H), 6.71 (br s, 4H, *Mes-H*), 2.23 (br s, 6H, *p-Mes-CH₃*), 1.95 (br s, 12H, *o-Mes-CH₃*) ppm.

^{19}F NMR (376 MHz, $CDCl_3$): δ = -65.01 (s) ppm.

^{1}H NMR (400 MHz, THF): δ = 7.88 – 7.81 (m, 1H), 7.69 – 7.58 (m, 2H), 7.55 – 7.47 (m, 1H), 6.69 (br s, 4H), 2.19 (br s, 6H), 1.94 (br s, 12H) ppm.

^{13}C NMR (126 MHz, CD_2Cl_2): δ = 169.05, 155.24, 154.8, 151.00, 141,11. 139.58, 135.03, 132.20, 130.82, 139.69, 128.64, 126.66, 117.53, 114.83, 23.31 (Mes-o-Me), 21.25 (Mes-p-Me)ppm.

^{11}B NMR (128 MHz, THF): δ = 67.1 (br s) ppm.

MS (EI): m/z calcd. for $C_{27}H_{26}BF_3N_2O$: 462.20903 Da; experim.: m/z = 447 Da $[M\text{-}CH_3]^+$, 343 Da $[M\text{-}Mes]^+$, 328 Da $[M\text{-}Mes\text{ -}CH_3]^+$.

Smp.: 115.5-116.5 °C.

1.3. References

(1) Brown, H. C.; Dodson, V. H. Studies in Stereochemistry. XXII. The Preparation and Reactions of Trimesitylborane. Evidence for the Non-Localized Nature of the Odd Electron in Triarylborane Radical Ions and Related Free Radicals 1. *J. Am. Chem. Soc.* **1957**, *79* (9), 2302–2306. https://doi.org/10.1021/ja01566a076.

(2) Schepper, J. D. W.; Orthaber, A.; Pammer, F. Preparation of Structurally and Electronically Diverse N → B-Ladder Boranes by [2 + 2 + 2] Cycloaddition. *J. Org. Chem.* **2021**, *86* (21), 14767–14776. https://doi.org/10.1021/acs.joc.1c01402.

(3) Schepper, J.; Orthaber, A.; Pammer, F. Tetrazole-Functionalized Organoboranes Exhibiting Dynamic Intramolecular N→B-Coordination and Cyanide-Selective Anion Binding. *Chem. – A Eur. J.* **2024**, *30* (37), e202401466. https://doi.org/10.1002/chem.202401466.

(4) Armarego, W. L. .; Perrin, D. D. *Purification of Laboratory Chemicals*, 4th ed.; Butterworth-Heinemann: Oxford, 1997.

(5) Fulmer, G. R.; Miller, A. J. M.; Sherden, N. H.; Gottlieb, H. E.; Nudelman, A.; Stoltz, B. M.; Bercaw, J. E.; Goldberg, K. I. NMR Chemical Shifts of Trace Impurities: Common Laboratory Solvents, Organics, and Gases in Deuterated Solvents Relevant to the Organometallic Chemist. *Organometallics* **2010**, *29* (9), 2176–2179. https://doi.org/10.1021/om100106e.

(6) Ando, S.; Matsuura, T. Substituent Shielding Parameters of Fluorine-19 NMR on Polyfluoroaromatic Compounds Dissolved in Dimethyl Sulphoxide- d 6. *Magn. Reson. Chem.* **1995**, *33* (8), 639–645. https://doi.org/10.1002/mrc.1260330805.

(7) Altomare, A.; Cascarano, G.; Giacovazzo, C.; Guagliardi, A.; Burla, M. C.; Polidori, G.; Camalli, M. SIR 92 – a Program for Automatic Solution of Crystal Structures by Direct Methods. *J. Appl. Crystallogr.* **1994**, *27* (3), 435–435. https://doi.org/10.1107/S002188989400021X.

(8) Sheldrick, G. M. A Short History of SHELX. *Acta Crystallogr. Sect. A Found. Crystallogr.* **2008**, *64* (1), 112–122. https://doi.org/10.1107/S0108767307043930.

(9) Frisch, M. J.; Trucks, G. W.; Schlegel, H. B.; Scuseria, G. E.; Robb, M. A.; Cheeseman, J. R.; Scalmani, G.; Barone, V.; Petersson, G. A.; Nakatsuji, H.; Li, X.; Caricato, M.; Marenich, A. V; Bloino, J.; Janesko, B. G.; Gomperts, R.; Mennucci, B.; Hratchian, H. P.; Ortiz, J. V; Izmaylov, A. F.; Sonnenberg, J. L.; Williams-Young, D.; Ding, F.; Lipparini, F.; Egidi, F.; Goings, J.; Peng, B.; Petrone, A.; Henderson, T.; Ranasinghe, D.; Zakrzewski, V. G.; Gao, J.; Rega, N.; Zheng, G.; Liang, W.; Hada, M.; Ehara, M.; Toyota, K.; Fukuda, R.; Hasegawa, J.; Ishida, M.; Nakajima, T.; Honda, Y.; Kitao, O.; Nakai, H.; Vreven, T.; Throssell, K.; Montgomery Jr., J. A.; Peralta, J. E.; Ogliaro, F.; Bearpark, M. J.; Heyd, J. J.; Brothers, E. N.; Kudin, K. N.; Staroverov, V. N.; Keith, T. A.; Kobayashi, R.; Normand, J.; Raghavachari, K.; Rendell, A. P.; Burant, J. C.; Iyengar, S. S.; Tomasi, J.; Cossi, M.; Millam, J. M.; Klene, M.; Adamo, C.; Cammi, R.; Ochterski, J. W.; Martin, R. L.; Morokuma, K.; Farkas, O.; Foresman, J. B.; Fox, D. J. Gaussian 16 {R}evision {C}.01. 2019.

(10) Friebolin, H.; Thiele, C. M. *Ein- Und Zweidimensionale NMR-Spektroskopie*, 5th ed.; Wiley-VCH, Weinheim, 2013.

(11) Koch, R.; Sun, Y.; Orthaber, A.; Pierik, A. J.; Pammer, F. Turn-on Fluorescence Sensors Based on Dynamic Intramolecular N→B-Coordination. *Org. Chem. Front.* **2020**, *7* (12), 1437–1452. https://doi.org/10.1039/d0qo00267d.

2. Supplementary Analytical Data

2.1. Analytical Data

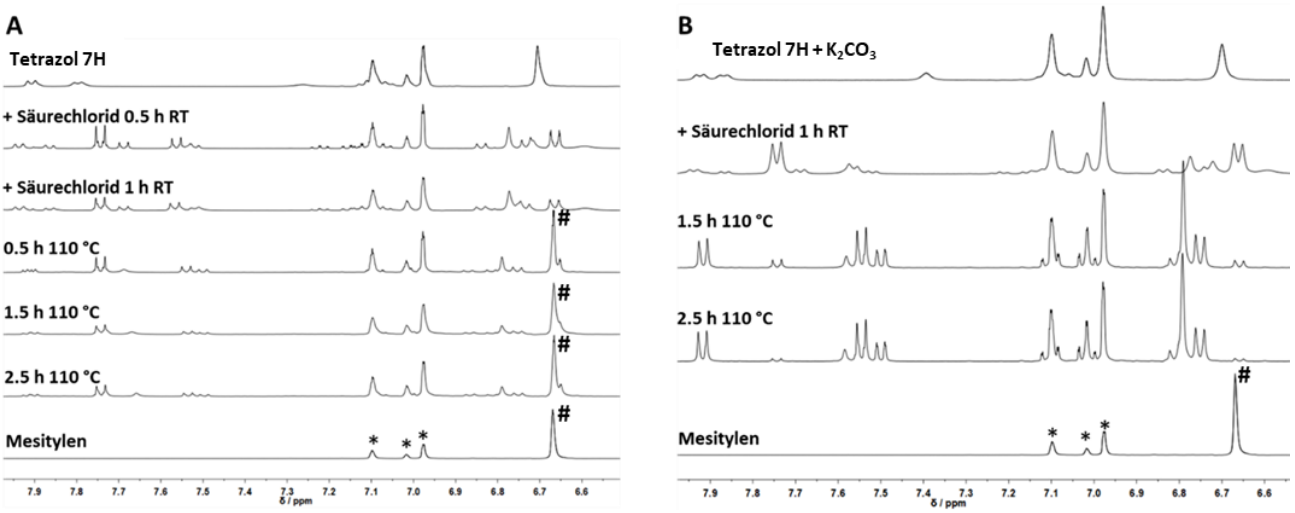

Figure S1: ^{1}H-NMR-Reaction control oft he reaction of 2H with p-toluoyl chloride in toluene-d_8 (*) without (A) and with (B) K_2CO_3. Bottom: Reference spectrum of mesitylene (#).

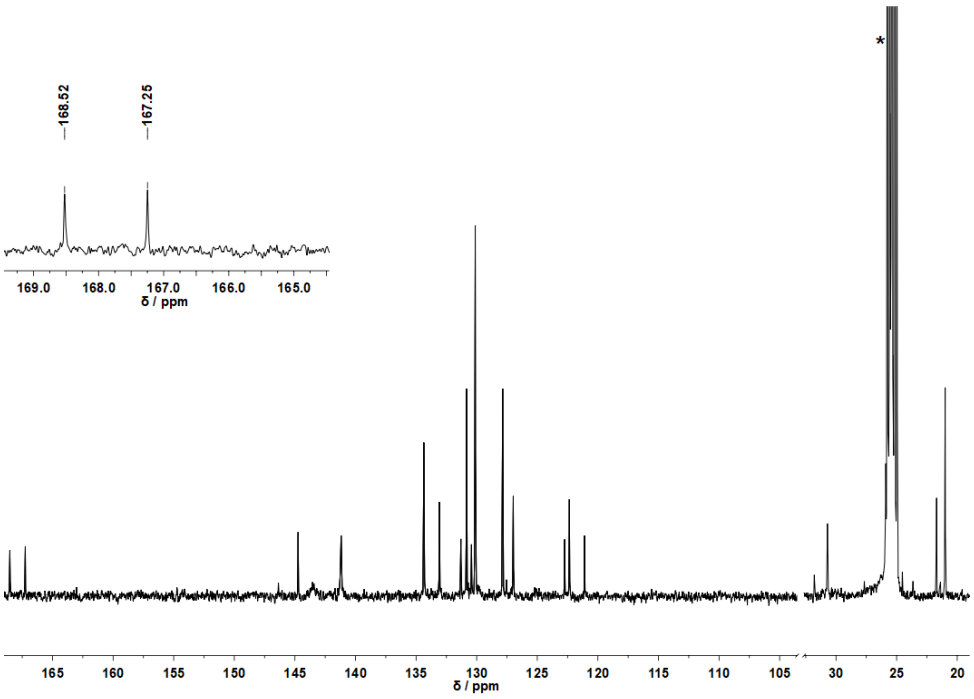

Figure S2. Exemplary ^{13}C-NMR-spectrum of Oxadiazol 4a in THF-d_8 (*).

2.2. Crystallographic Data

2.2.1. Structural data for CCDC-2514226 (4a)

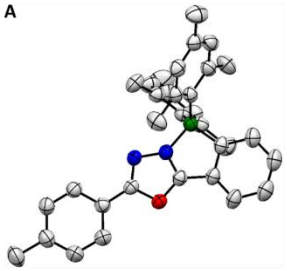

Table S1: Crystal data and structural refinement for 2-(2-(Dimesitylboryl)phenyl)-5-(p-tolyl)-1,3,4-oxadiazole (4a).

Identification code	**CCDC-2514226**
Empirical formula	$C_{33}H_{33}BN_2O$
Formula weight	484.42
Temperature/K	301.9(6)
Crystal system	triclinic
Space group	P-1
a/Å	9.7571(5)
b/Å	11.1700(7)
c/Å	14.0701(9)
α/°	99.257(5)
β/°	101.748(5)
γ/°	108.129(5)
Volume/Å³	1384.75(15)
Z	2
ρ_{calc}g/cm³	1.162
μ/mm⁻¹	0.531
F(000)	516
Crystal size/mm³	0.232 × 0.232 × 0.225
Radiation	Cu Kα (λ = 1.54184)
2Θ range for data collection/°	8.582 to 146.048
Index ranges	-8 ≤ h ≤ 12, -13 ≤ k ≤ 13, -16 ≤ l ≤ 17
Reflections collected	20186
Independent reflections	5343 [R_{int} = 0.0255, R_{sigma} = 0.0283]
Data/restraints/parameters	5343/0/341
Goodness-of-fit on F²	1.048
Final R indexes [I>=2σ (I)]	R_1 = 0.0514, wR_2 = 0.1310
Final R indexes [all data]	R_1 = 0.0656, wR_2 = 0.1453
Largest diff. peak/hole / e Å⁻³	0.19/-0.18

2.2.2. Structural data for CCDC-2514223 (4b)

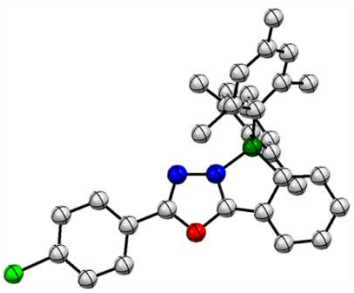

Table S2: Crystal data and structural refinement for 2-(4-Chlorophenyl)-5-(2-(dimesitylboryl)phenyl)-1,3,4-oxadiazole (4b).+

Identification code	**CCDC-2514223**
Empirical formula	$C_{32}H_{30}BClN_2O$
Formula weight	504.84
Temperature/K	150.00(14)
Crystal system	triclinic
Space group	P-1
a/Å	9.9216(5)
b/Å	11.0600(6)
c/Å	13.9944(5)
α/°	102.348(4)
β/°	104.003(4)
γ/°	110.321(5)
Volume/Å³	1320.27(12)
Z	2
ρ_{calc}g/cm³	1.27
μ/mm⁻¹	1.489
F(000)	532
Crystal size/mm³	0.241 × 0.194 × 0.129
Radiation	Cu Kα (λ = 1.54184)
2Θ range for data collection/°	6.89 to 145.642
Index ranges	-10 ≤ h ≤ 12, -13 ≤ k ≤ 13, -17 ≤ l ≤ 14
Reflections collected	18552
Independent reflections	5076 [R_{int} = 0.0228, R_{sigma} = 0.0235]
Data/restraints/parameters	5076/0/340
Goodness-of-fit on F²	1.05
Final R indexes [I>=2σ (I)]	R_1 = 0.0443, wR_2 = 0.1169
Final R indexes [all data]	R_1 = 0.0516, wR_2 = 0.1250
Largest diff. peak/hole / e Å⁻³	0.28/-0.27

2.2.3. Structural data for CCDC-2514225 (4c)

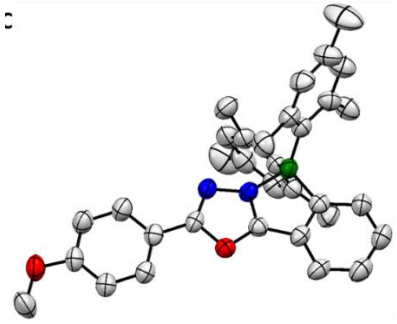

Table S3: Crystal data and structural refinement for 2-(2-(Dimesitylboryl)phenyl)-5-(4-methoxyphenyl)-1,3,4-oxadiazole (4c).+

Identification code	**CCDC-2514225**
Empirical formula	$C_{33}H_{33}BN_2O_2$
Formula weight	500.42
Temperature/K	302.9(9)
Crystal system	orthorhombic
Space group	$Pna2_1$
a/Å	8.7084(3)
b/Å	32.0567(13)
c/Å	10.0958(3)
α/°	90
β/°	90
γ/°	90
Volume/Å³	2818.37(17)
Z	4
ρ_{calc}g/cm³	1.179
μ/mm⁻¹	0.565
F(000)	1064
Crystal size/mm³	0.479 × 0.079 × 0.053
Radiation	Cu Kα (λ = 1.54184)
2Θ range for data collection/°	9.184 to 145.952
Index ranges	-10 ≤ h ≤ 7, -38 ≤ k ≤ 39, -5 ≤ l ≤ 12
Reflections collected	14530
Independent reflections	3634 [R_{int} = 0.0334, R_{sigma} = 0.0321]
Data/restraints/parameters	3634/1/350
Goodness-of-fit on F²	1.076
Final R indexes [I>=2σ (I)]	R_1 = 0.0519, wR_2 = 0.1226
Final R indexes [all data]	R_1 = 0.0645, wR_2 = 0.1345
Largest diff. peak/hole / e Å⁻³	0.13/-0.20
Flack parameter	0.0(5)

2.2.4. Structural data for CCDC-2514224 (4f)

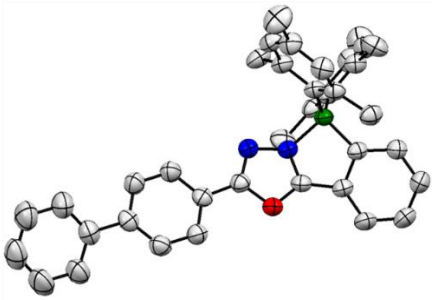

Table S4: Crystal data and structural refinement for 2-([1,1'-Biphenyl]-4-yl)-5-(2-(dimesitylboryl)phenyl)-1,3,4-oxadiazole (4f).

Identification code	**CCDC-2514224**
Empirical formula	$C_{38}H_{35}BN_2O$
Formula weight	546.49
Temperature/K	300(3)
Crystal system	monoclinic
Space group	$P2_1/c$
a/Å	13.5714(2)
b/Å	10.65747(17)
c/Å	21.9263(4)
α/°	90
β/°	104.8563(17)
γ/°	90
Volume/Å³	3065.35(9)
Z	4
ρ_{calc}g/cm³	1.184
μ/mm⁻¹	0.539
F(000)	1160
Crystal size/mm³	0.305 × 0.105 × 0.093
Radiation	Cu Kα (λ = 1.54184)
2Θ range for data collection/°	8.344 to 145.914
Index ranges	-16 ≤ h ≤ 10, -13 ≤ k ≤ 12, -26 ≤ l ≤ 27
Reflections collected	25494
Independent reflections	5952 [R_{int} = 0.0268, R_{sigma} = 0.0232]
Data/restraints/parameters	5952/0/386
Goodness-of-fit on F²	1.039
Final R indexes [I>=2σ (I)]	R_1 = 0.0473, wR_2 = 0.1303
Final R indexes [all data]	R_1 = 0.0556, wR_2 = 0.1420
Largest diff. peak/hole / e Å⁻³	0.23/-0.15

2.2.5. Structural data for CCDC-2514222 (8b)

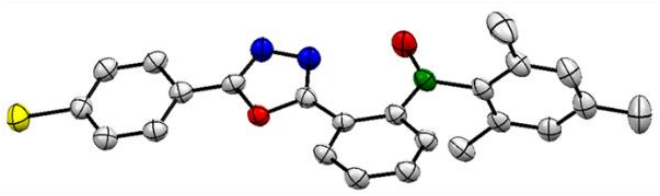

Table S5: Crystal data and structural refinement for 2-(4-chlorophenyl)-5-(2-(hydroxy(mesityl)boryl)phenyl)-1,3,4-oxadiazole (8b).

Identification code	**CCDC-2514222**
Empirical formula	$C_{23}H_{20}BClN_2O_2$
Formula weight	402.67
Temperature/K	150.05(10)
Crystal system	triclinic
Space group	P-1
a/Å	8.7343(5)
b/Å	9.8964(6)
c/Å	13.1346(10)
α/°	111.079(7)
β/°	94.791(6)
γ/°	102.413(5)
Volume/Å³	1018.35(13)
Z	2
ρ_{calc}g/cm³	1.313
μ/mm⁻¹	1.83
F(000)	420
Crystal size/mm³	0.175 × 0.129 × 0.103
Radiation	Cu Kα (λ = 1.54184)
2Θ range for data collection/°	7.328 to 145.66
Index ranges	-6 ≤ h ≤ 10, -12 ≤ k ≤ 12, -16 ≤ l ≤ 15
Reflections collected	6844
Independent reflections	3885 [R_{int} = 0.0372, R_{sigma} = 0.0417]
Data/restraints/parameters	3885/0/266
Goodness-of-fit on F²	1.036
Final R indexes [I>=2σ (I)]	R_1 = 0.0527, wR_2 = 0.1448
Final R indexes [all data]	R_1 = 0.0676, wR_2 = 0.1572
Largest diff. peak/hole / e Å⁻³	0.37/-0.31

2.3. UV-vis Data

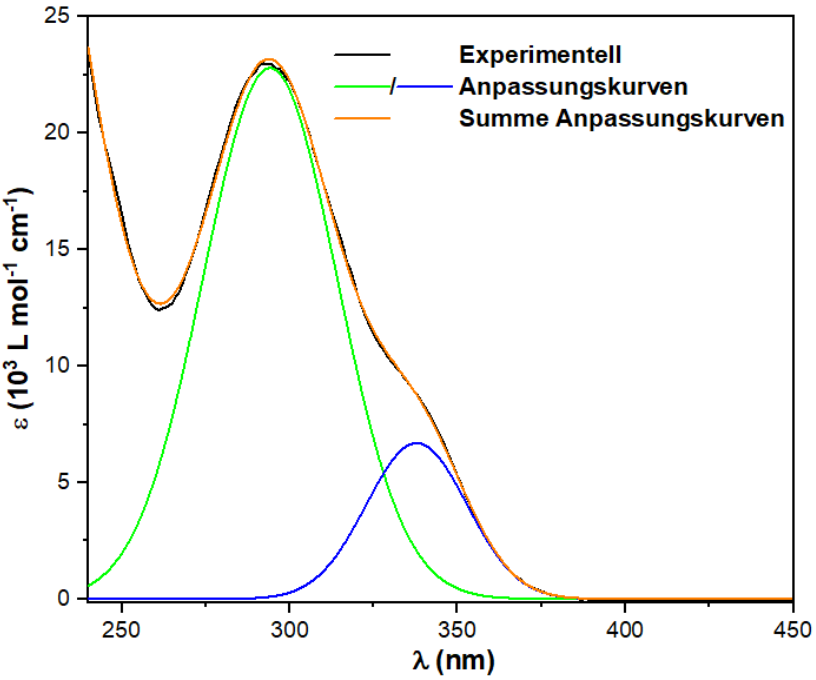

Modell	Gauss		
Gleichung	y=y0 + (A/(w*sqrt(pi/2)))*exp(-2*((x-xc)/w)^2)		
Zeichnen	Peak1(ext)	Peak2(ext)	Peak3(ext)
y0	0 ± 0	0 ± 0	0 ± 0
xc	210 ± 0	294.13252 ± 0.07268	337.79122 ± 0.24997
w	53.26411 ± 0.32289	39.83995 ± 0.25041	29.93291 ± 0.31962
A	2909299.0258 ± 9982.	1138242.84191 ± 7766	251193.48807 ± 5003.650
Chi-Quadr Reduzie	14583.72692		
R-Quadrat(COD)	0.99978		
Kor. R-Quadrat	0.99977		

Figure S3. Deconvolution of the absorption spectrum of 4a.

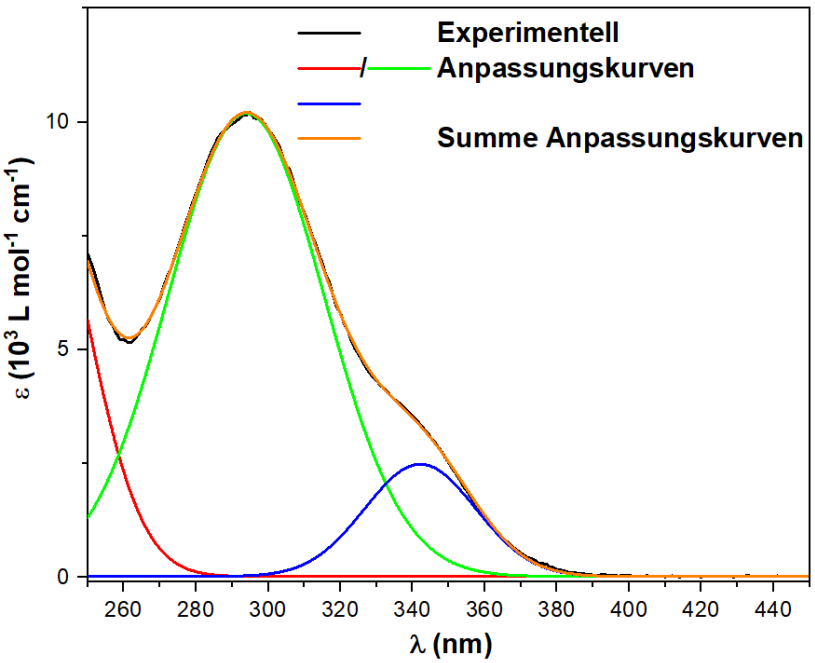

Modell	Gauss		
Gleichung	y=y0 + (A/(w*sqrt(pi/2)))*exp(-2*((x-xc)/w)^2)		
Zeichnen	Peak1(G)	Peak2(G)	Peak3(G)
y0	20 ± 0	20 ± 0	20 ± 0
xc	234.22022 ± 0.46097	293.86363 ± 0.06322	342.11045 ± 0.27418
w	30.50219 ± 0.60773	43.22093 ± 0.2778	30.67414 ± 0.36709
A	365713.09347 ± 11825.69744	550972.14981 ± 3348.55448	94865.12393 ± 2059.61797
Chi-Quadr Reduziert	2796.33197		
R-Quadrat(COD)	0.99979		
Kor. R-Quadrat	0.99978		

Figure S4. Deconvolution of the absorption spectrum of 4b.

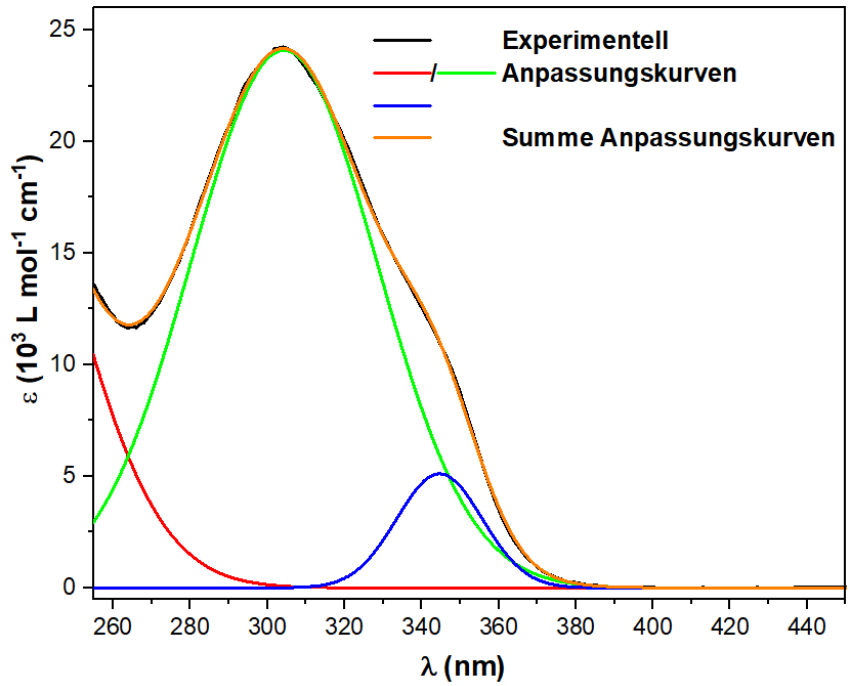

Modell	Gauss		
Gleichung	y=y0 + (A/(w*sqrt(pi/2)))*exp(-2*((x-xc)/w)^2)		
Zeichnen	Peak1(ext)	Peak2(ext)	Peak3(ext)
y0	0 ± 0	0 ± 0	0 ± 0
xc	223.04986 ± 1.57737	304.33456 ± 0.07444	344.65021 ± 0.13356
w	47.90358 ± 1.70099	48.17371 ± 0.38613	22.1566 ± 0.37058
A	1518367.0463 ± 103521.792	1454593.6754 ± 11914.886	141937.3049 ± 5697.20516
Chi-Quadr Reduziert	12231.19726		
R-Quadrat(COD)	0.99983		
Kor. R-Quadrat	0.99983		

Figure S5. Deconvolution of the absorption spectrum of 4c.

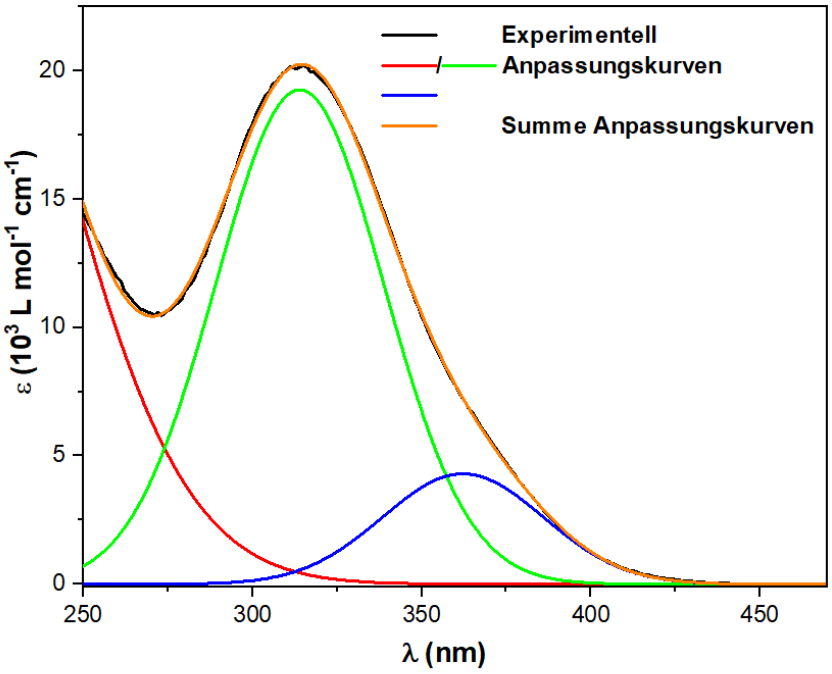

Modell	Gauss		
Gleichung	y=y0 + (A/(w*sqrt(pi/2)))*exp(-2*((x-xc)/w)^2)		
Zeichnen	Peak1(ext)	Peak2(ext)	Peak3(ext)
y0	0 ± 0	0 ± 0	0 ± 0
xc	200.80593 ± 0	313.95649 ± 0.40931	362.21356 ± 1.8983
w	77.37218 ± 0.64299	49.73523 ± 0.64409	47.60466 ± 1.57794
A	3073310.07323 ± 9675.8	1200871.95022 ± 28182.2	256614.06273 ± 24062.17232
Chi-Quadr Reduziert	20264.38971		
R-Quadrat(COD)	0.9996		
Kor. R-Quadrat	0.99959		

Figure S6. Deconvolution of the absorption spectrum of 4d.

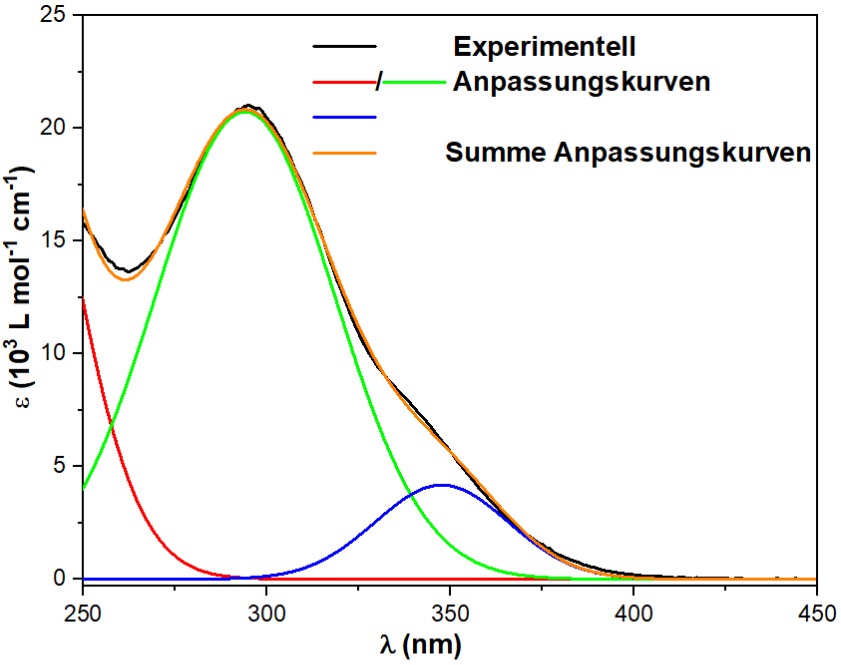

Modell	Gauss		
Gleichung	y=y0 + (A/(w*sqrt(pi/2)))*exp(-2*((x-xc)/w)^2)		
Zeichnen	Peak1(ext)	Peak2(ext)	Peak3(ext)
y0	0 ± 0	0 ± 0	0 ± 0
xc	223.71032 ± 0	294.07283 ± 0.16167	347.5907 ± 0.89575
w	39.54817 ± 0.51709	48.77999 ± 0.69641	36.26665 ± 1.09545
A	1472063.98881 ± 12006.4	1267474.07428 ± 18156.8	189693.70792 ± 11438.626
Chi-Quadr Reduziert	48161.50795		
R-Quadrat(COD)	0.9991		
Kor. R-Quadrat	0.99909		

Figure S7. Deconvolution of the absorption spectrum of 4e.

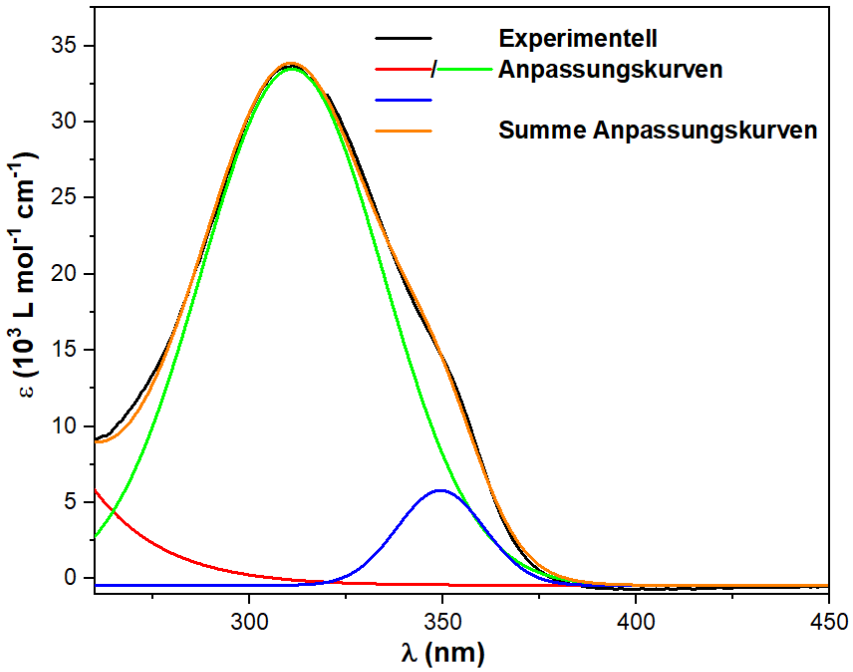

Modell	Gauss		
Gleichung	y=y0 + (A/(w*sqrt(pi/2)))*exp(-2*((x-xc)/w)^2)		
Zeichnen	Peak1(ext)	Peak2(ext)	Peak3(ext)
y0	-434.32085 ± 0	-434.32085 ± 0	-434.32085 ± 0
xc	-298.69223 ± 0	310.95577 ± 0.15298	349.32784 ± 0.30296
w	204.7755 ± 0	47 ± 0.25238	22.60605 ± 0.67843
A	4.65865E12 ± 0	1997535.42414 ± 11277.369	176662.75505 ± 10177.0251
Chi-Quadr Reduziert	117333.41115		
R-Quadrat(COD)	0.99907		
Kor. R-Quadrat	0.99905		

Figure S8. Deconvolution of the absorption spectrum of 4f.

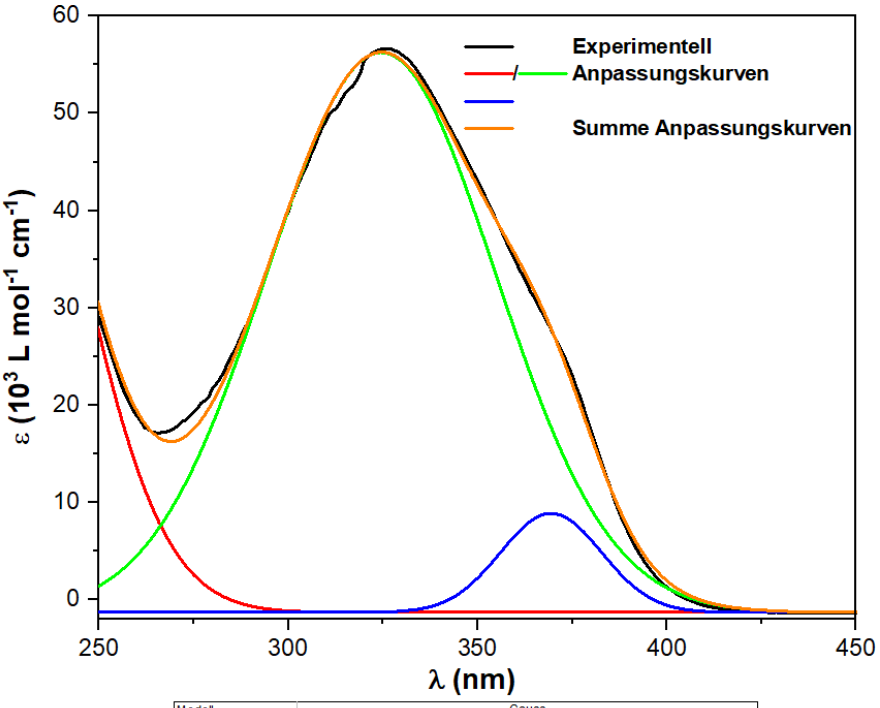

Modell	Gauss		
Gleichung	y=y0 + (A/(w*sqrt(pi/2)))*exp(-2*((x-xc)/w)^2)		
Zeichnen	Peak1(ext)	Peak2(ext)	Peak3(ext)
y0	-1316.07757 ± 45.35764	-1316.07757 ± 45.35764	-1316.07757 ± 45.35764
xc	220 ± 0	324.55199 ± 0.12568	369.42393 ± 0.2974
w	46.08018 ± 0.27717	60.31273 ± 0	26.66898 ± 0.64648
A	3893561.15759 ± 20226.6	4352622.31951 ± 9989.9	340294.9416 ± 10903.7065
Chi-Quadr Reduziert	407391.95494		
R-Quadrat(COD)	0.99897		
Kor. R-Quadrat	0.99895		

Figure S9. Deconvolution of the absorption spectrum of 4g.

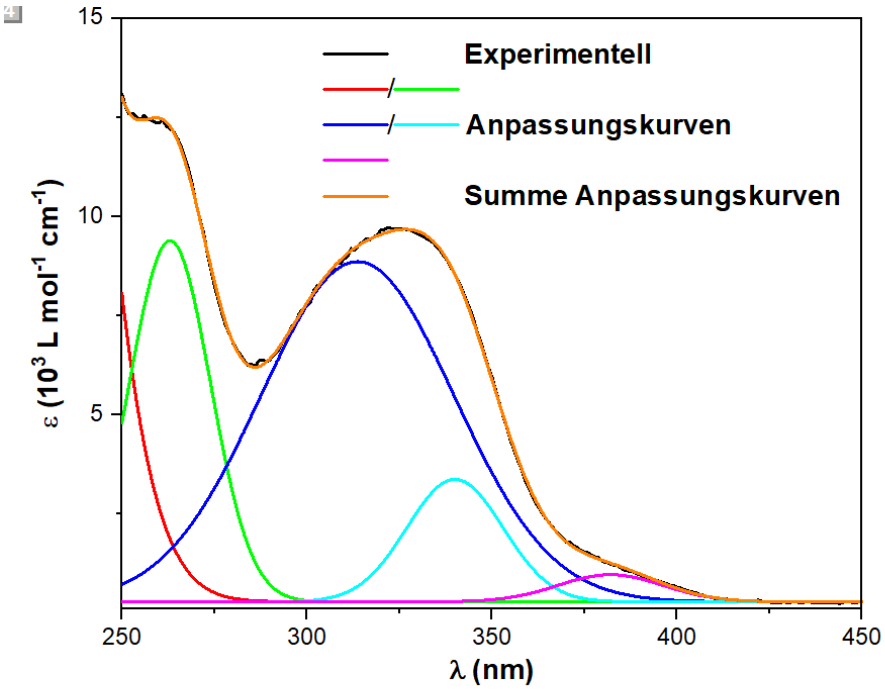

Modell	Gauss				
Gleichung	y=y0 + (A/(w*sqrt(pi/2)))*exp(-2*((x-xc)/w)^2)				
Zeichnen	Peak1(195)	Peak2(195)	Peak3(195)	Peak4(195)	Peak5(195)
y0	274.88497 ± 2.80522	274.88497 ± 2.80522	274.88497 ± 2.80522	274.88497 ± 2.80522	274.88497 ± 2.80522
xc	216.51788 ± 5.28431	262.98974 ± 0.29652	313.65489 ± 1.30332	339.99939 ± 0.18499	382.00755 ± 2.15443
w	36.11845 ± 4.24043	21.89476 ± 0.35348	52.15727 ± 2.10084	25.9104 ± 1.34643	28.36237 ± 1.96703
A	1966015.16606 ± 606069.72644	249940.79241 ± 14918.66531	560872.67366 ± 32097.22818	100371.79428 ± 22857.29158	24249.30004 ± 5431.68616
Chi-Quadr Reduziert	1417.63258				
R-Quadrat (COD)	0.99993				
Kor. R-Quadrat	0.99993				

Figure S10. Deconvolution of the absorption spectrum of 4h.

2.4. NMR and MS Data

2.4.1. ^{11}B NMR

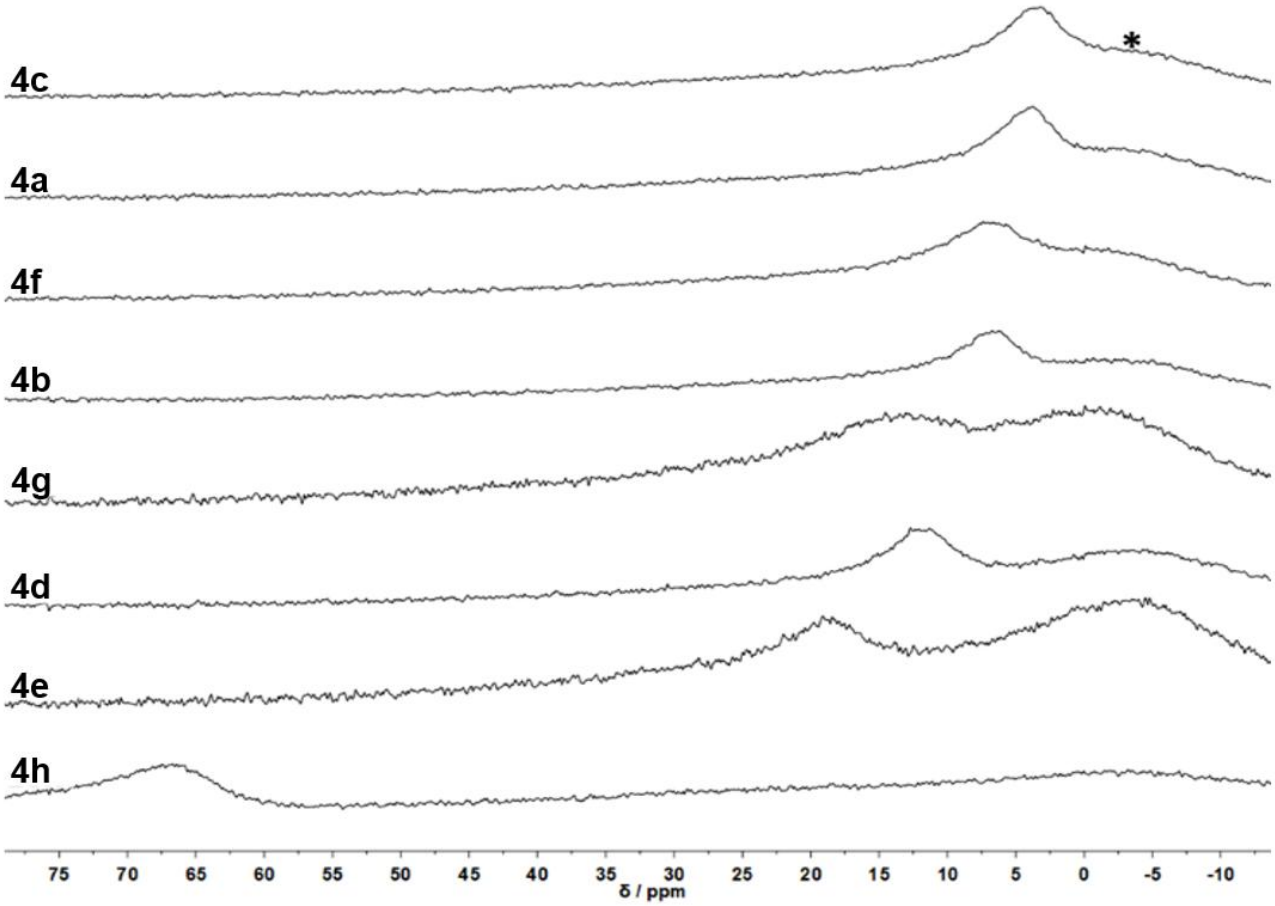

Figure S11. ^{11}B-NMR-Spektra of 4a – 4f and 4h in THF-d_8 and of 4g in. * Background glass-signal.

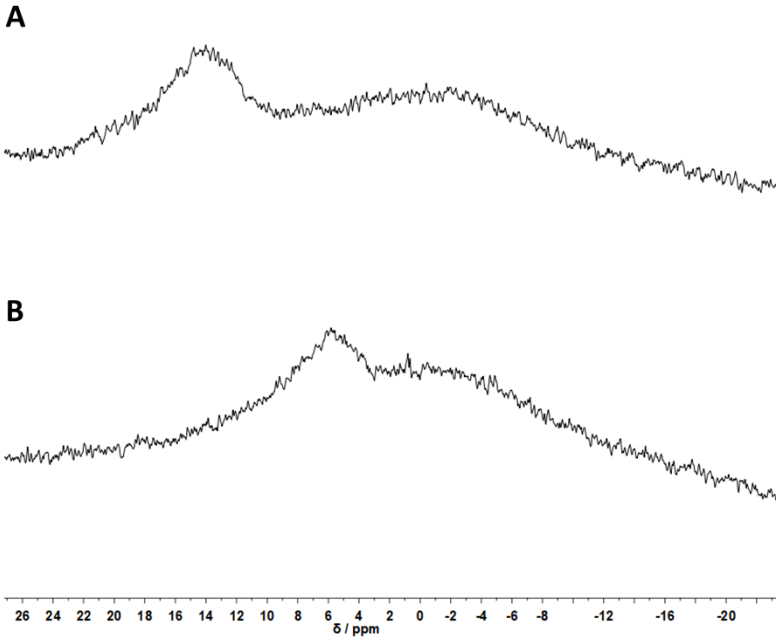

Figure S12. ^{11}B-NMR-Spektra of 4b before (A) and after (B) addition of von TBAF in $CDCl_3$.

2.4.2. Variable Temperature NMR

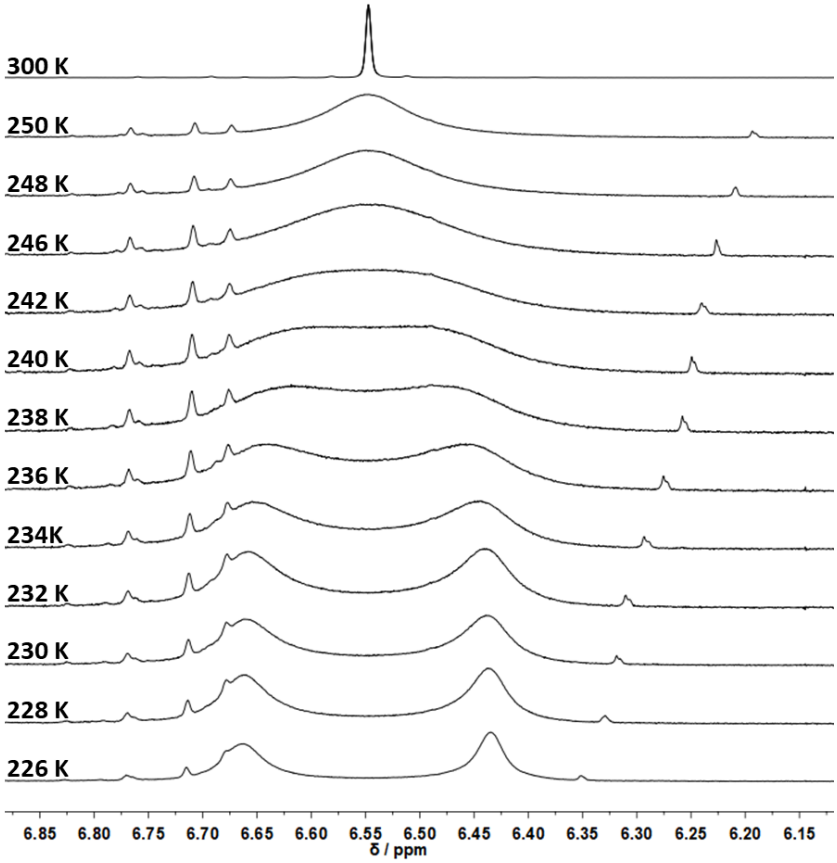

Figure S13. Section of variable-temperature 1H-NMR spectra of 4a in THF-d_8; The signals of the aromatic mesityl-protons are depicted.

To derive the activation barrier for rotation about the CPh-B bond for several the borane, the coalescence temperature T_C wasexperimentally determined via variable temperature NMR-spectroscopy (VT-NMR).[10] From Tc and signal splitting (Δv) of the frozen signals, the rotation barriers ∆GC (see Table 5) can be calculated with the following approximate relationship:

$$\Delta G_C \approx \alpha \cdot T_C[9.972+\log(T_C/\Delta v)] \qquad [1]$$

with $\alpha \cdot = 1.914 \cdot 10^{-2}$ kJ·mol^{-1}·K^{-1}; Δv: signal splitting in Hz, determined fr0m the lowest temperature spectra.

2.4.3. NMR Spectra

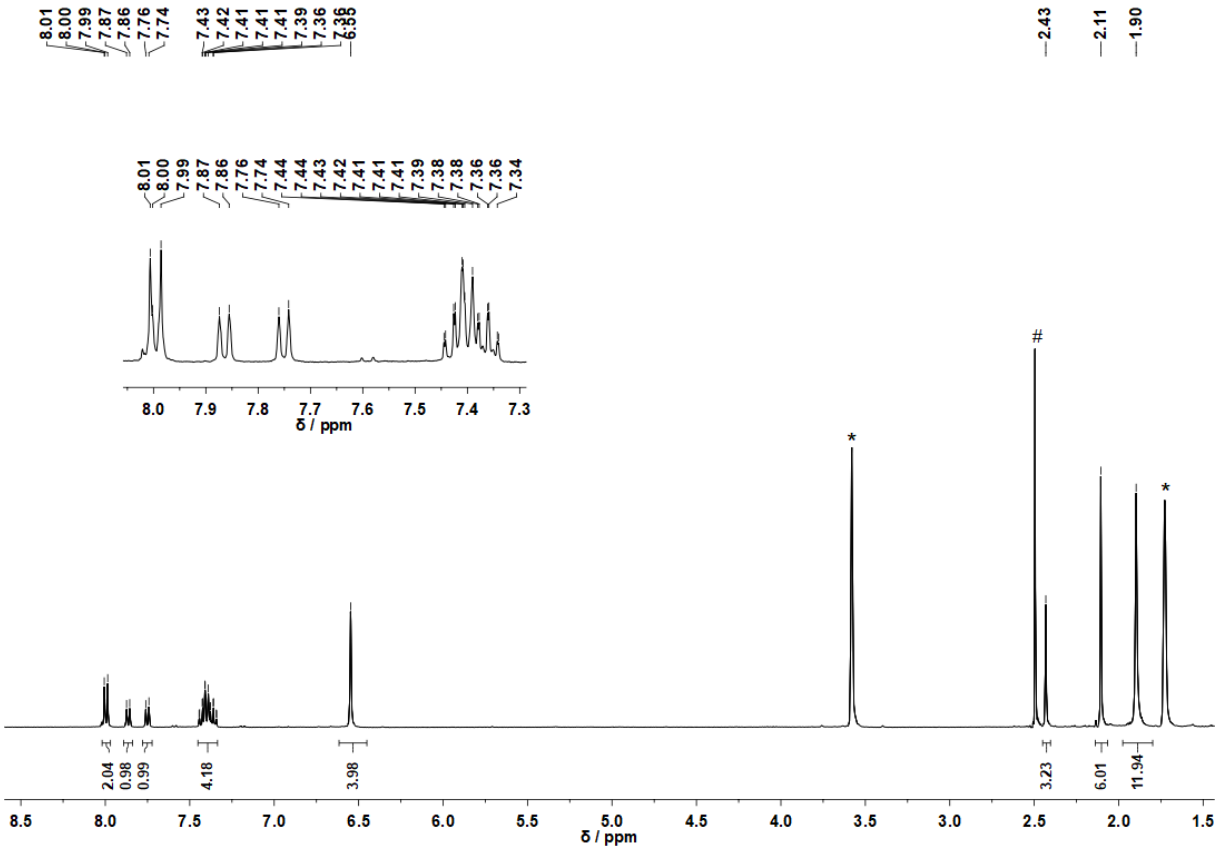

Figure S14. ^{1}H-NMR-Spectrum of 4a in THF-d_8 (*); H_2O (#).

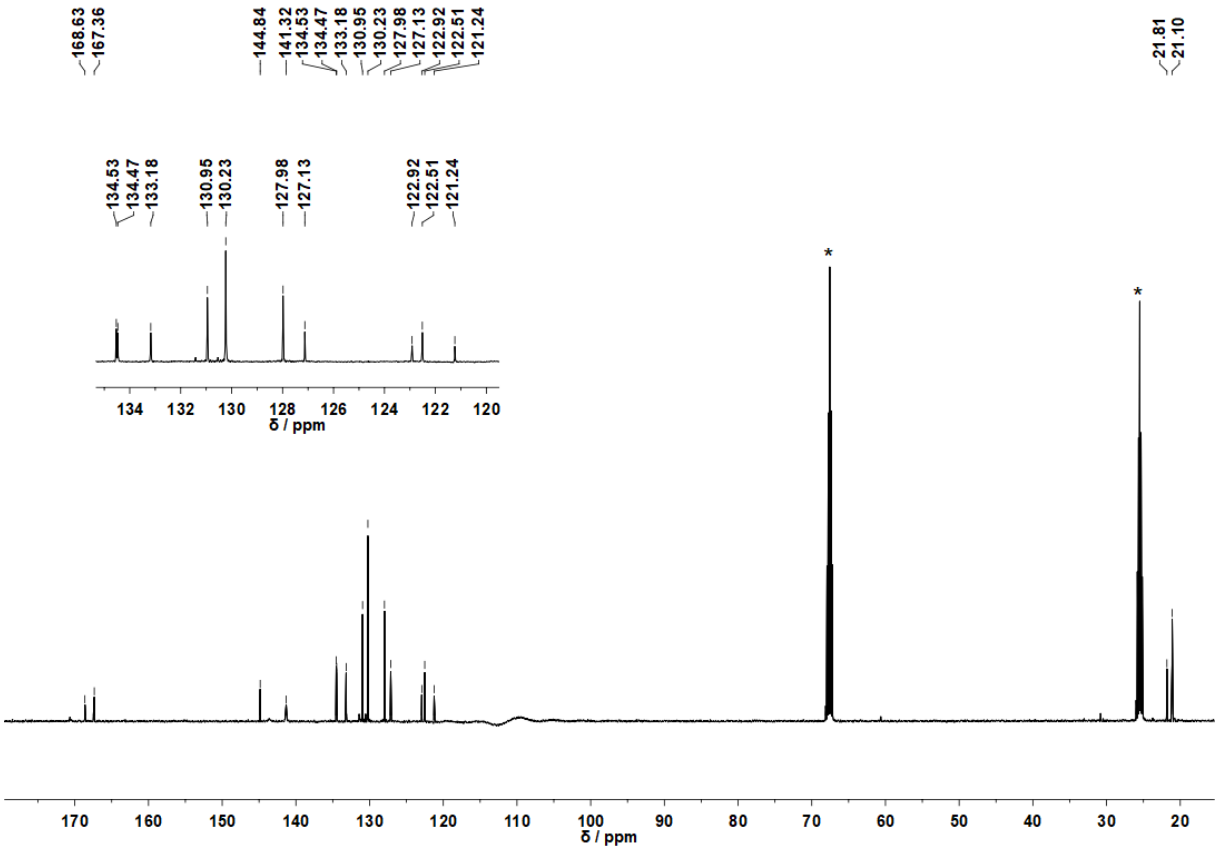

Figure S15. Udeft-Spectrum of 4a in THF-d_8 (*).

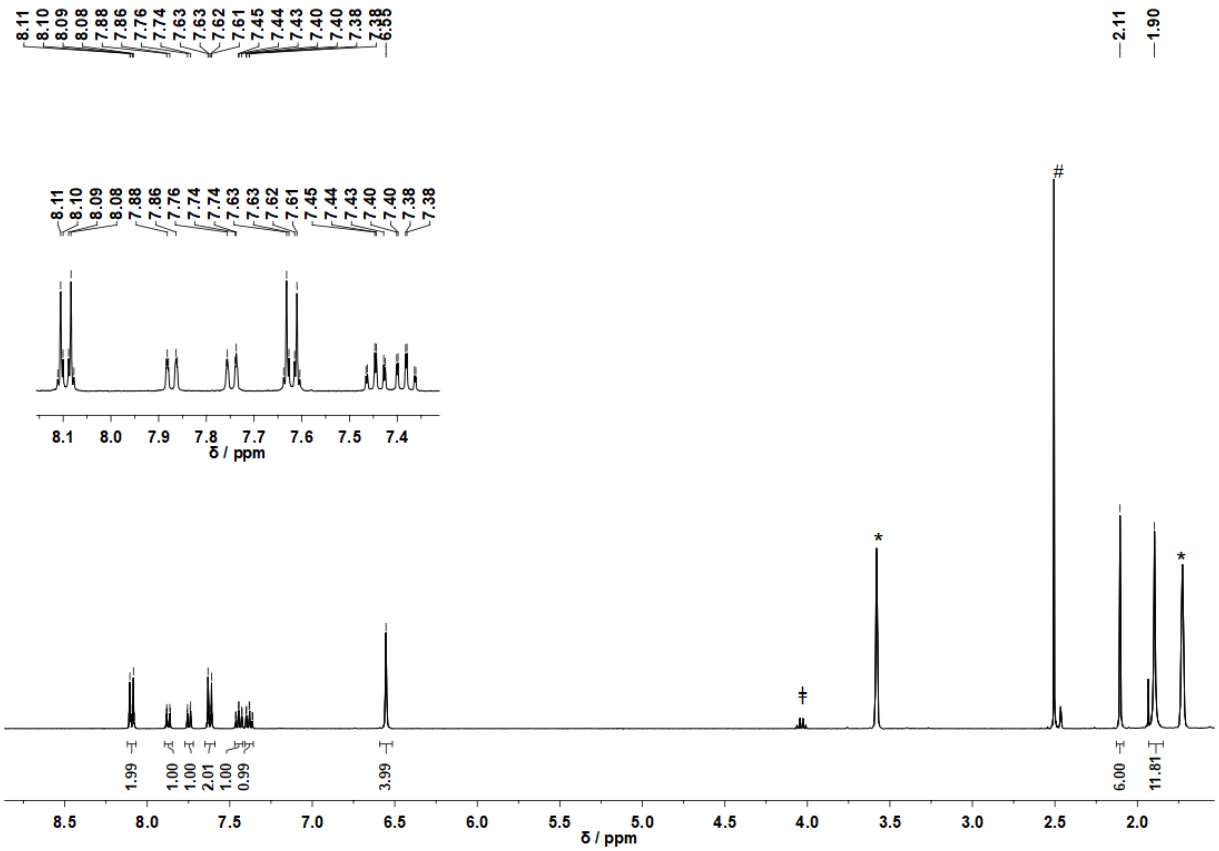

Figure S16.[1]H-NMR-Spectrum of 4b in THF-d_8 (*); H_2O (#); EtOAc (‡).

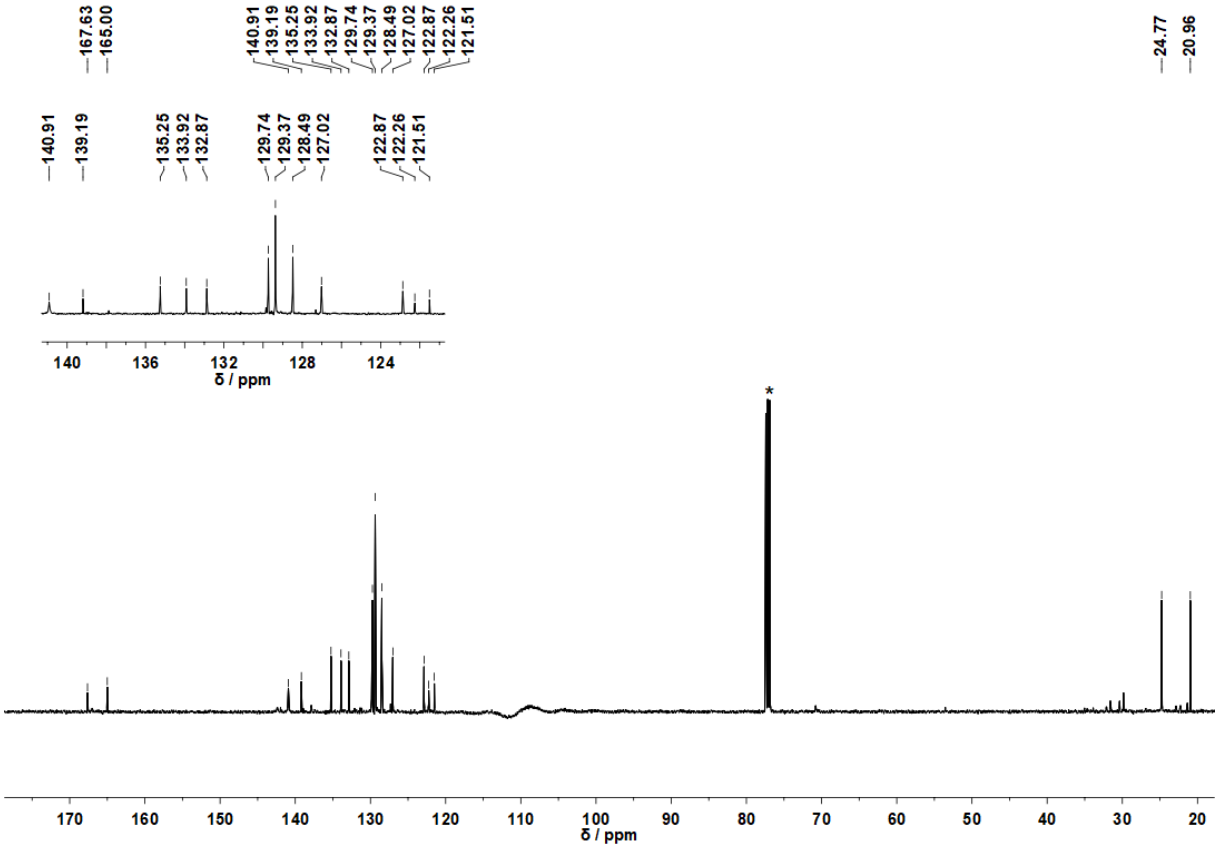

Figure S17.udeft-Spectrum of 4b in $CDCl_3$ (*).

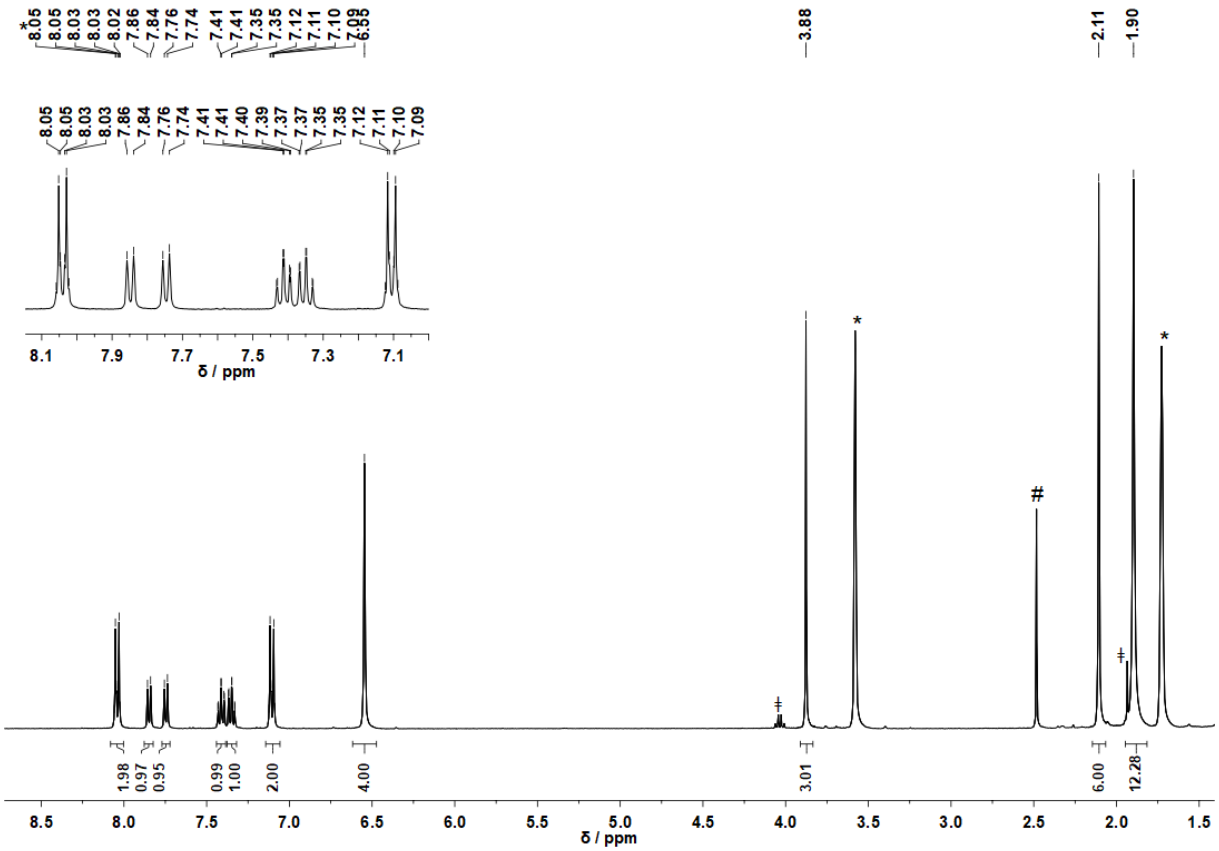

Figure S18. ^{1}H-Spectrum of 4c in THF-d_8 (*); H_2O (#); EtOAc (‡).

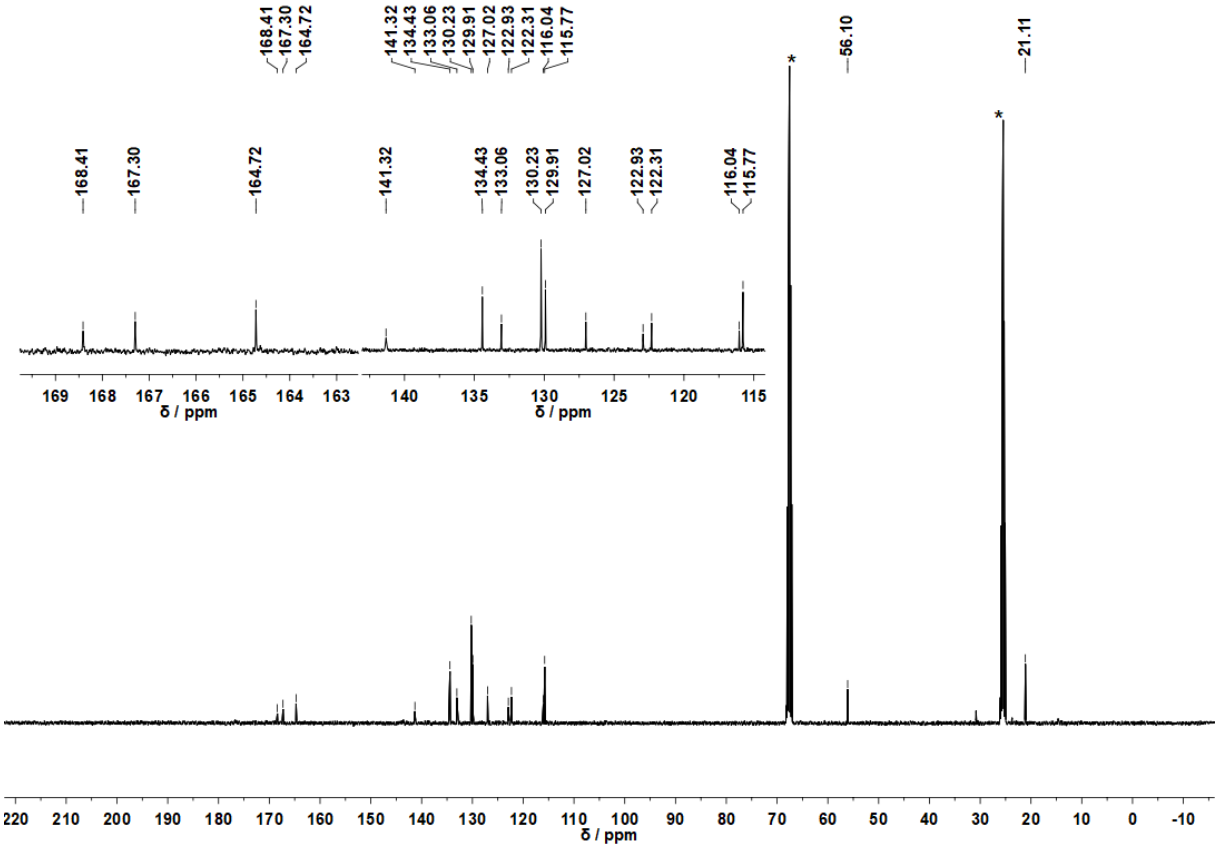

Figure S19.^{13}C-NMR-Spectrum of 4c THF-d_8 (*).

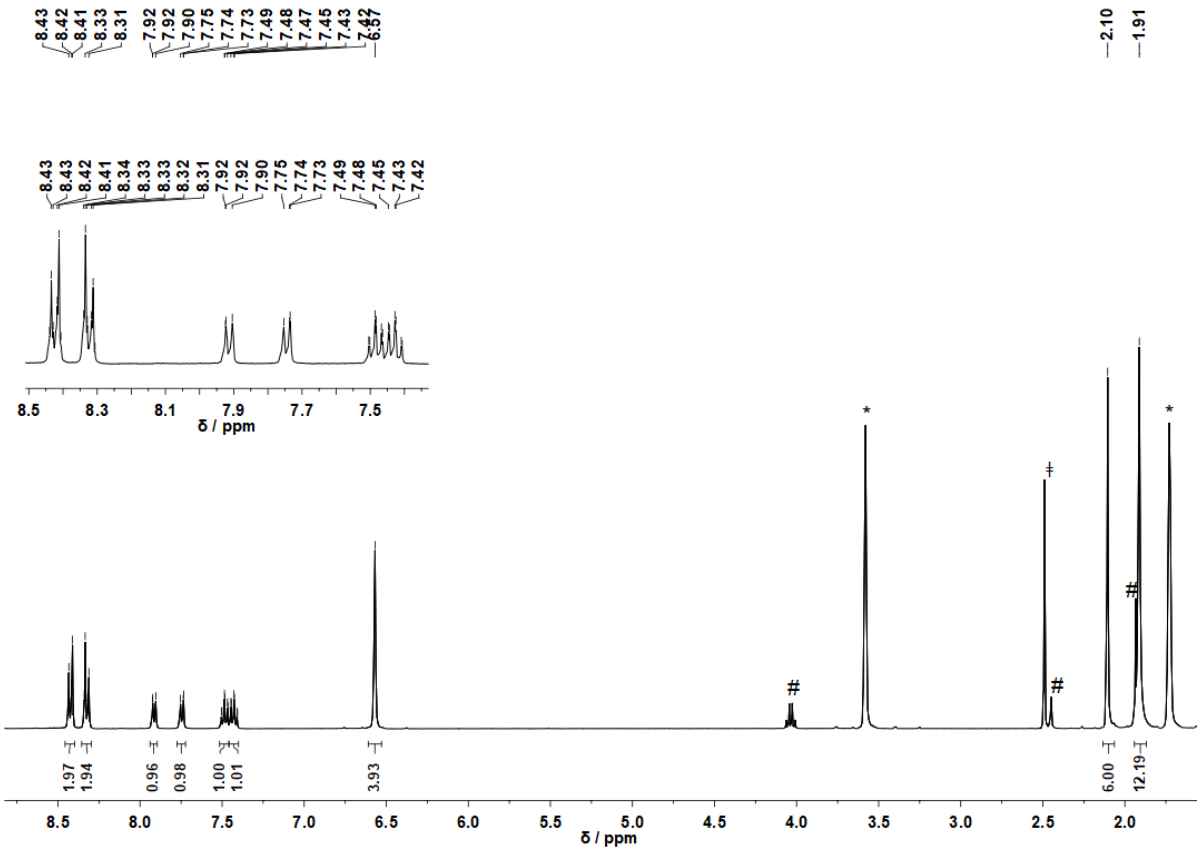

Figure S20.[1]H-NMR-Spectrum of 4d in THF-d_8 (*); H_2O (‡); EtOAc (#).

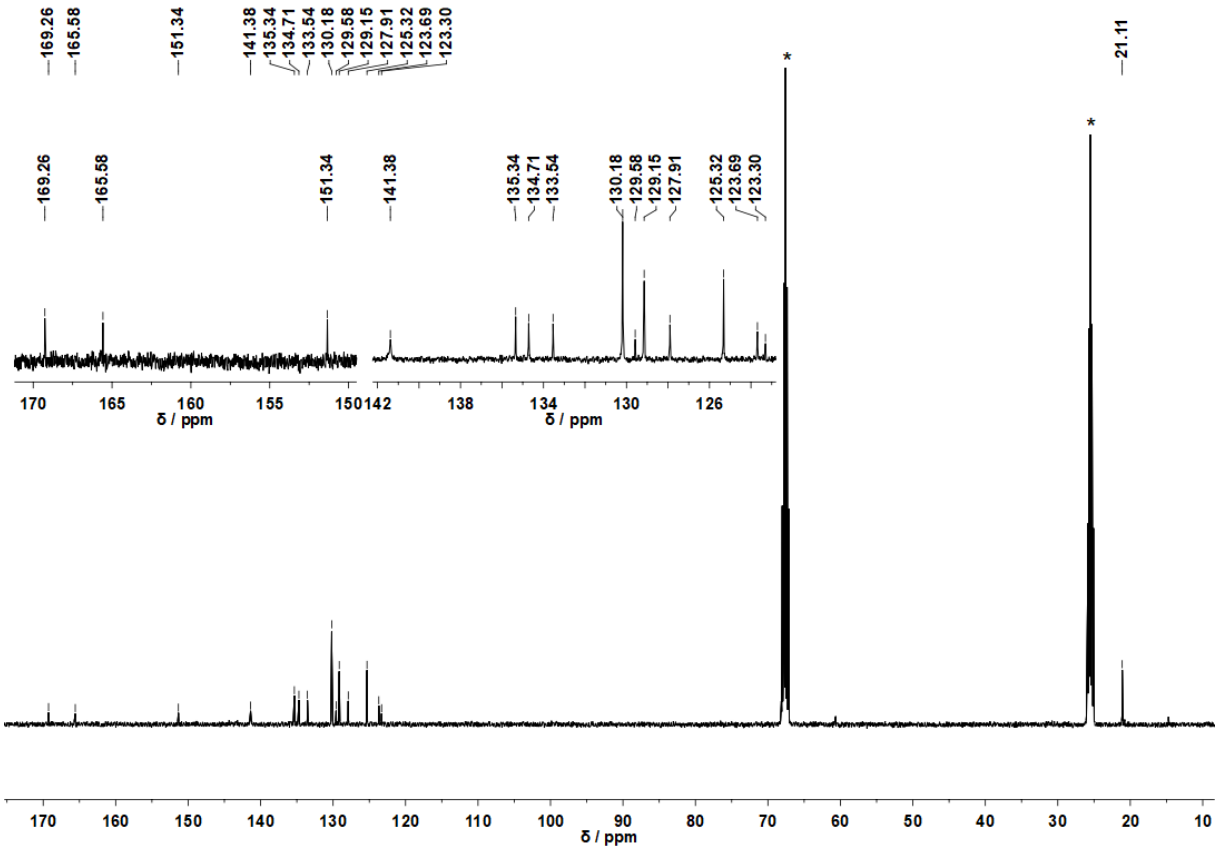

Figure S21. [13]C-NMR-Spectrum of 4d in THF-d_8 (*).

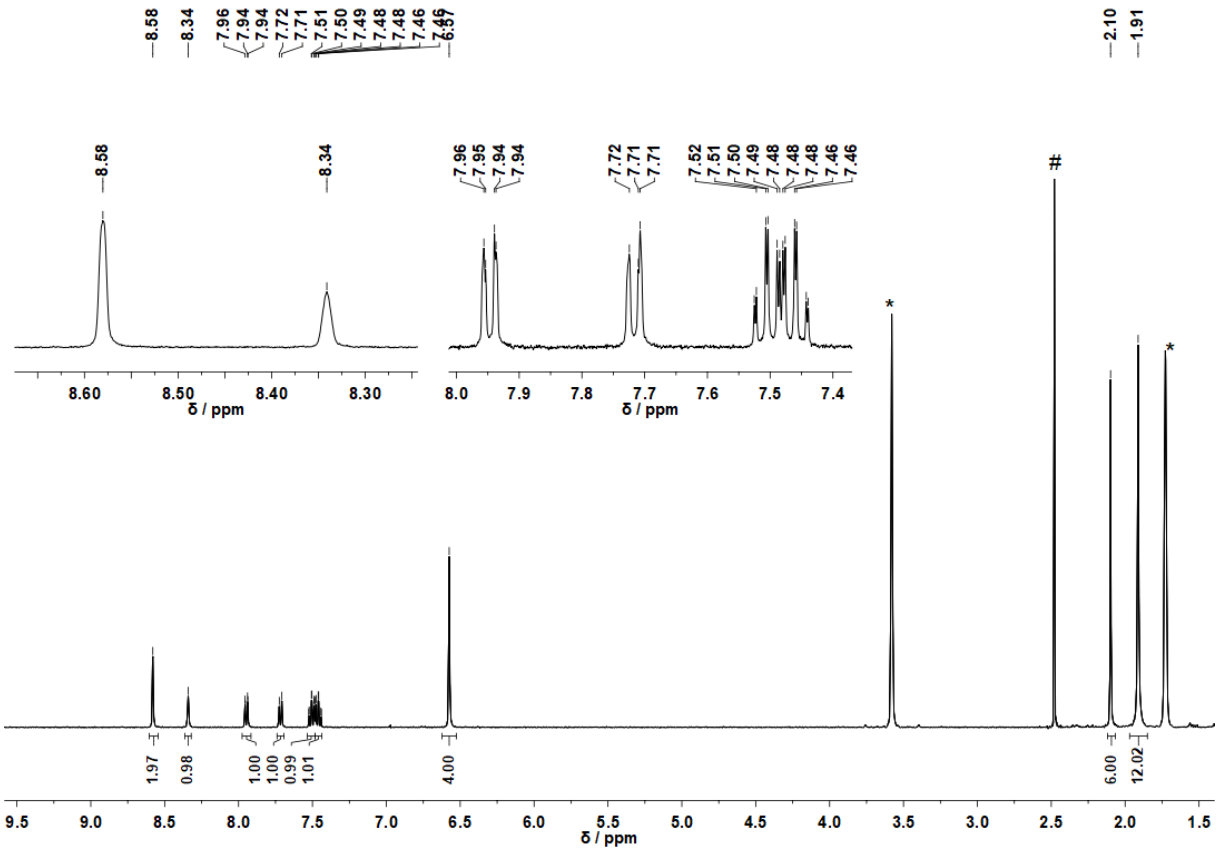

Figure S22.^{1}H-NMR-Spectrum of 4e in THF-d_8 (*); H_2O (#).

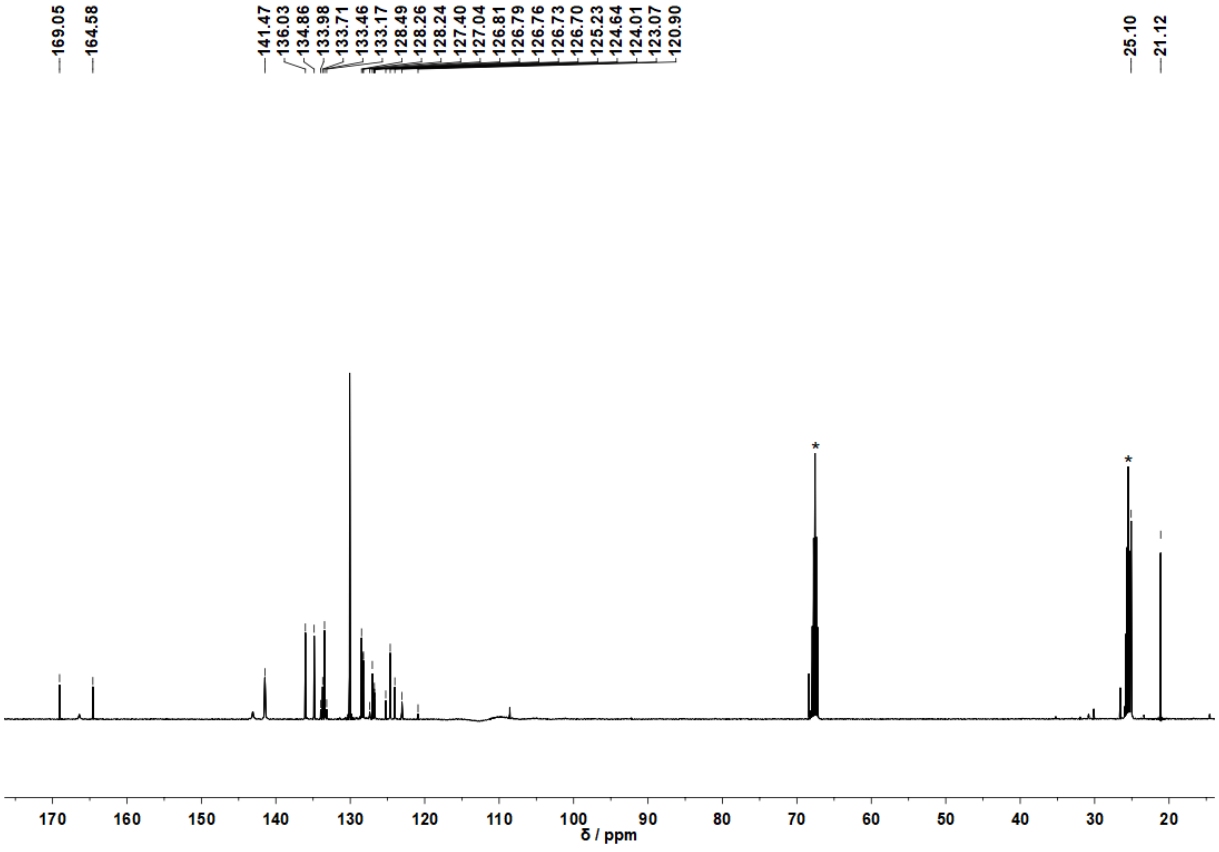

Figure S23. udeft-Spectrum of 4e in THF-d_8 (*).

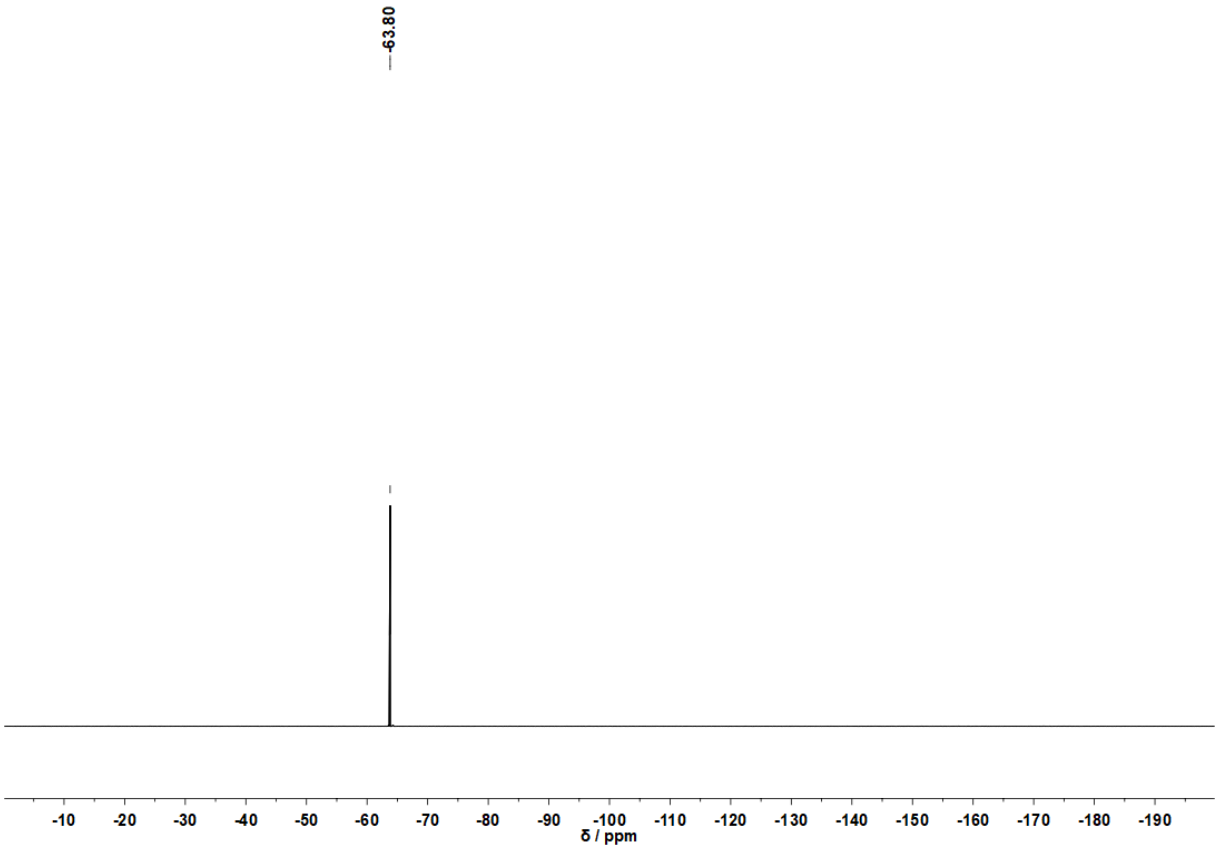

Figure S24. ^{19}F-NMR-Spectrum of 4e in THF-d_8.

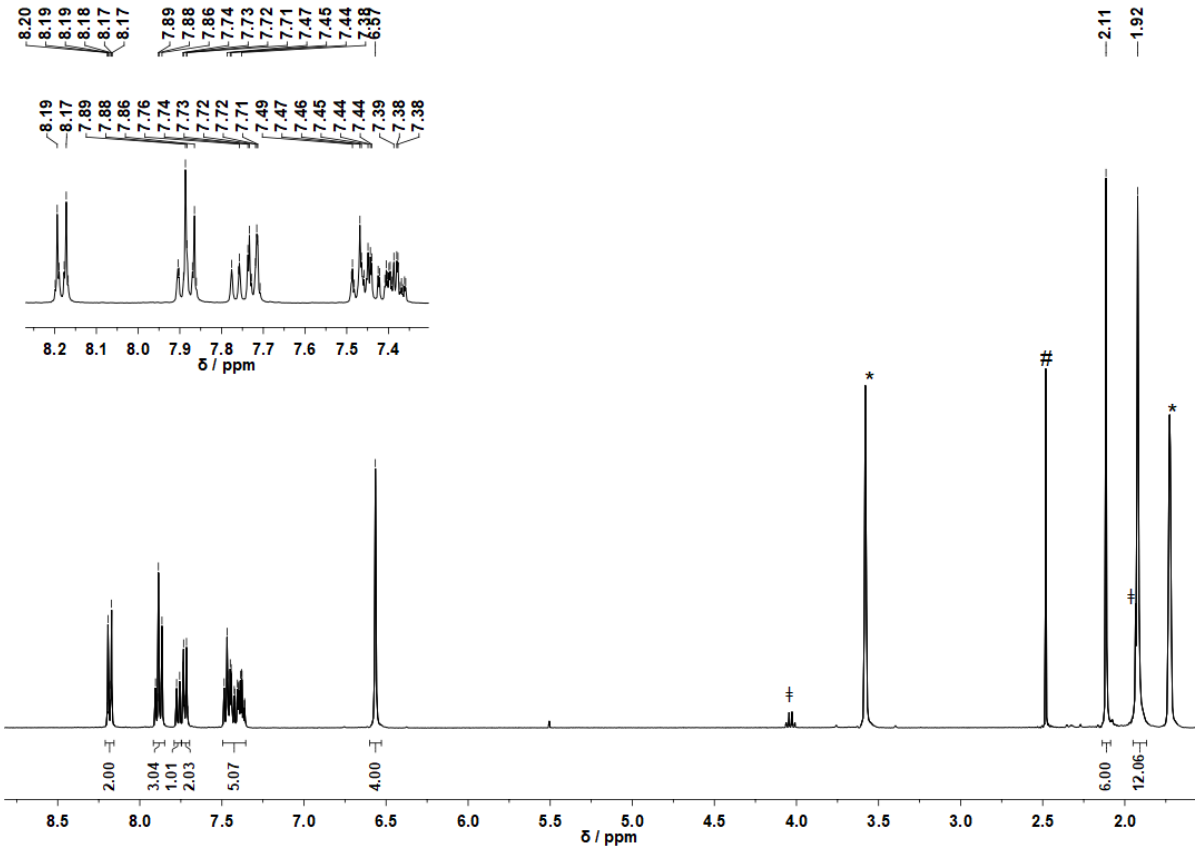

Figure S25. ^{1}H-NMR-Spectrum of 4f in THF-d_8 (*); H_2O (#); EtOAc (‡).

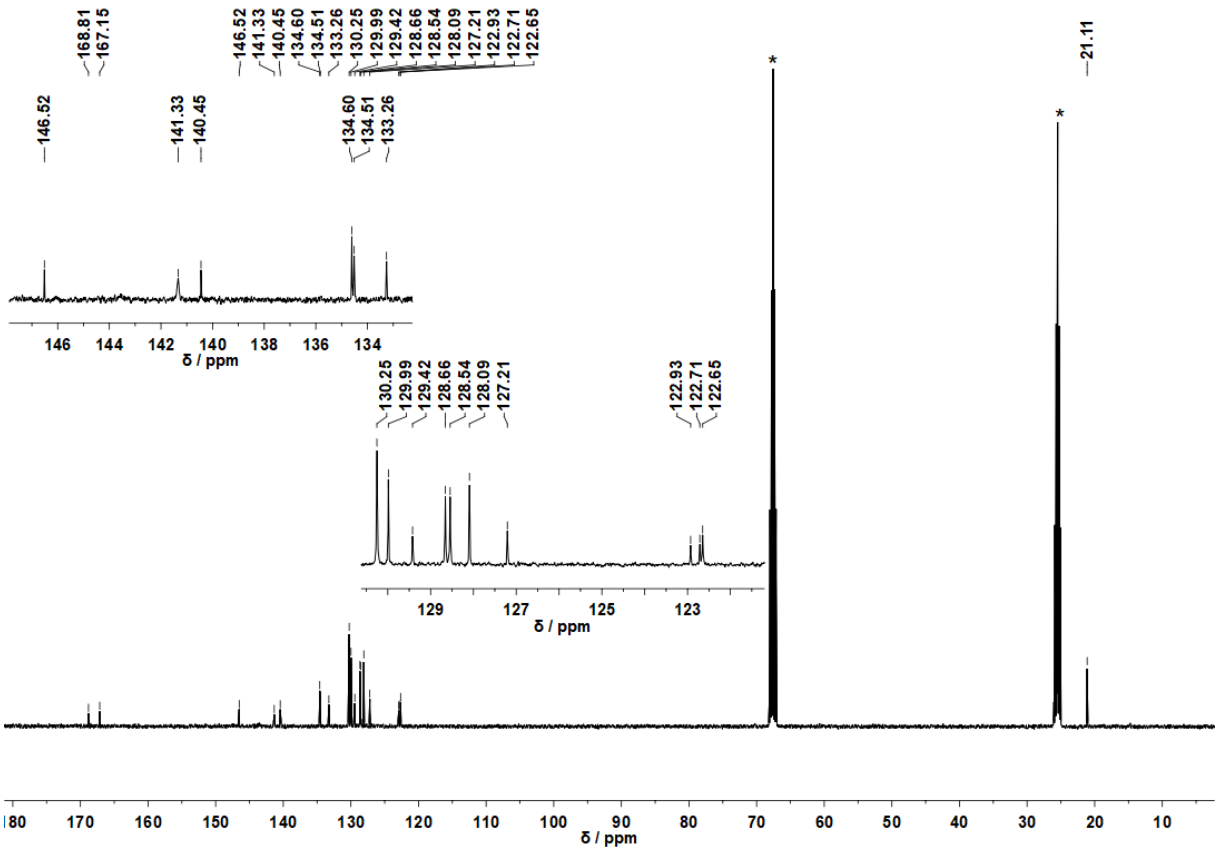

Figure S26. ^{13}C-NMR-Spectrum of 4f in THF-d_8 (*).

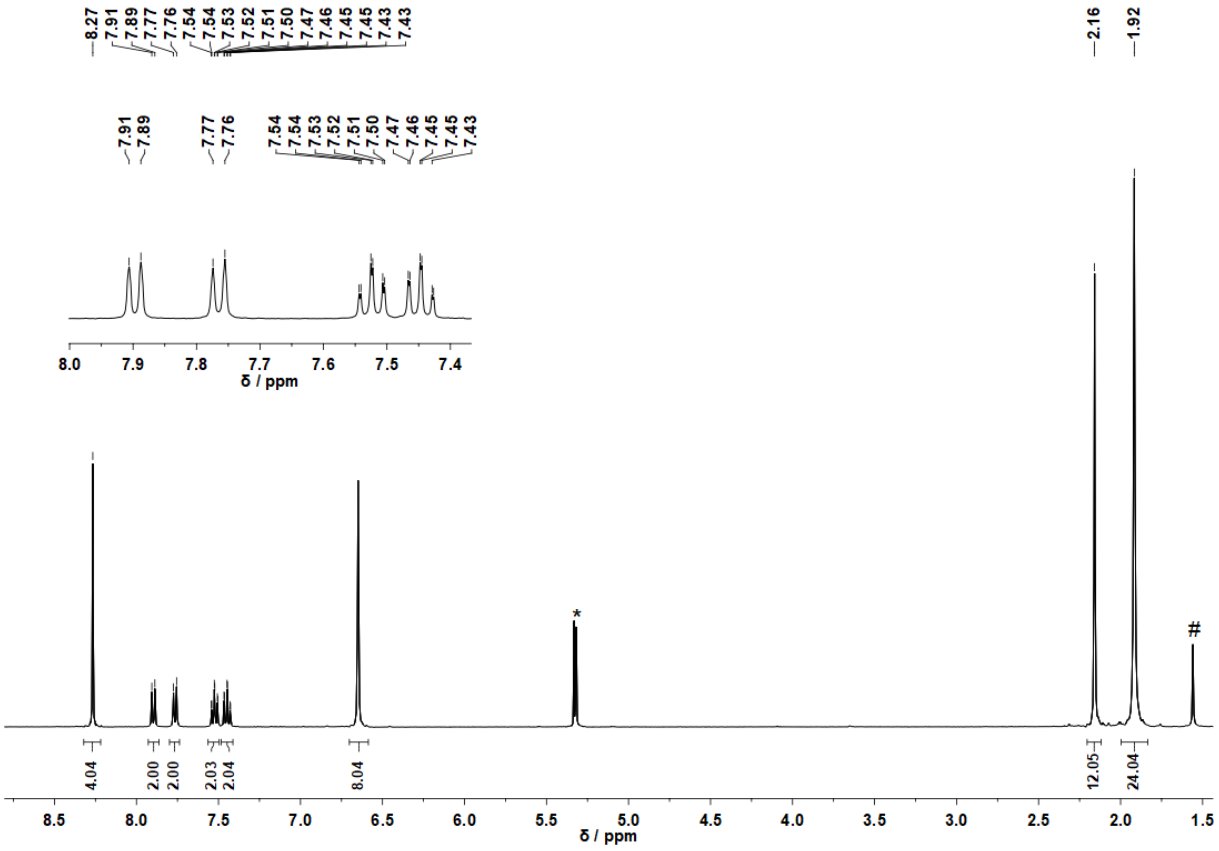

Figure S27. ^{1}H-NMR-Spectrum of 4g in CD_2Cl_2 (*); H_2O (#).

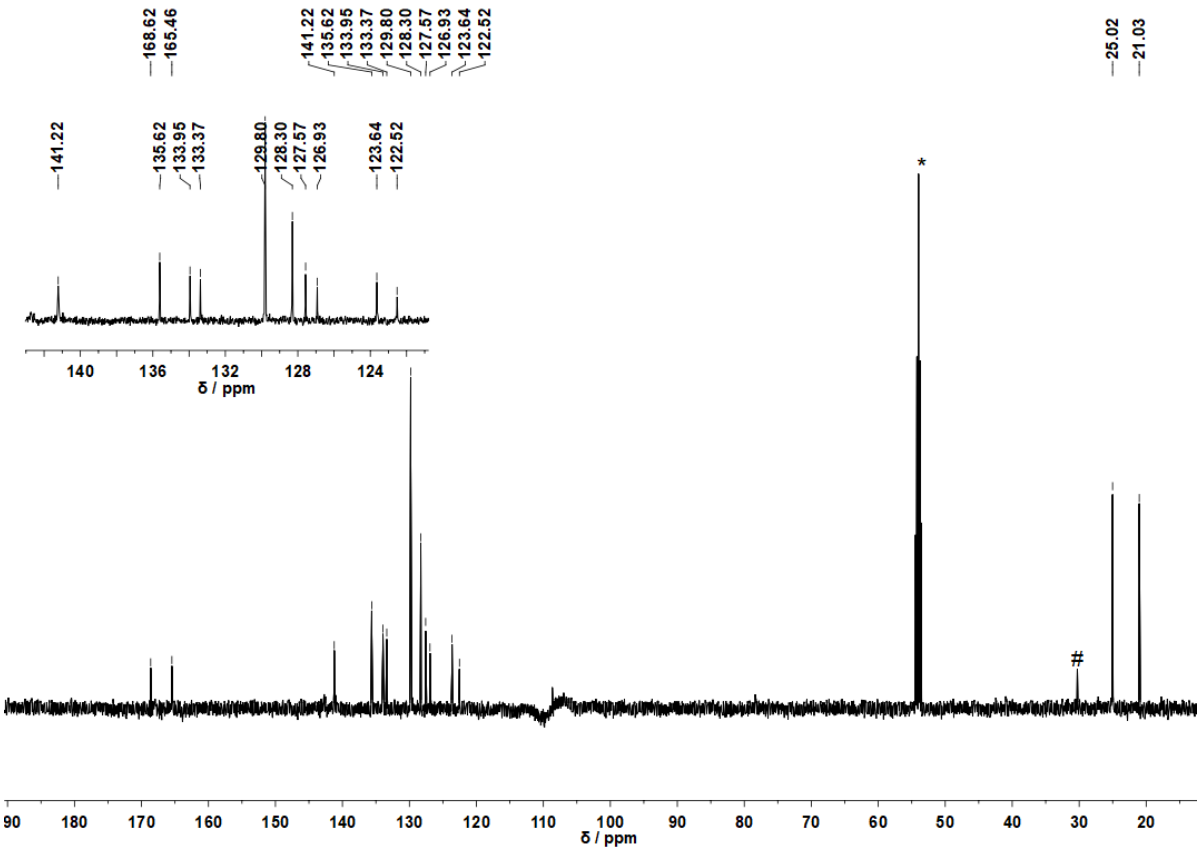

Figure S28. udeft-Spectrum of 4g in CD_2Cl_2 (*); grease (#).

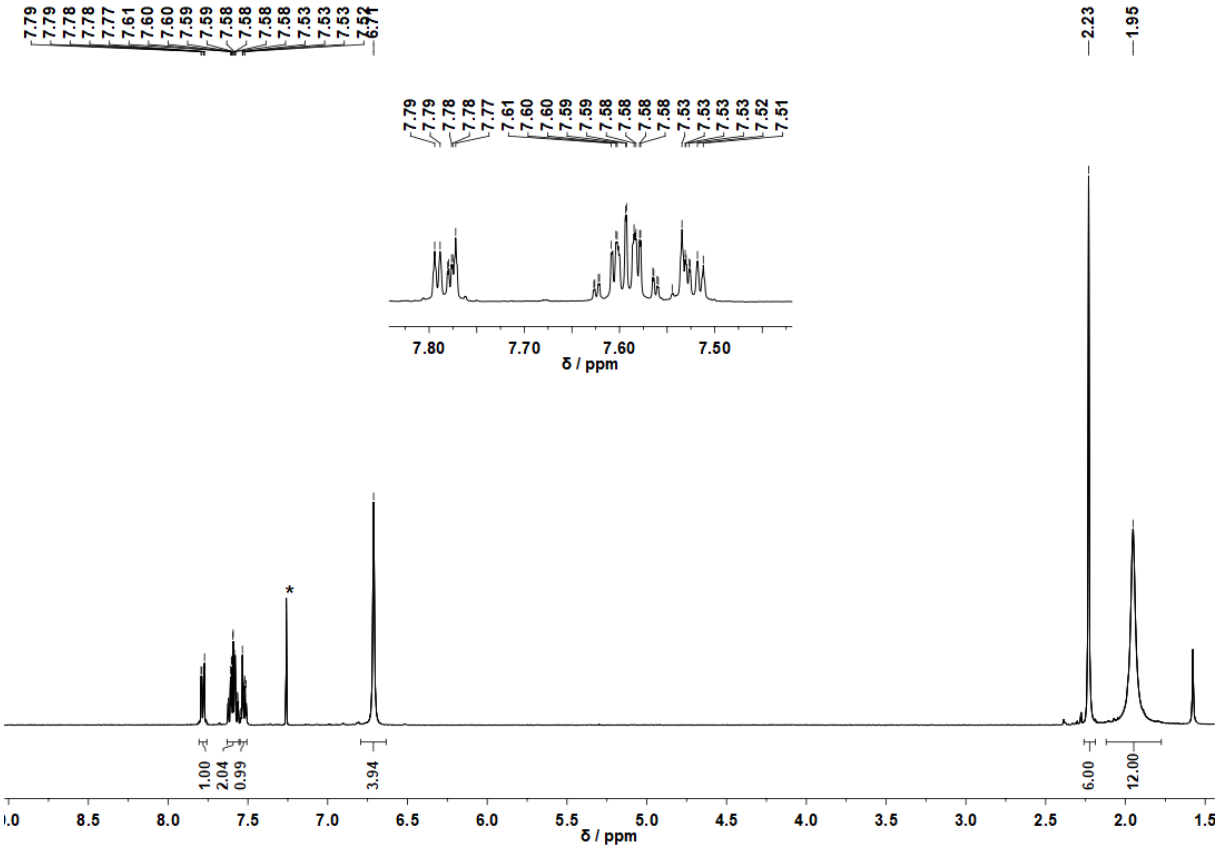

Figure S29. ^{1}H-NMR-Spectrum of 4h in $CDCl_3$ (*).

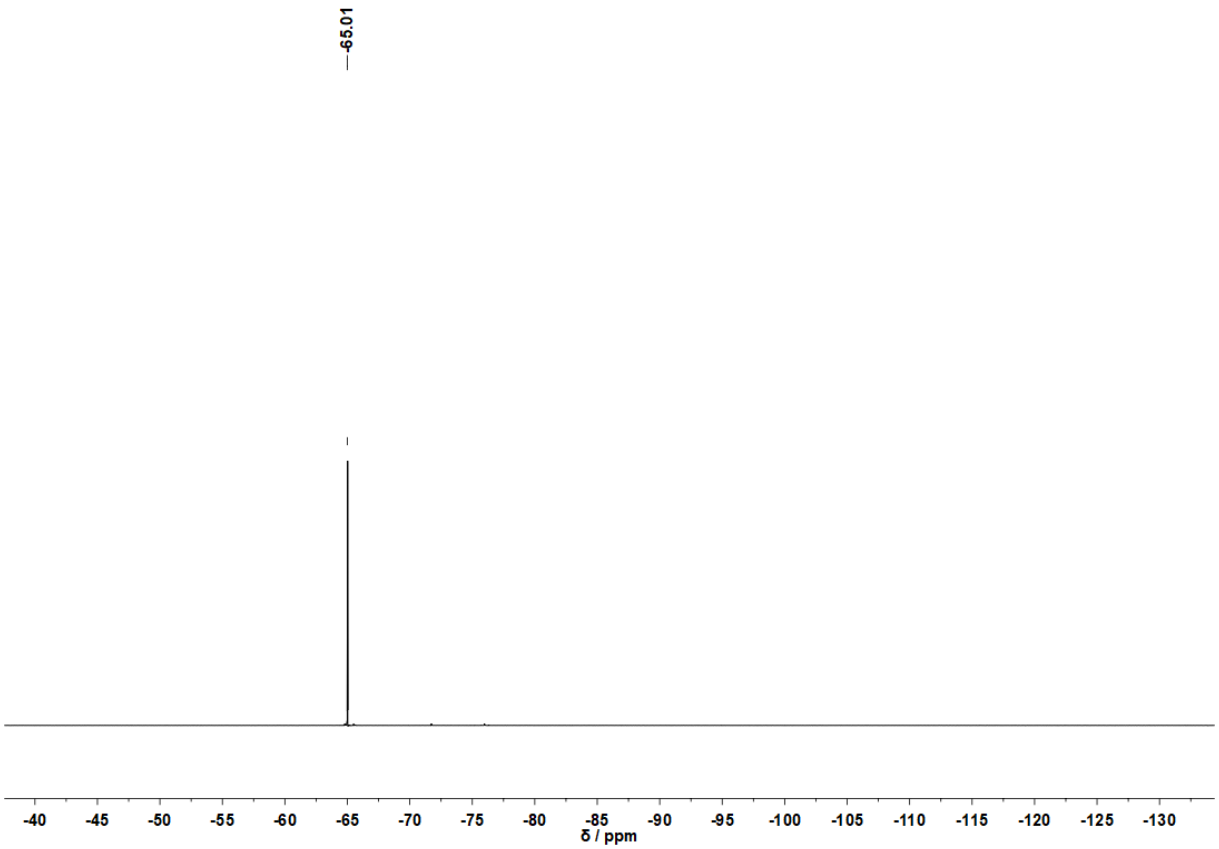

Figure S30. ^{19}F-NMR-Spectrum of 4h in $CDCl_3$.

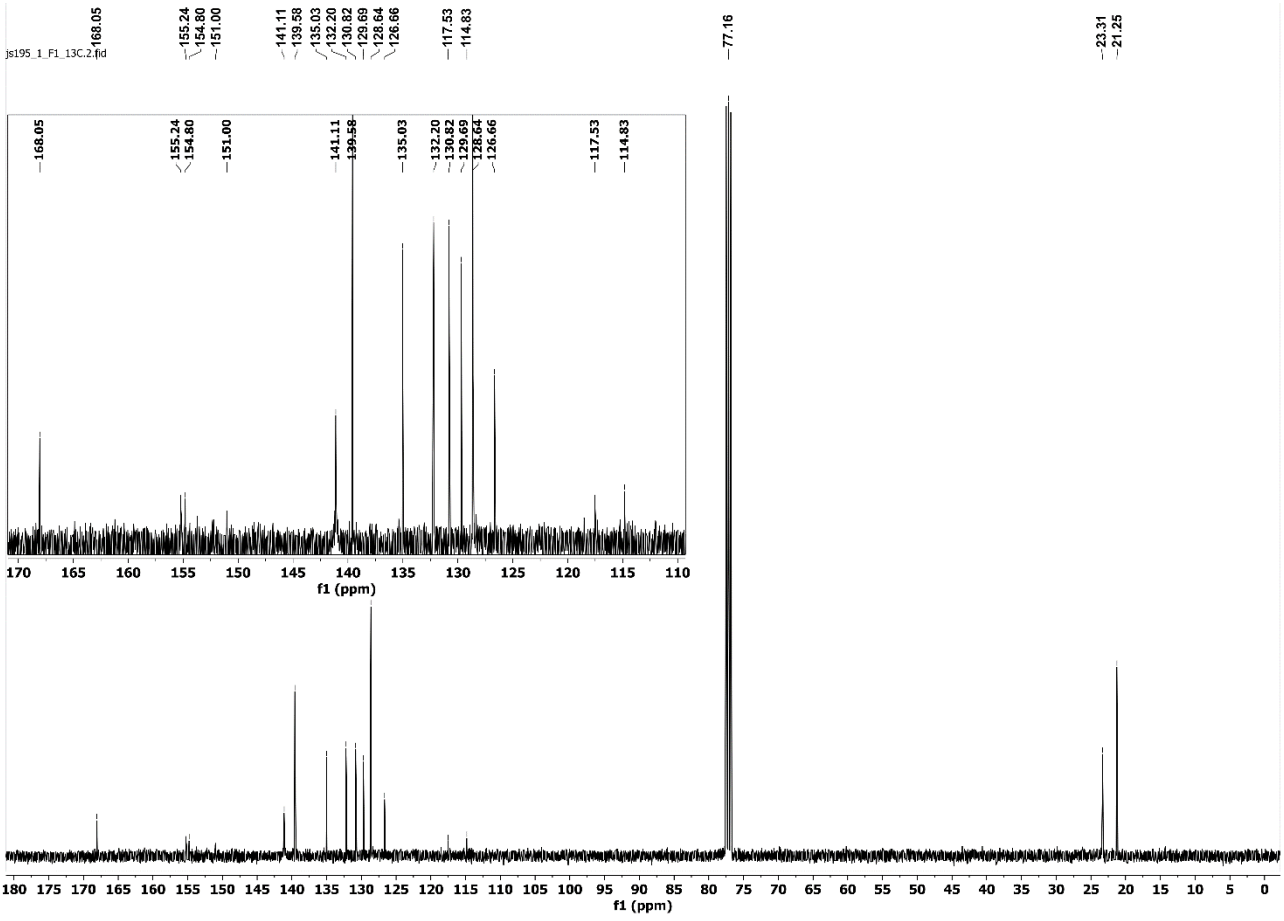

Figure S31. 13C-NMR-Spectrum of 4h in $CDCl_3$.

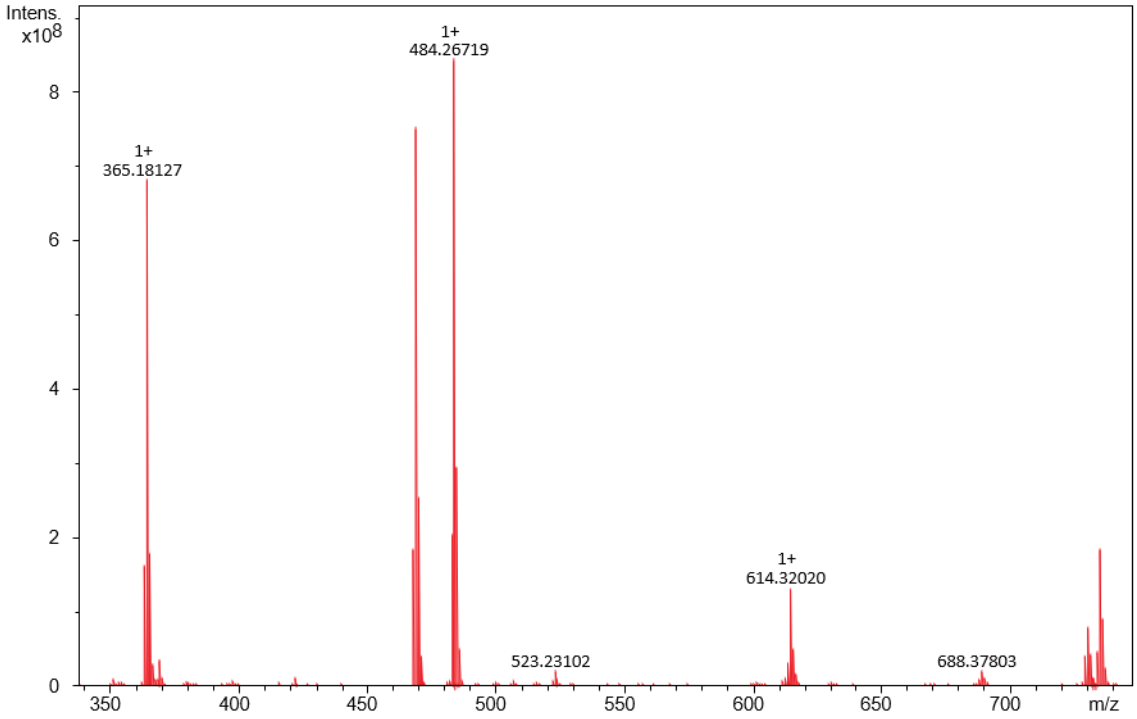

Figure S32. MALDI-MS-Spectrum of 4a; Matrix: DCTB.

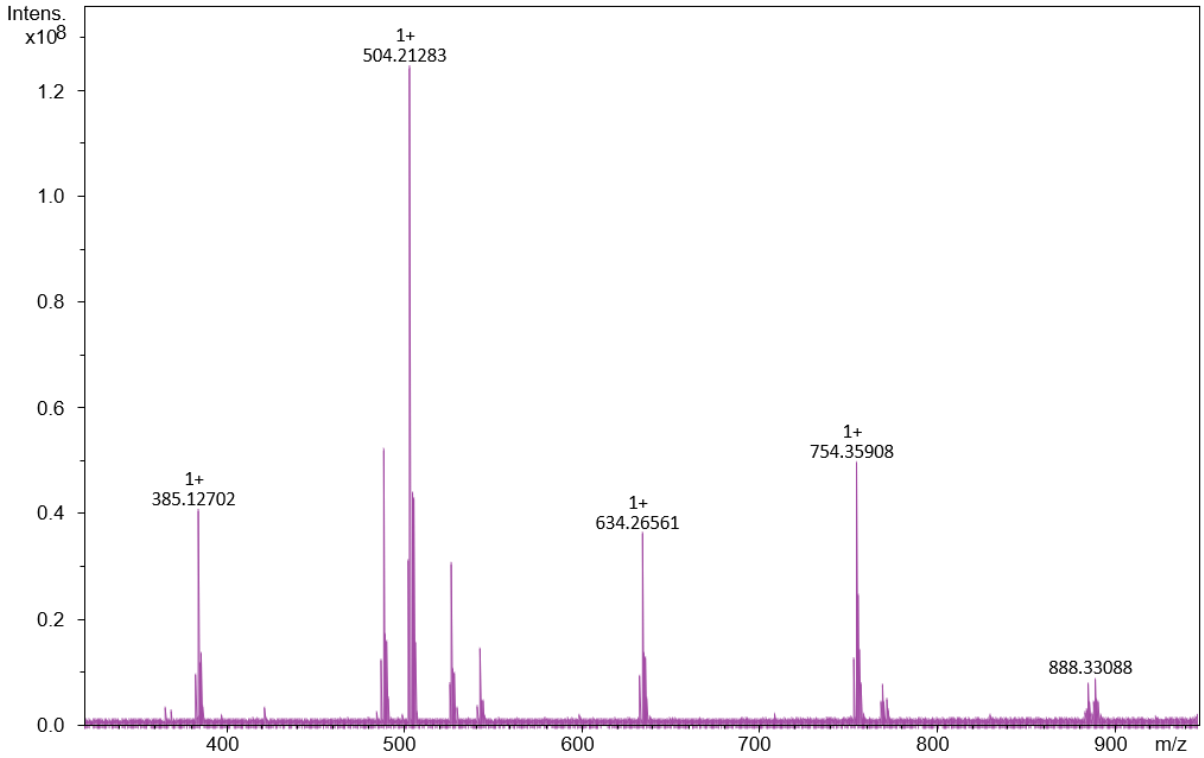

Figure S33. MALDI-MS-Spectrum of 4b; Matrix: DCTB.

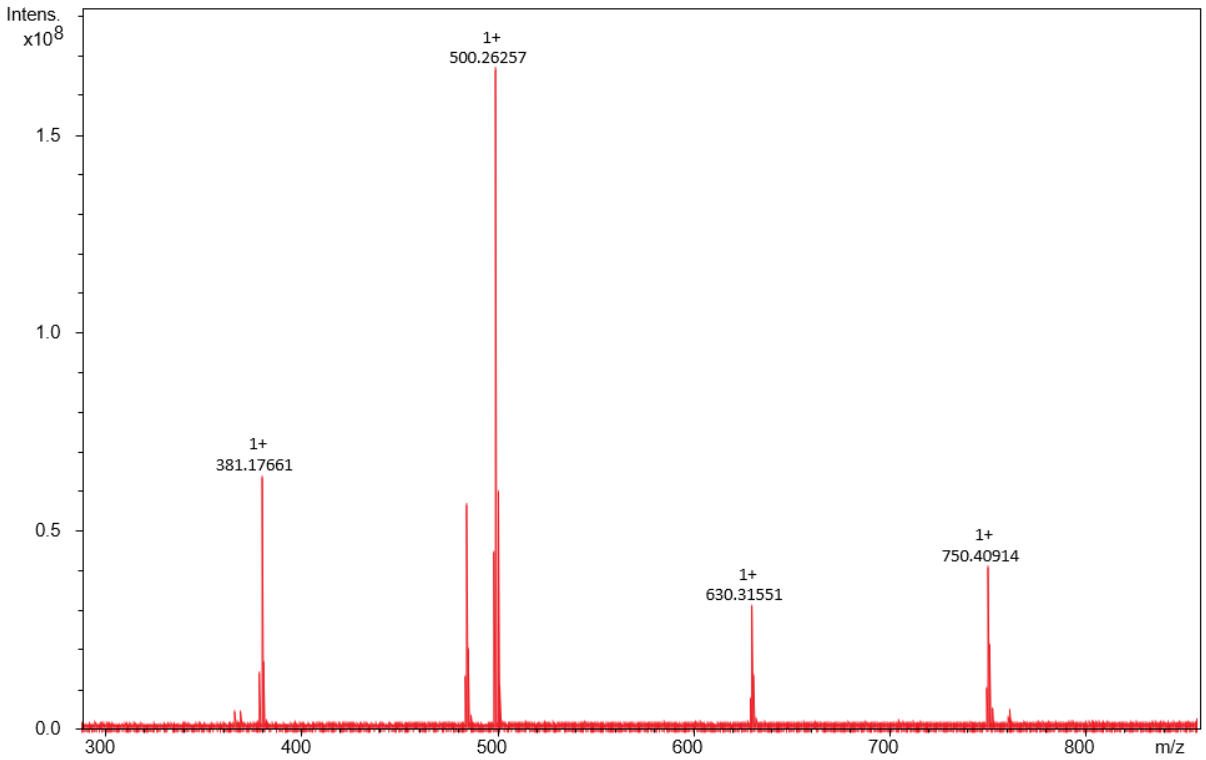

Figure S34. MALDI-MS-Spectrum of 4c; Matrix: DCTB.

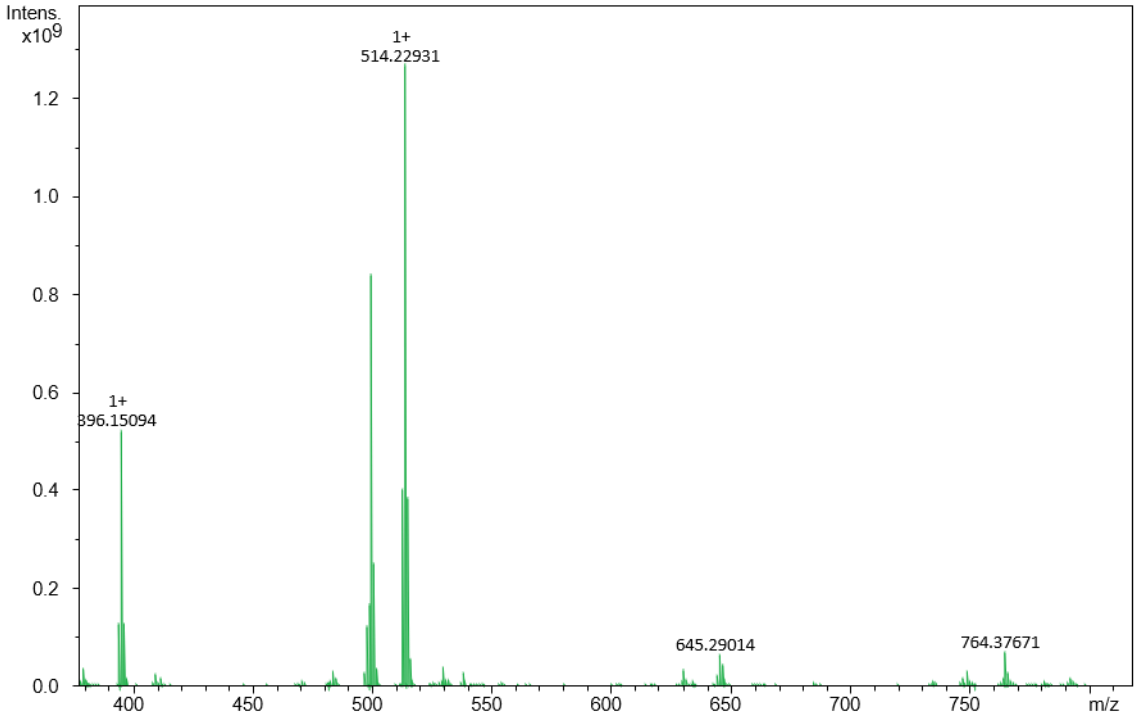

Figure S35. MALDI-MS-Spectrum of 4d; Matrix: DCTB.

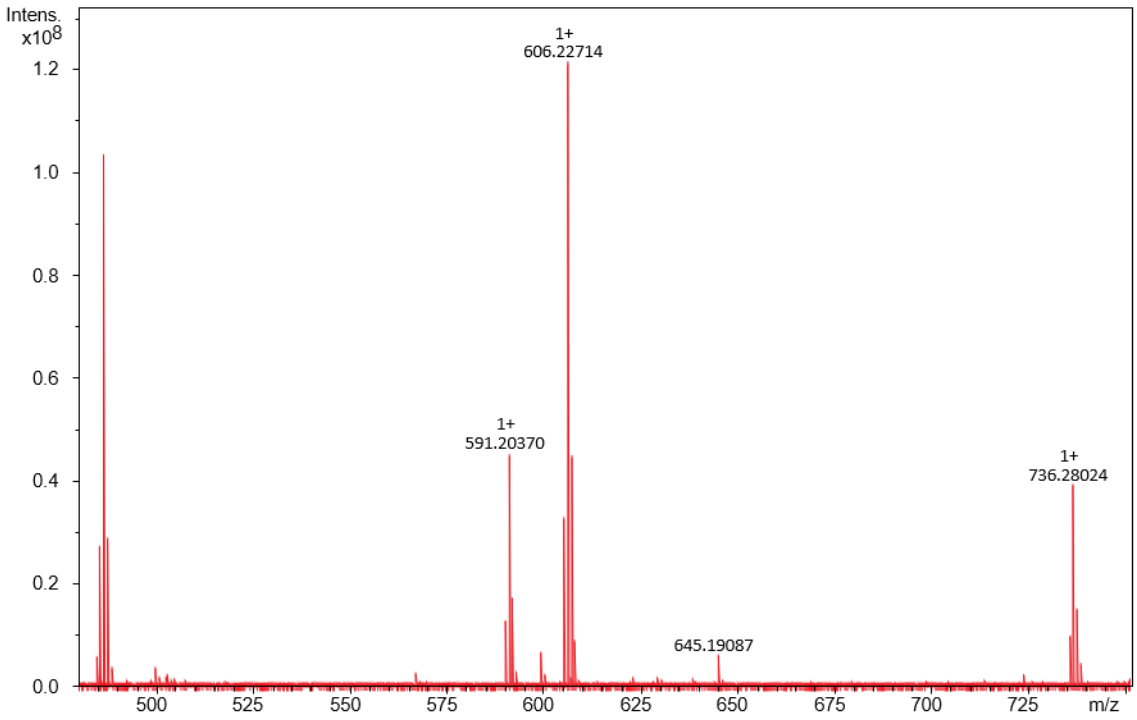

Figure S36. MALDI-MS-Spectrum of 4e; Matrix: DCTB.

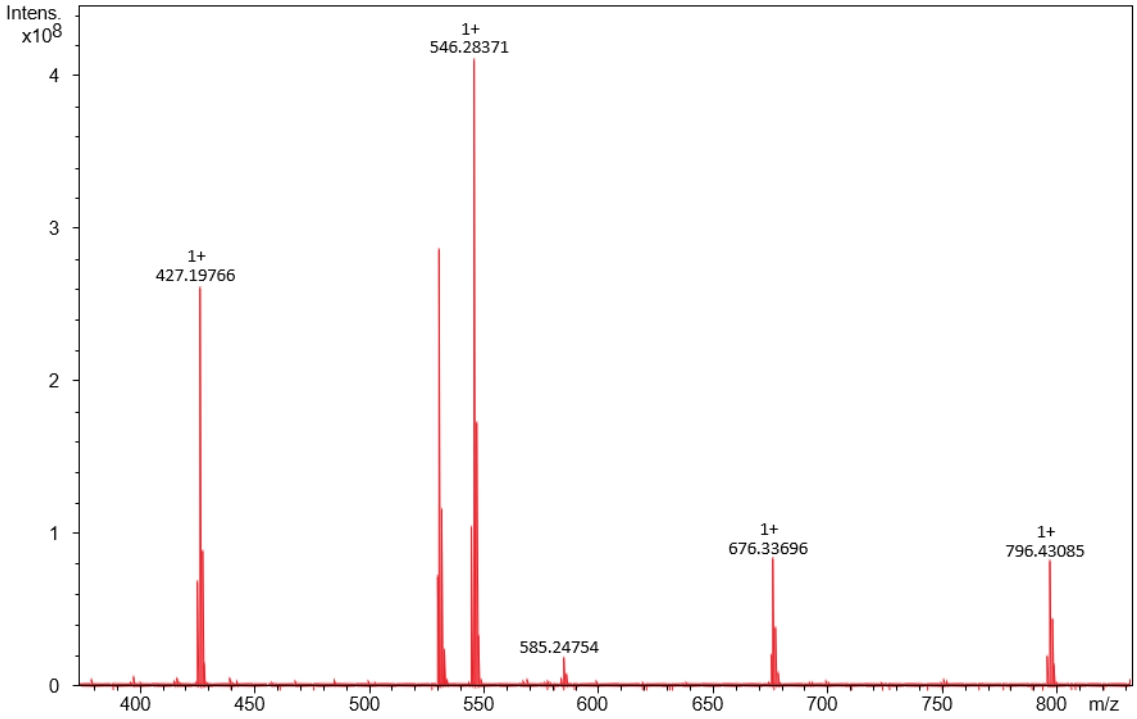

Figure S37. MALDI-MS-Spectrum of 4f; Matrix: DCTB.

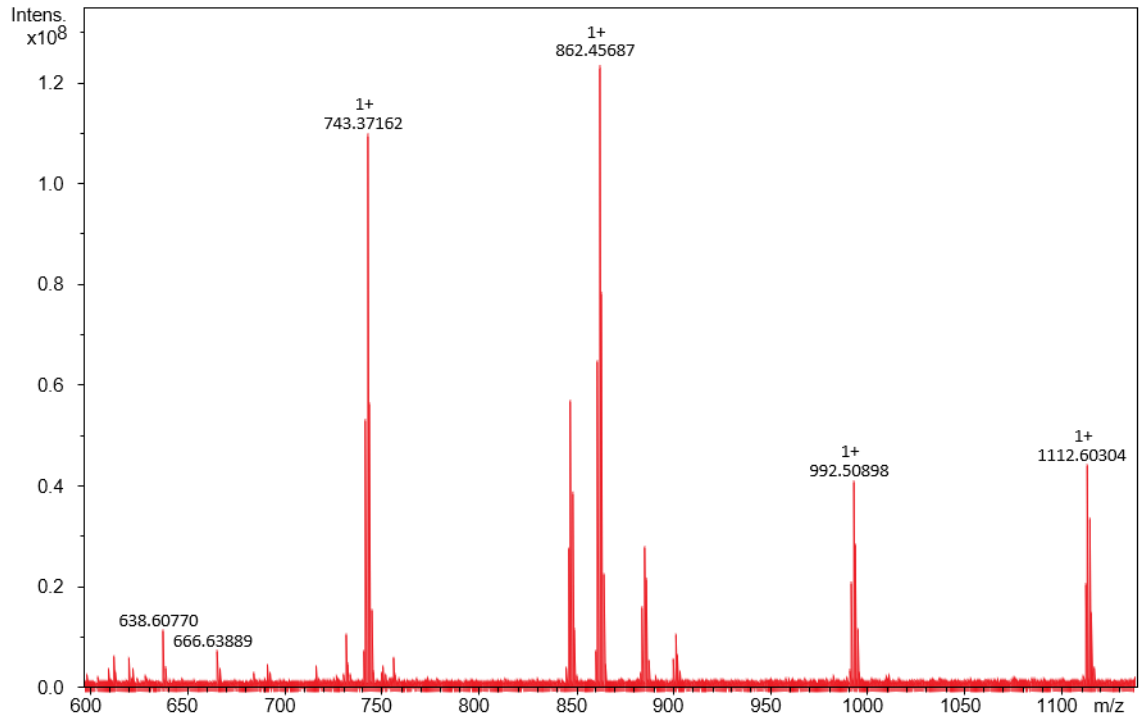

Figure S38. MALDI-MS-Spectrum of 4g; Matrix: DCTB.

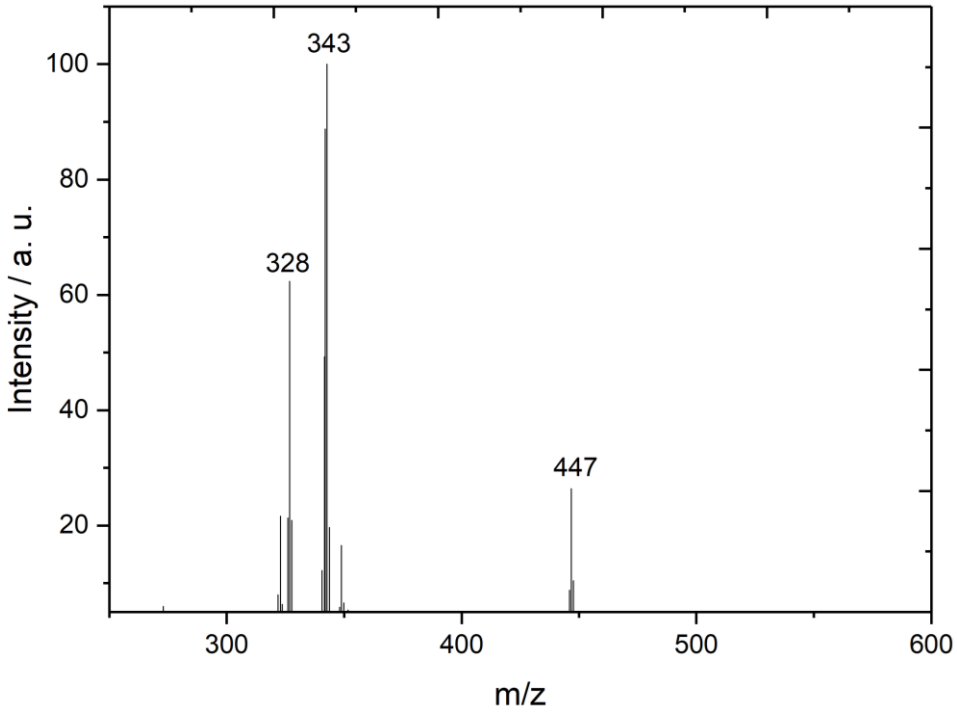

Figure S39. EI-MS-Spectrum of 4h.

2.5. Electrochemical Data

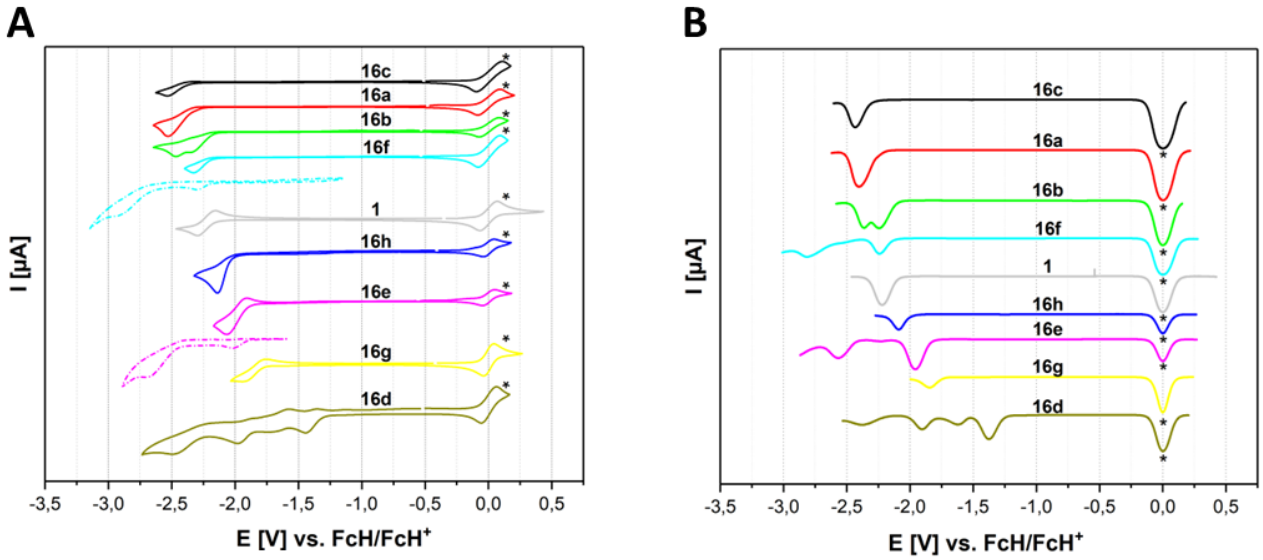

Figure S40. Cyclic voltammograms (A) and square wave voltammograms (B) of the oxadiazoles 4a - 4h in THF with 0.1 M $[NnBu_4][PF_6]$; Scan speeds: 200 mV/s (A) and 100 mV/s (B); * internal standard ferrocene.

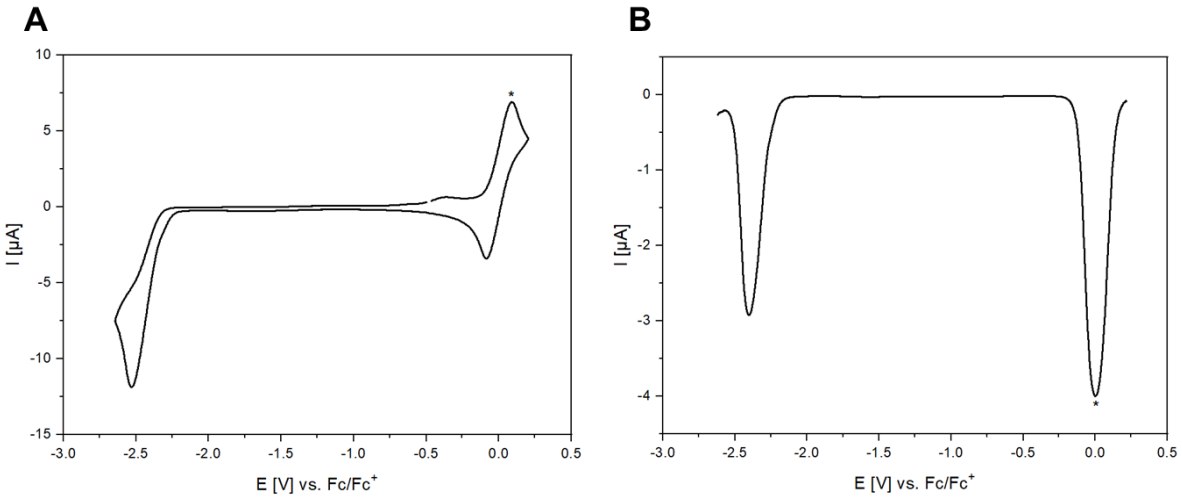

Figure S41. Cyclic voltammogramm (A) und Square-Wave voltammogramm (B) of compound 4a in THF mit 0.1 M $[NnBu_4][PF_6]$; Scanspeed: 100 mV/s; *internal standard ferrocene.

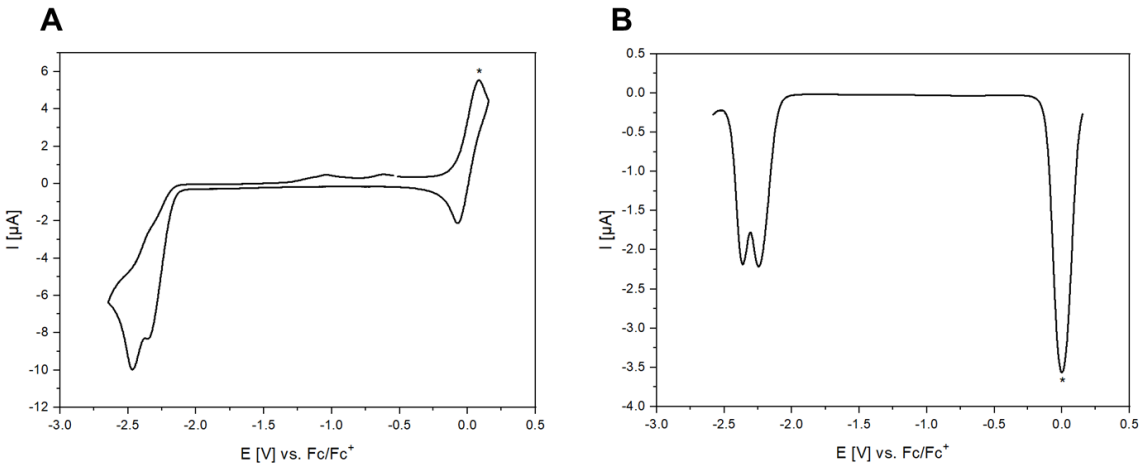

Figure S42. Cyclic voltammogramm (A) und Square-Wave voltammogramm (B) of compound 4b in THF mit 0.1 M [NnBu$_4$][PF$_6$]; Scanspeed: 100 mV/s; *internal standard ferrocene.

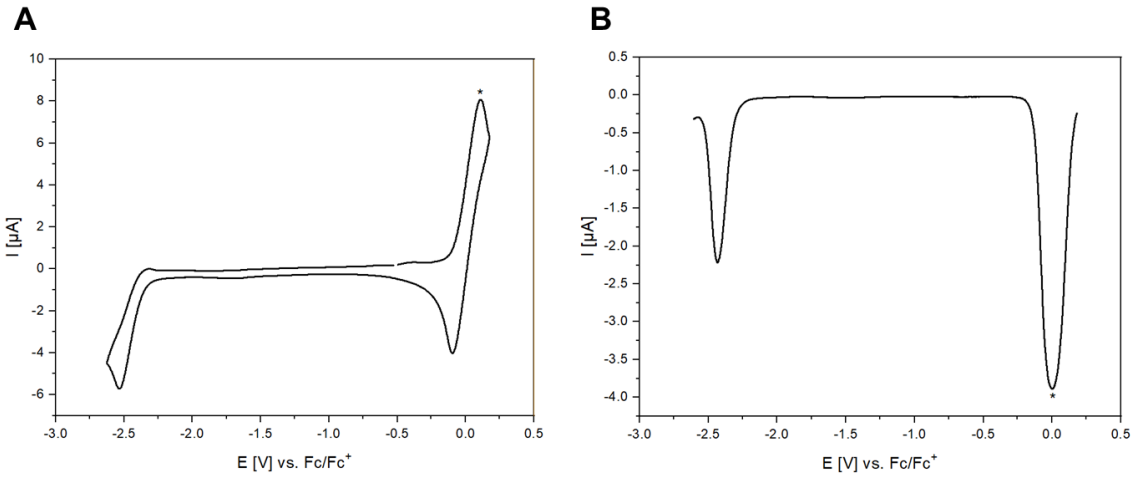

Figure S43. Cyclic voltammogramm (A) und Square-Wave voltammogramm (B) of compound 4c in THF mit 0.1 M [NnBu$_4$][PF$_6$]; Scanspeed: 100 mV/s; *internal standard ferrocene.

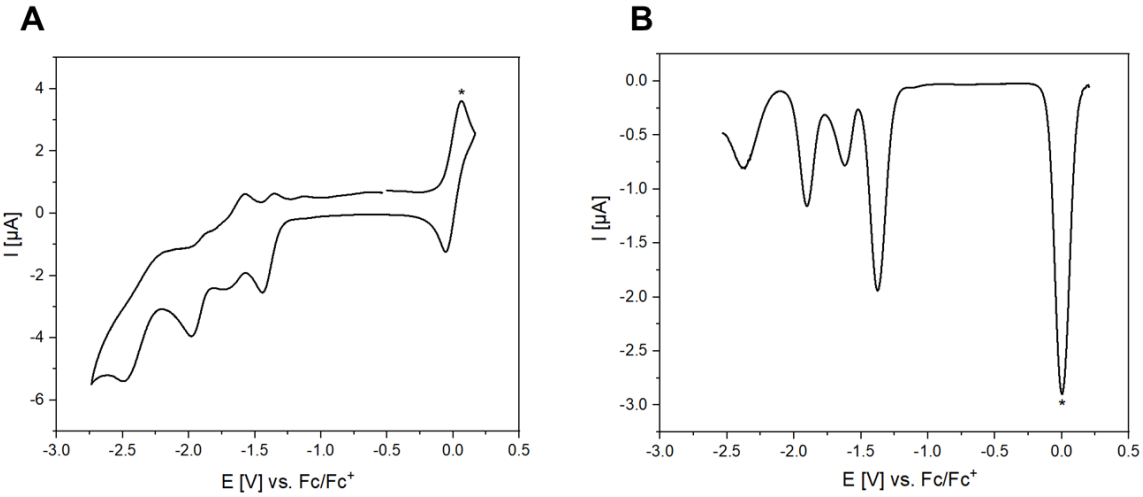

Figure S44. Cyclic voltammogramm (A) und Square-Wave voltammogramm (B) of compound 4d in THF mit 0.1 M [NnBu$_4$][PF$_6$]; Scanspeed: 100 mV/s; *internal standard ferrocene.

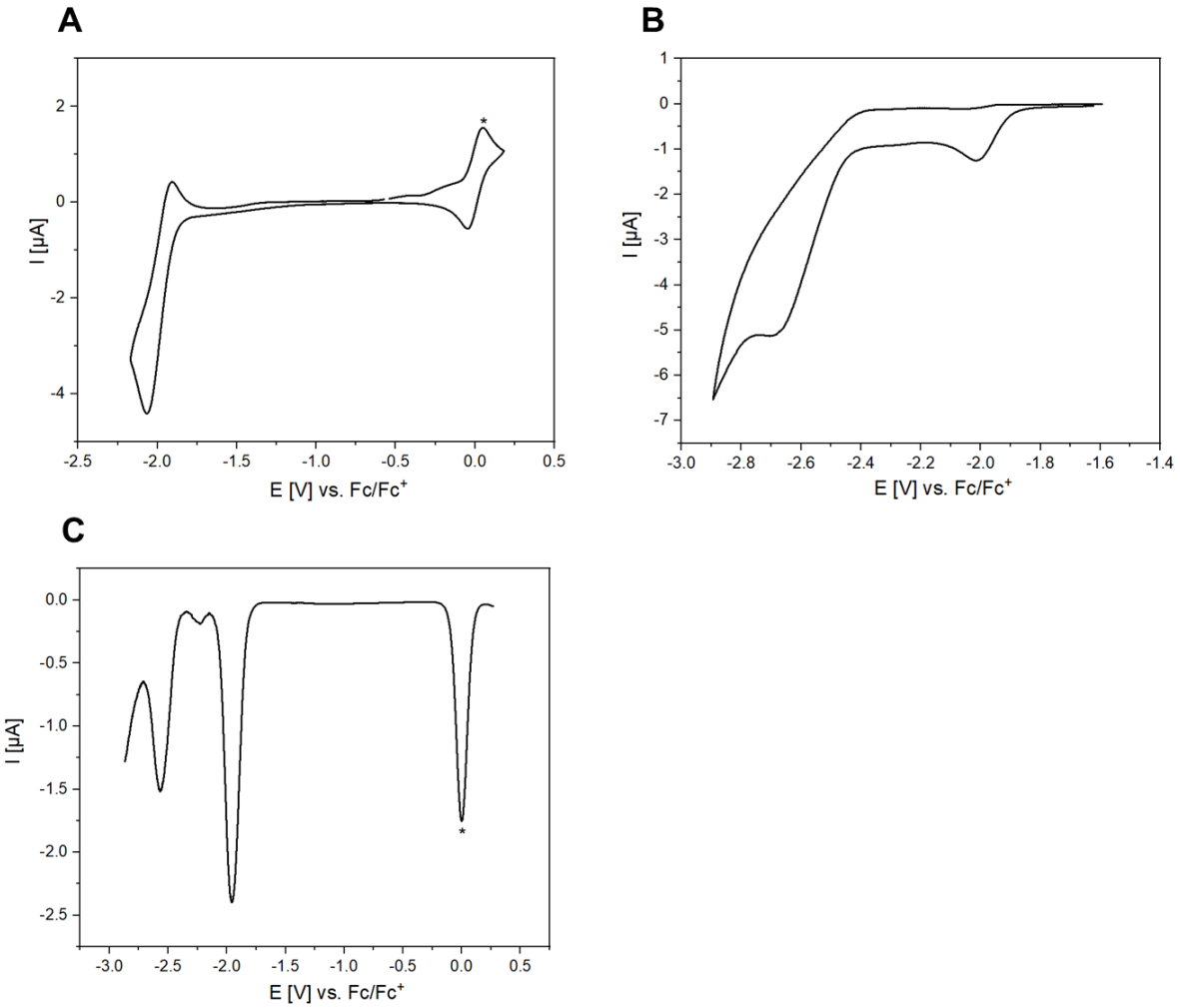

Figure S45. Cyclic voltammogramm (A, B) und Square-Wave voltammogramm (C) of compound 4e in THF mit 0.1 M [NnBu$_4$][PF$_6$]; Scanspeed: 100 mV/s; *internal standard ferrocene.

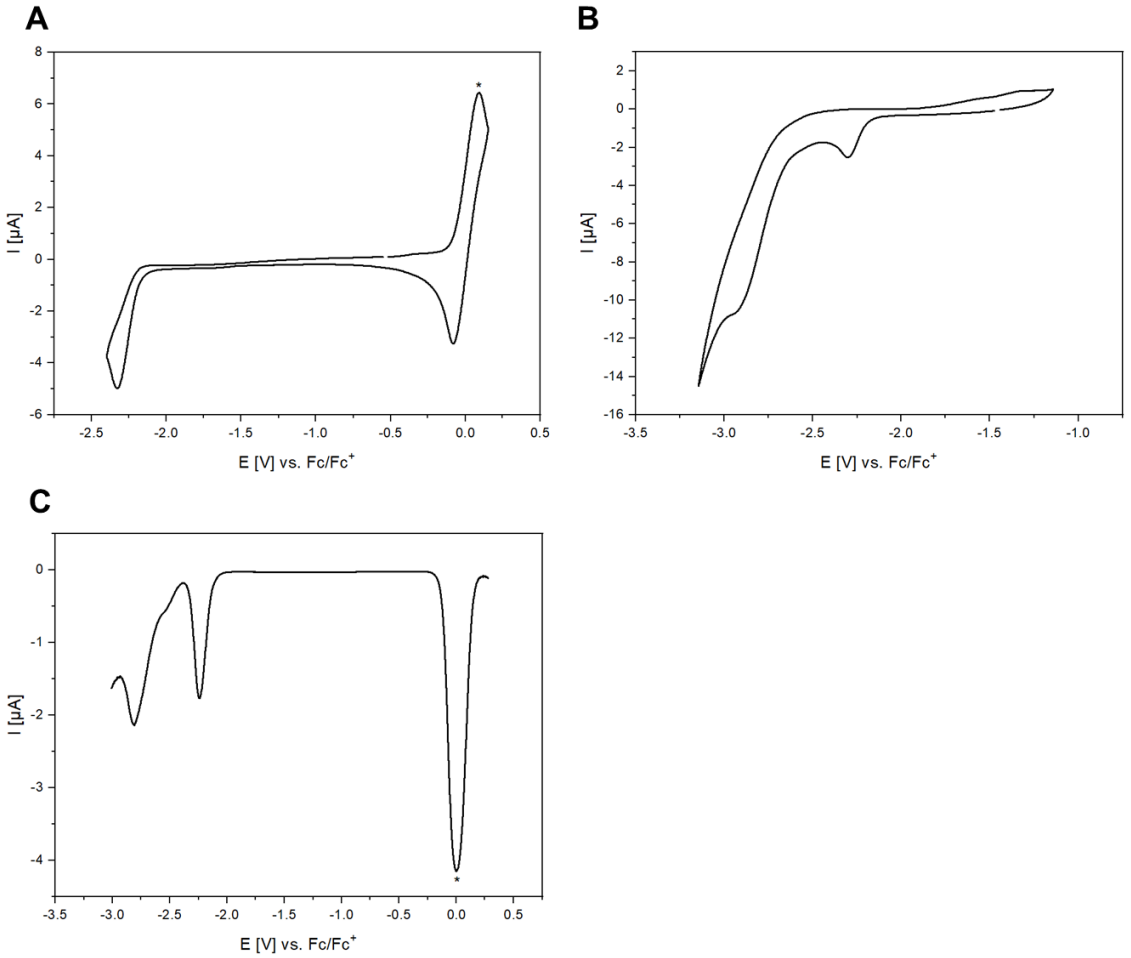

Figure S46. Cyclic voltammogramm (A, B) und Square-Wave voltammogramm (C) of compound 4f in THF mit 0.1 M [NnBu$_4$][PF$_6$]; Scanspeed: 100 mV/s; *internal standard ferrocene.

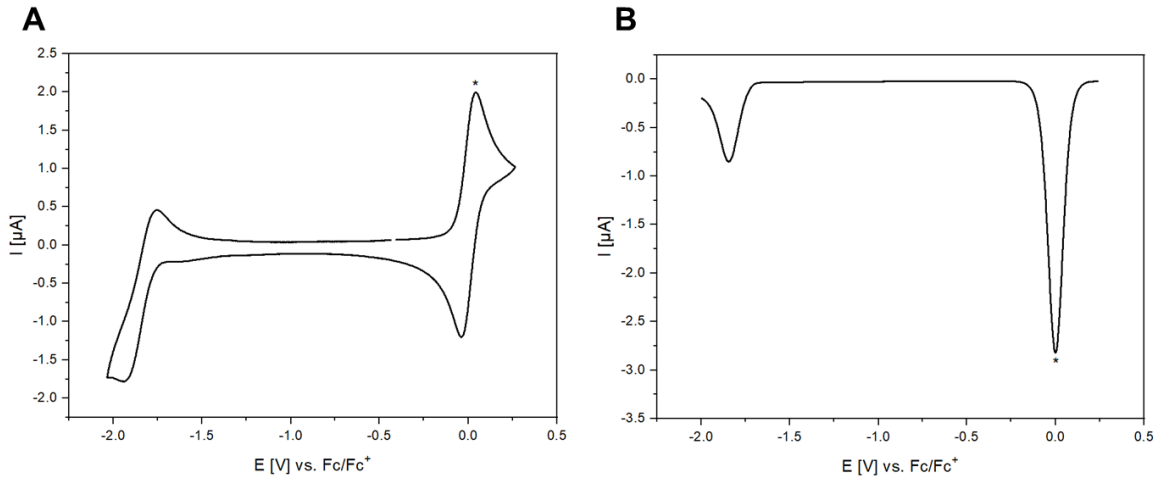

Figure S47. Cyclic voltammogramm (A) und Square-Wave voltammogramm (B) of compound 4g in THF mit 0.1 M [NnBu$_4$][PF$_6$]; Scanspeed: 100 mV/s; *internal standard ferrocene.

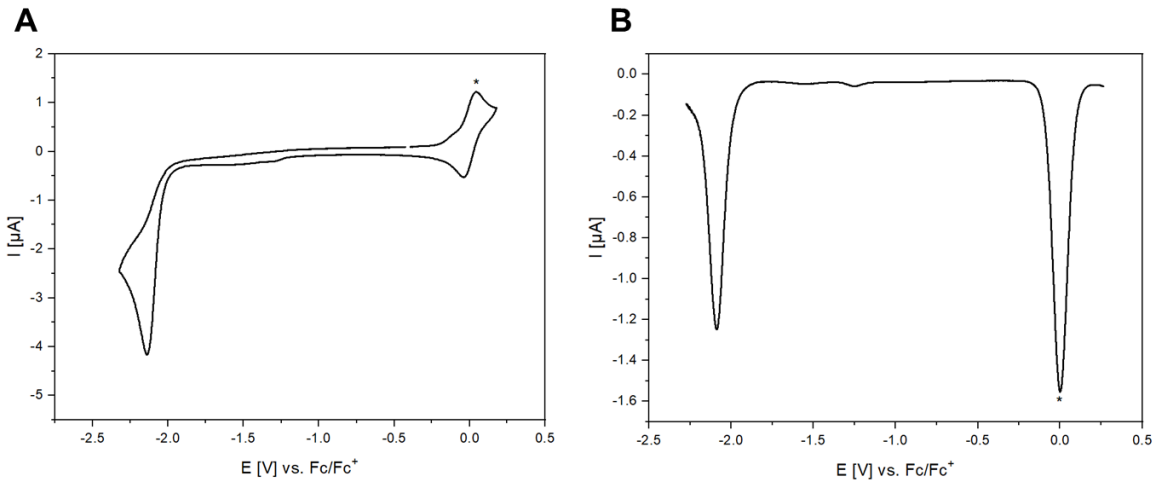

Figure S48. Cyclic voltammogramm (A) und Square-Wave voltammogramm (B) of compound 4h in THF mit 0.1 M [NnBu$_4$][PF$_6$]; Scanspeed: 100 mV/s; *internal standard ferrocene.

2.6. Computational Study

2.6.1. Frontier Orbital Plots

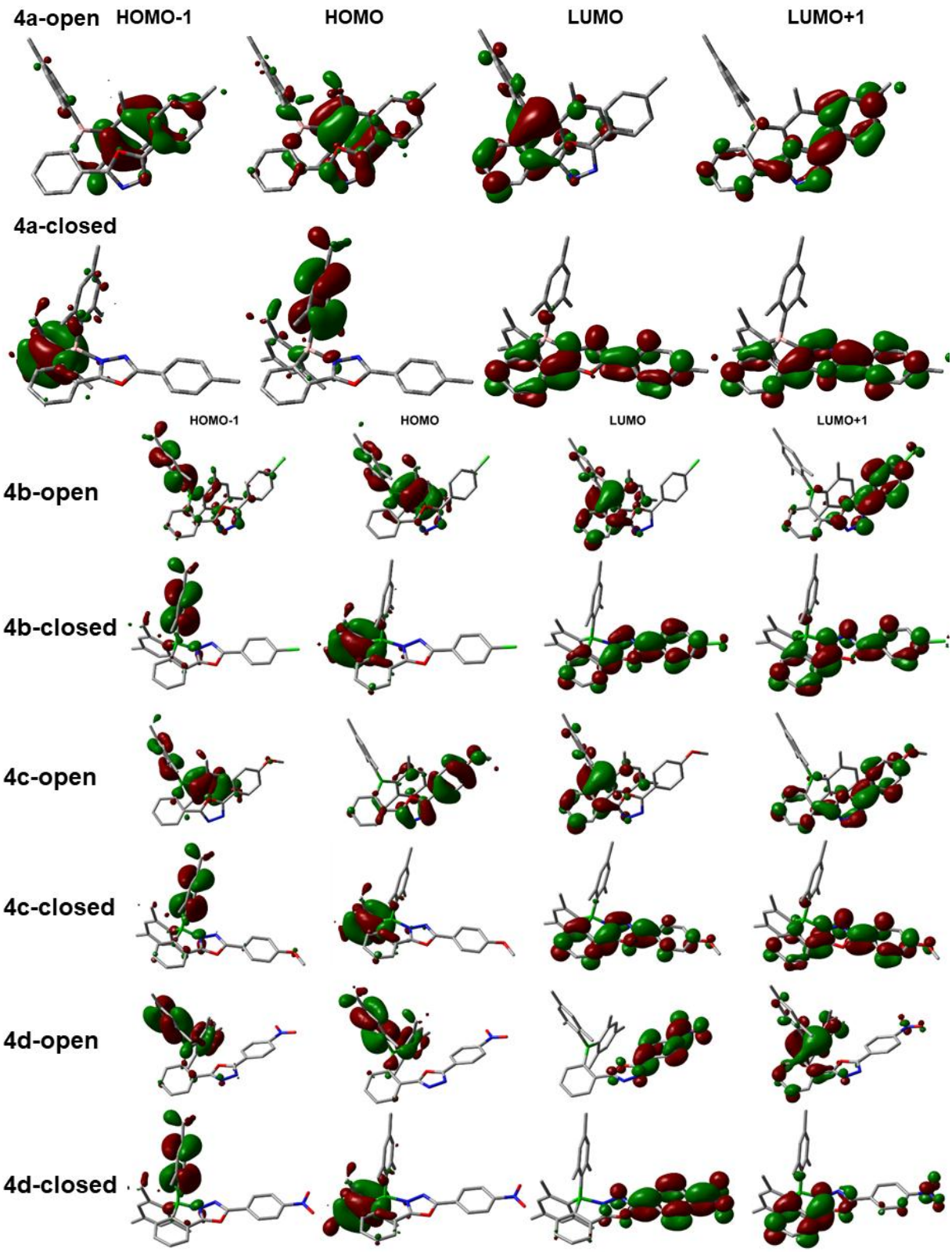

Figure S49. Kohn-Sham-Frontier orbitals of *open* and *closed* conformers of compounds 4a-4d; Plots generated with GaussView 6.0. Iso-value 0.035.

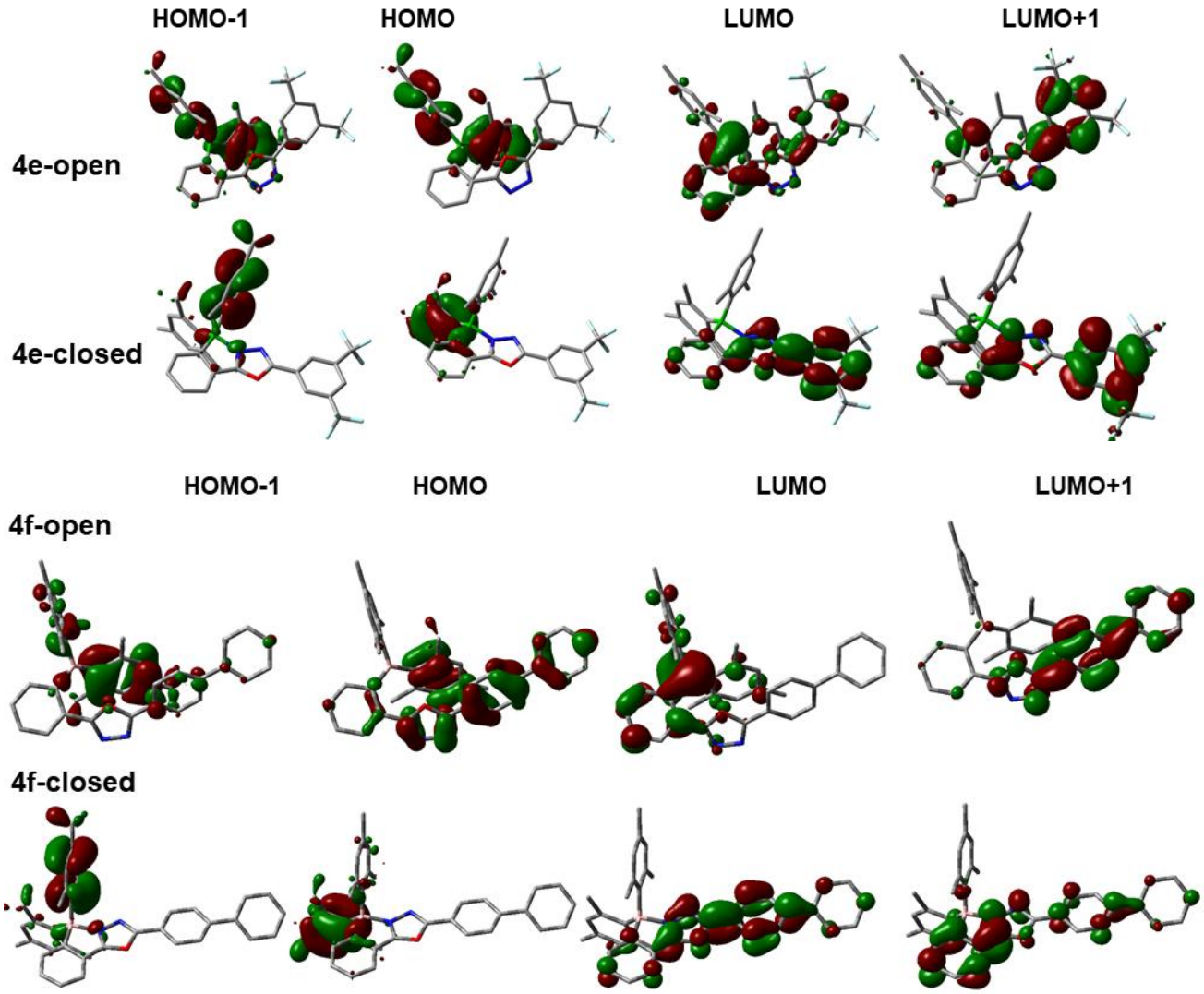

Figure S50. Kohn-Sham-Frontier orbitals of *open* and *closed* conformers of compounds 4e, 4f; Plots generated with GaussView 6.0. Iso-value 0.035.

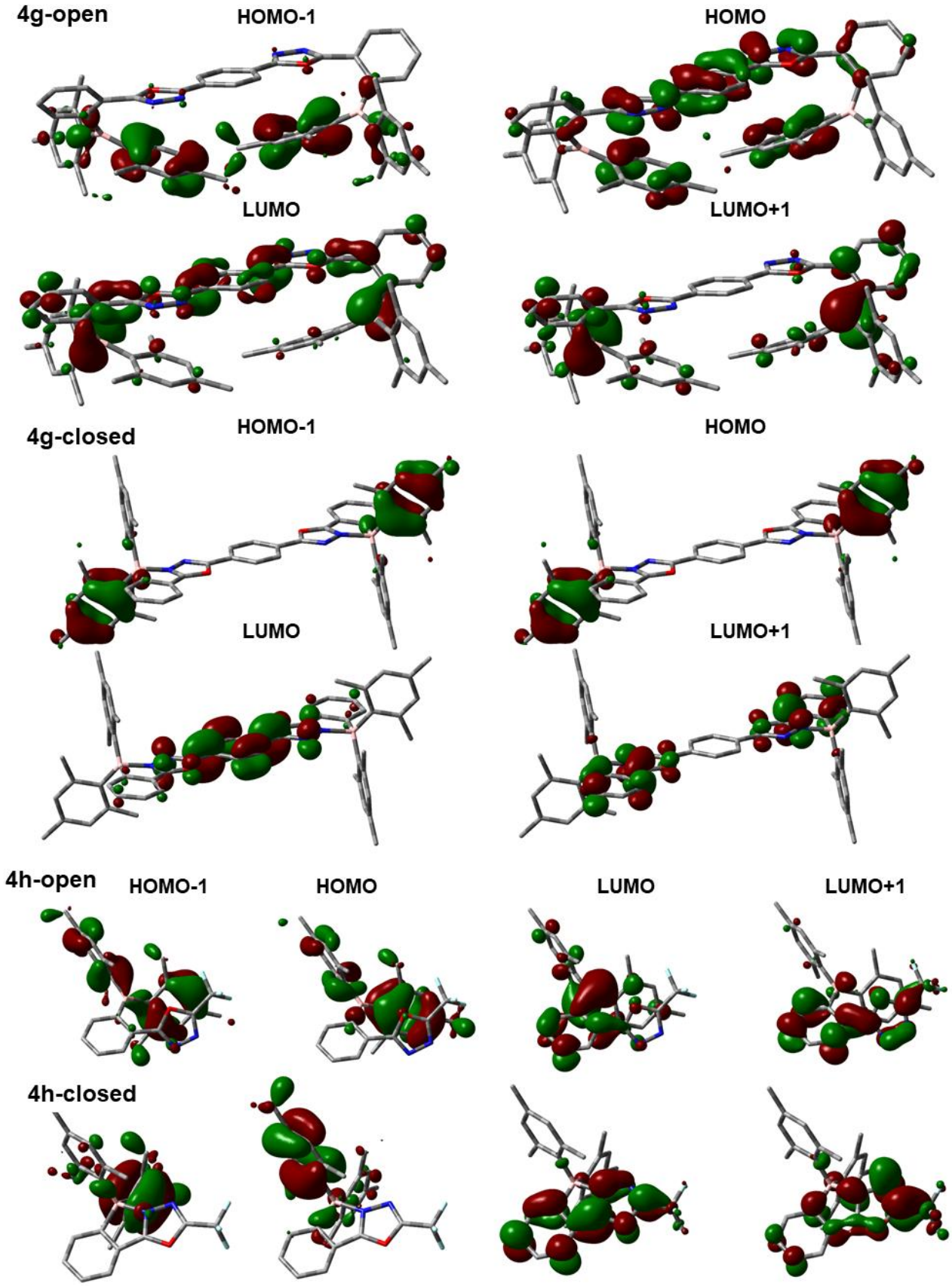

Figure S51. Kohn-Sham-Frontier orbitals of *open* and *closed* conformers of compounds 4g-4h; Plots generated with GaussView 6.0. Iso-value 0.035.

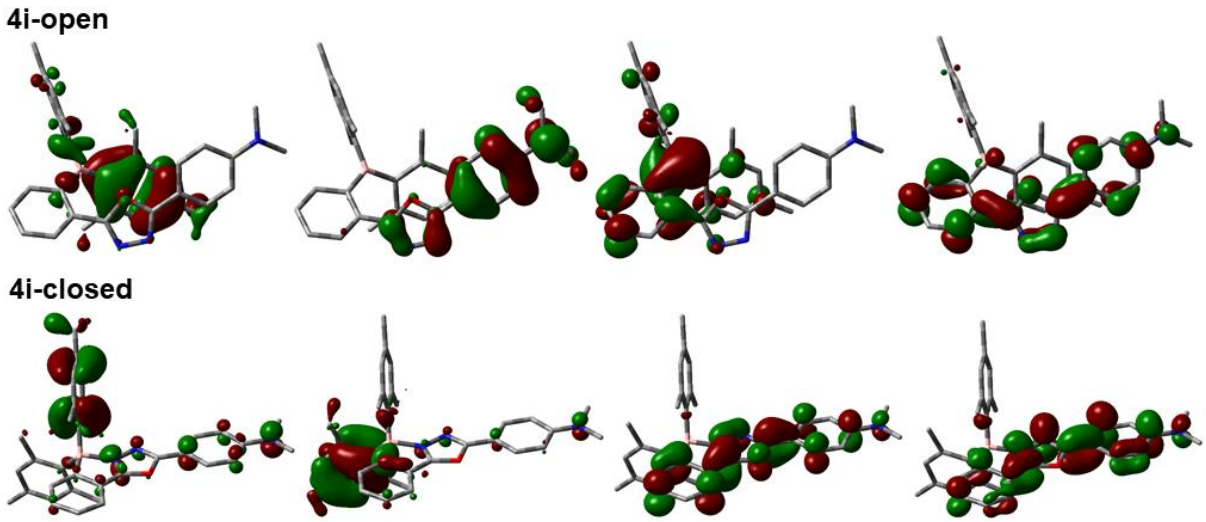

Figure S52. Kohn-Sham-Frontier orbitals of *open* and *closed* conformers of compound 4i; Plots generated with GaussView 6.0. Iso-value 0.035.

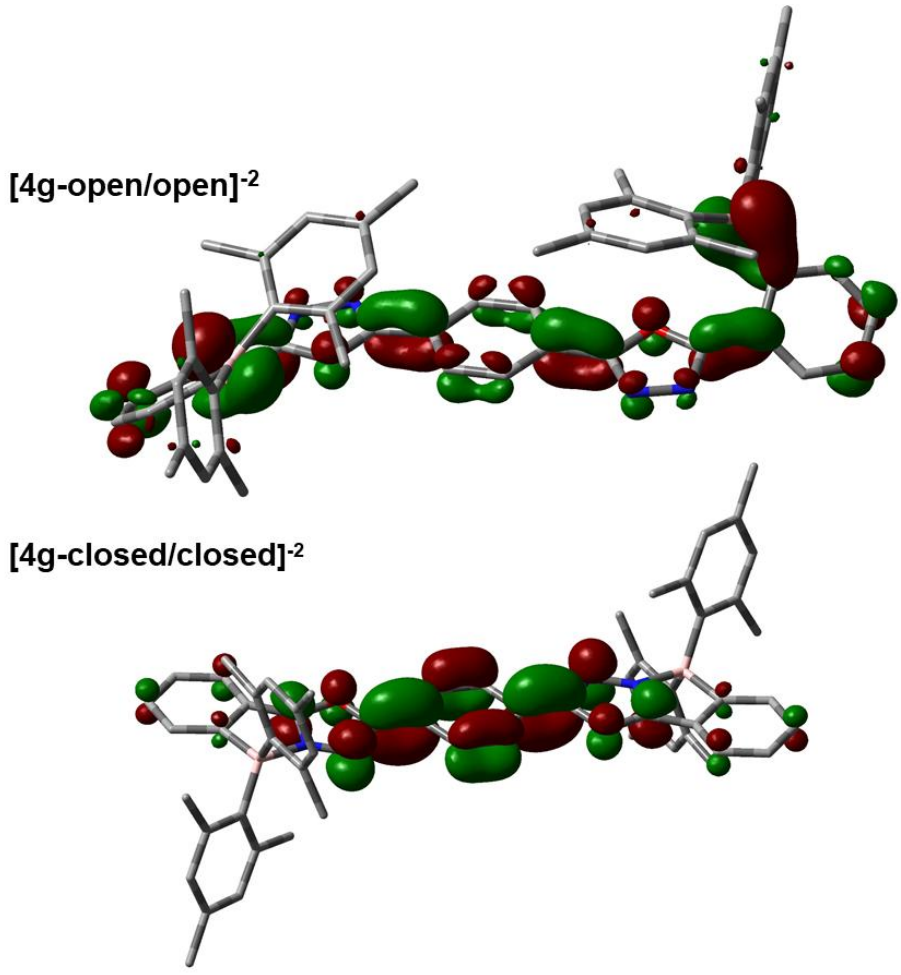

Figure S53. Kohn-Sham-Frontier orbitals of *open/open*$^{-2}$ and *closed/closed*$^{-2}$ conformers of compounds 4g; Plots generated with GaussView 6.0. Iso-value 0.035.

2.6.2. Spin Density Plots

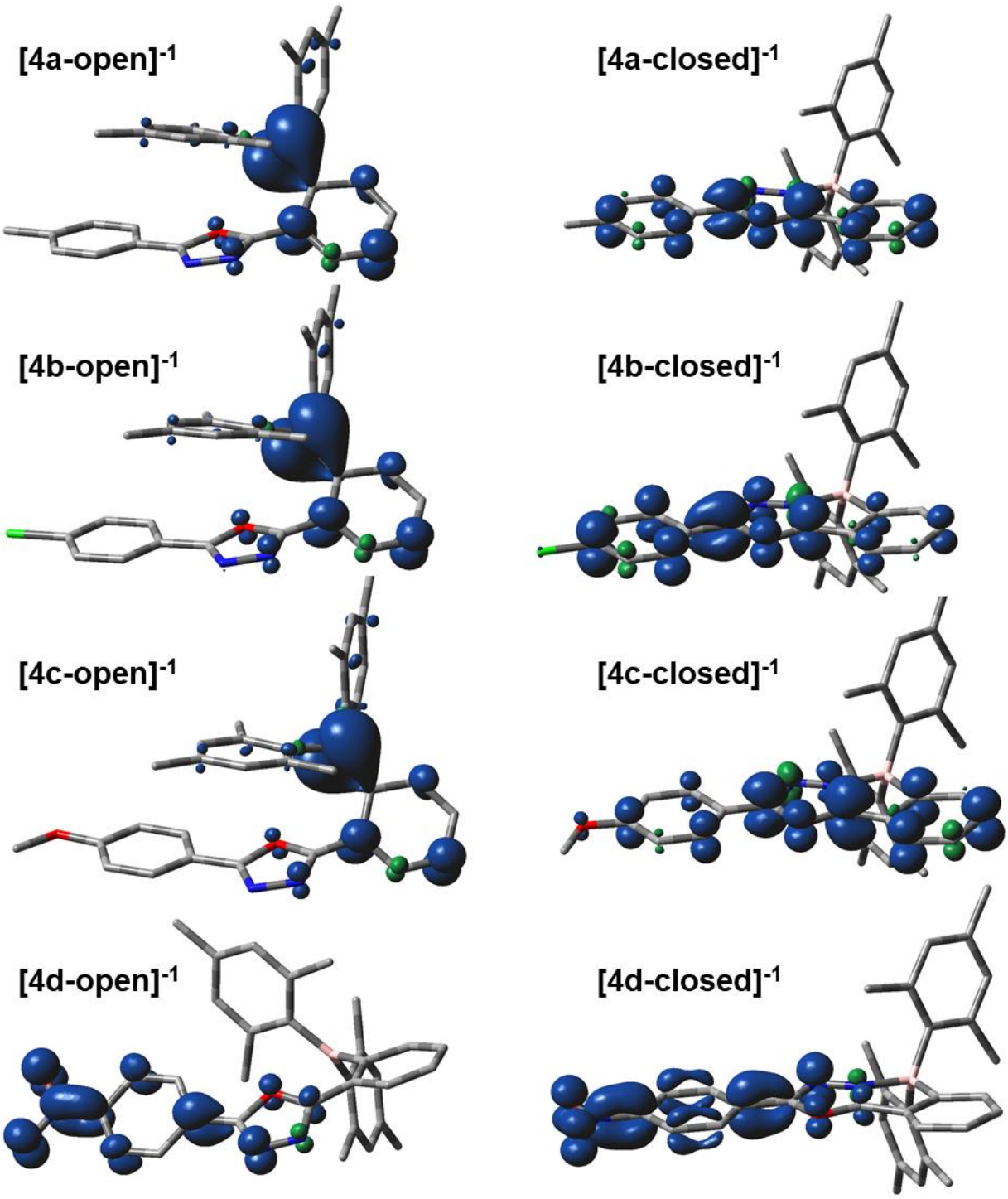

Figure S54. Spin density plots of *open* and *closed* conformers. Plots generated with GaussView 6.0. Spin density 0.004.

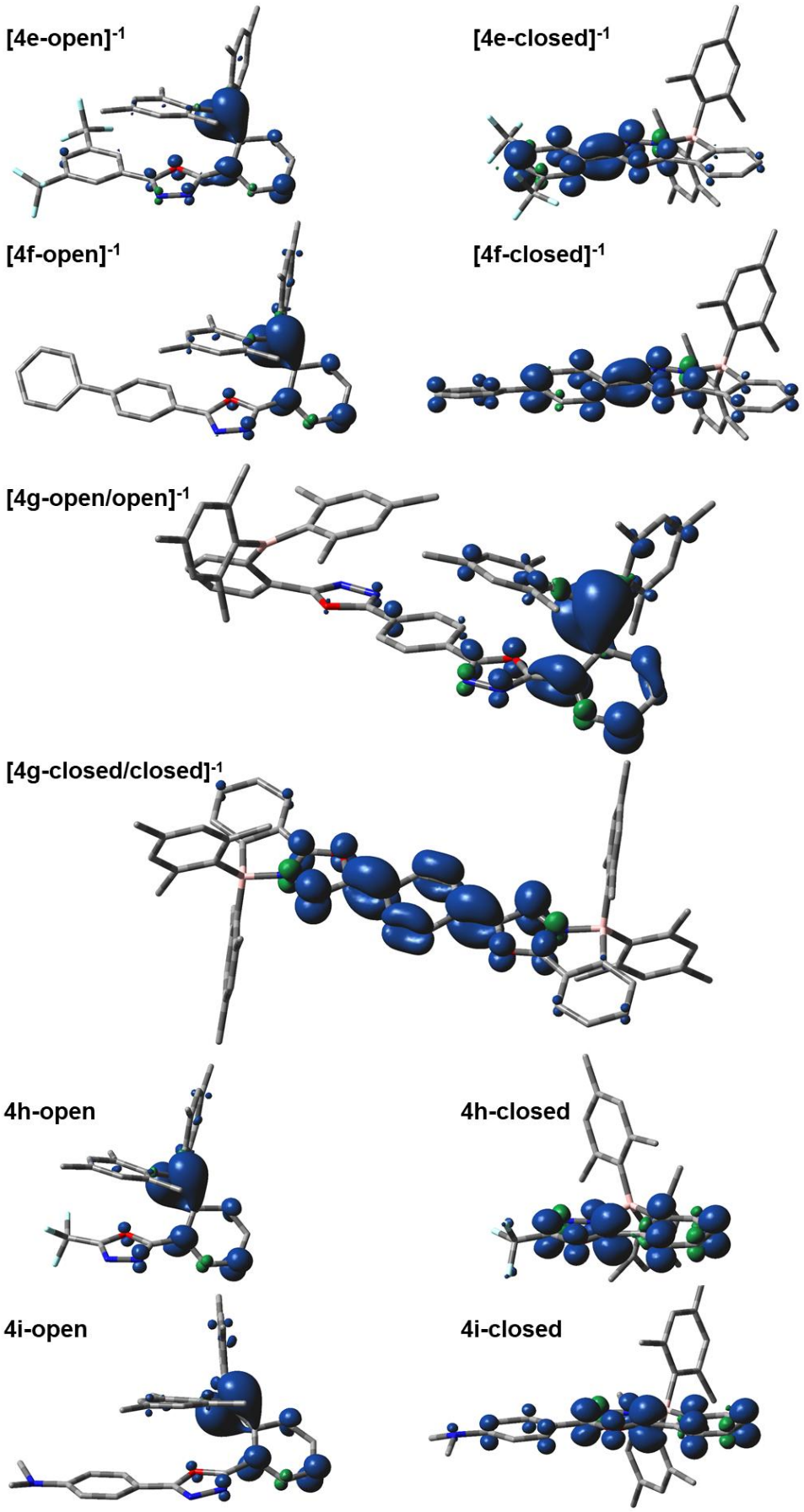

Figure S55. Spin density plots of *open* and *closed* conformers. Plots generated with GaussView 6.0. 4e, 4f, 4h, 4i: Spin density 0.004. 4h: Spin density 0.002

2.6.3. Simulated UV-Vis Spectra

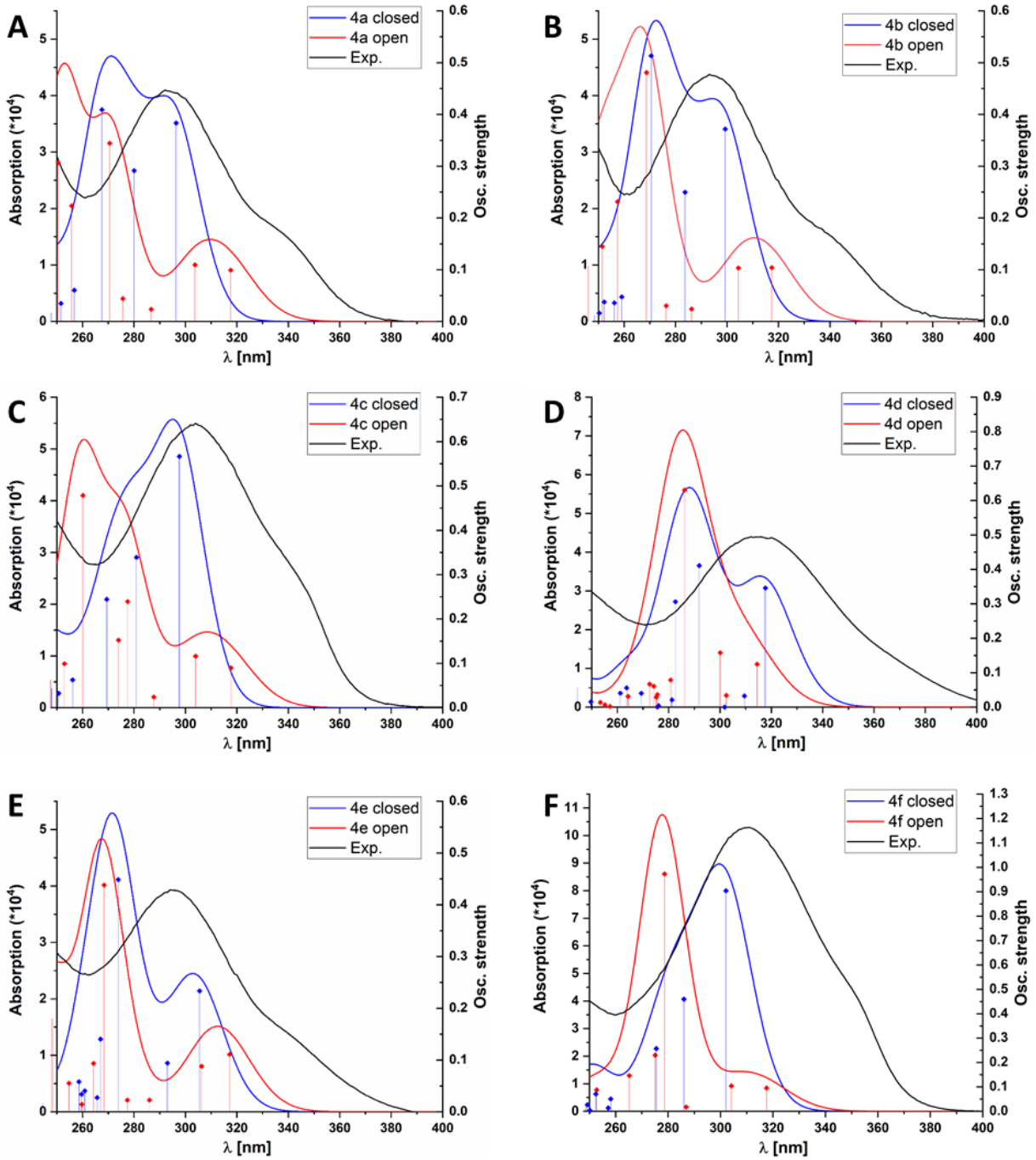

Figure S56. UV-vis spectra of *open* and *closed* conformers of compounds 4a-4f modelled by TDDFT and corresponding experimental absorption spectra.
Experimental spectra arbitrarily scaled to fit graph. Level of theory: m062x/def2-tzvp, solvent model: PCM, solvent dichloromethane

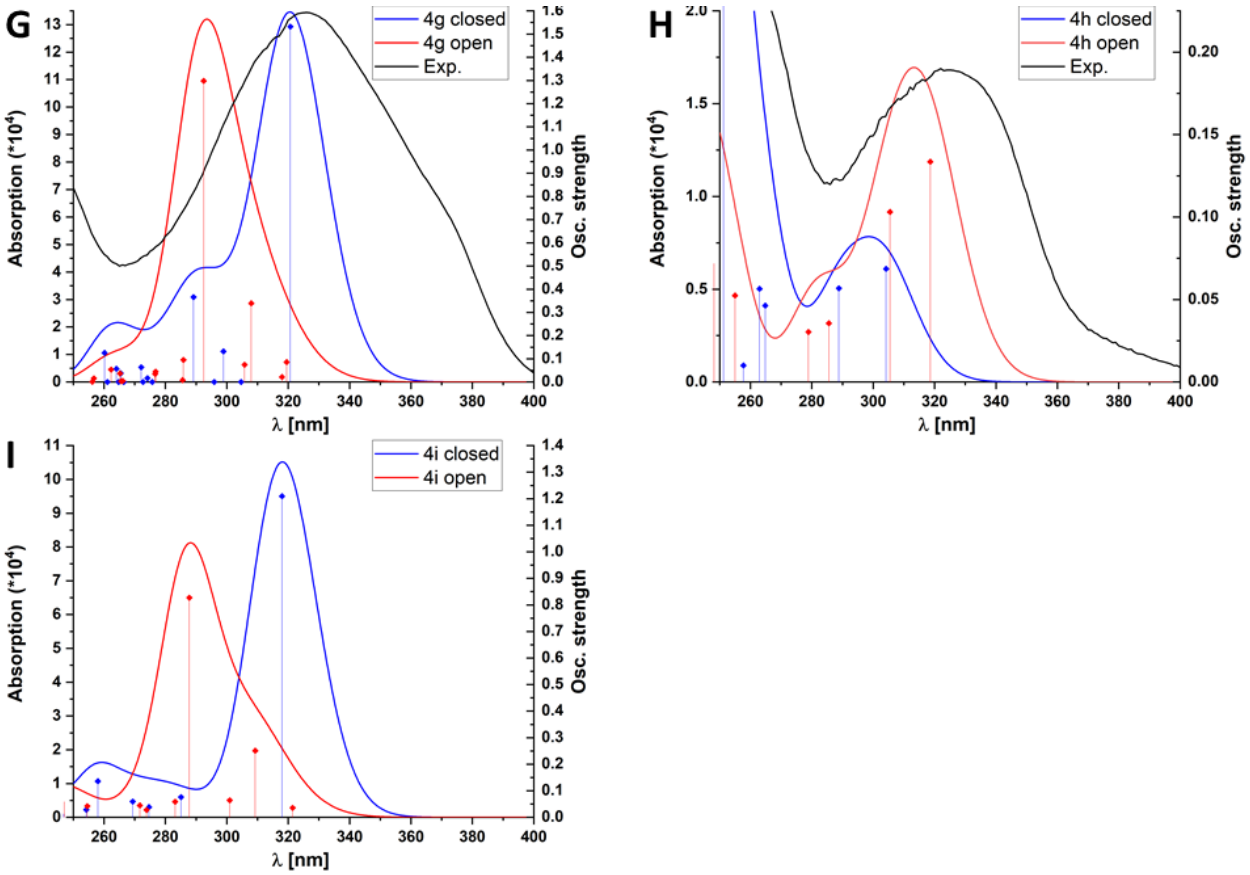

Figure S57. UV-vis spectra of *open* and *closed* conformers of compounds 4g-4i modelled by TDDFT and corresponding experimental absorption spectra.
Experimental spectra arbitrarily scaled to fit graph. No experimental spectrum available for 4i. Level of theory: m062x/def-tzvp, solvent model: PCM, solvent dichloromethane

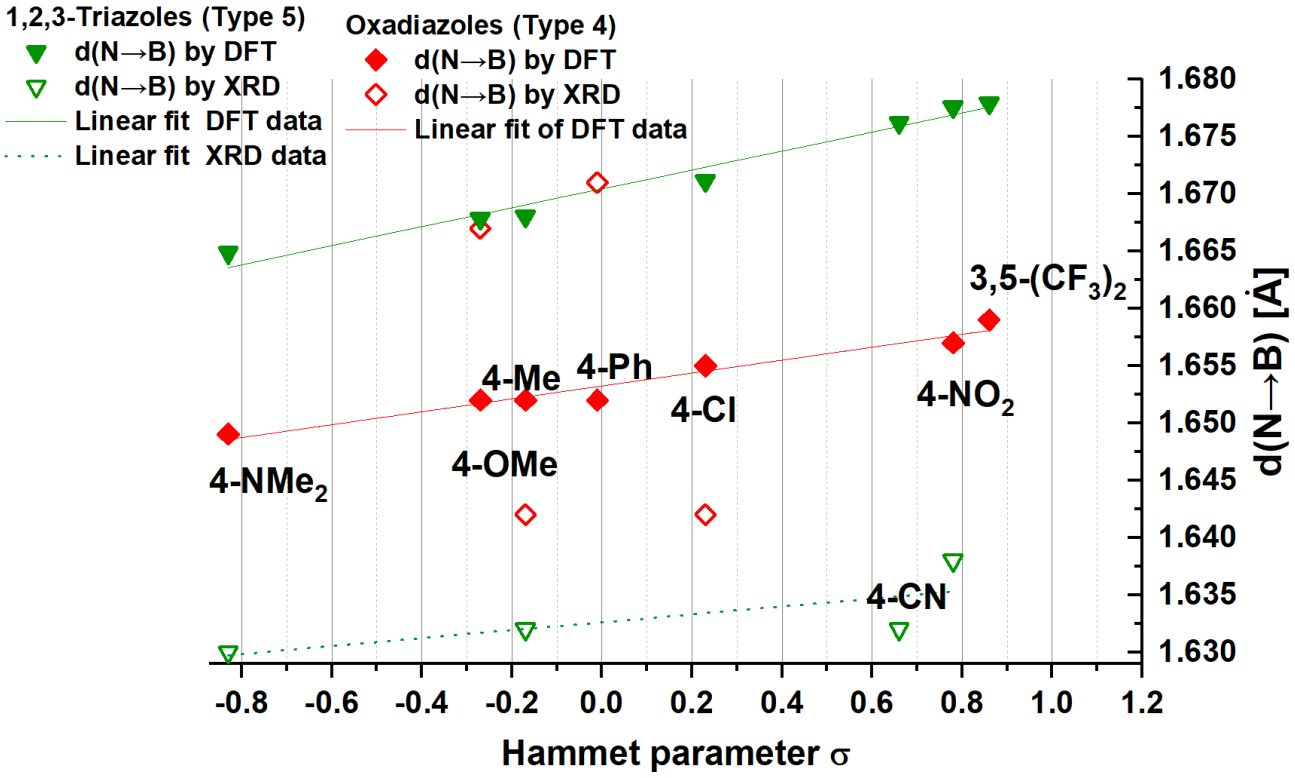

Figure S58. Correlation of N→B bond length in experimental and computed structures.
Data for oxadiazole-based N→B-ladder boranes (◇, ◆, —) produced herein. Level of theory: M06-2X/tzvp.
Data for 1,2,3-triazole-based (type 5) N→B-ladder boranes (▼,▽,—) adopted from Ref. [11]. Level of theory: B3LYP-D3/tzvp.

Table S 6. Computed electronic transitions for open-conformers

4a (Me) open				
No.	**Wave-length (nm)**	**Osc. Strength (f)**	**Major contribs**	**Minor contribs**
1	317.6	0.099	**H-1->LUMO (17%), HOMO->LUMO (73%)**	H-10->LUMO (2%)
2	303.7	0.109	H-2->LUMO (66%), H-1->LUMO (18%)	H-8->LUMO (2%), H-5->LUMO (3%), H-3->LUMO (2%)
3	286.7	0.024	H-3->LUMO (26%), H-2->LUMO (19%), H-1->LUMO (31%)	H-4->LUMO (4%), HOMO->LUMO (8%)
4	275.7	0.044	H-4->LUMO (49%), H-3->LUMO (31%)	H-4->L+1 (2%), H-4->L+4 (3%), H-1->LUMO (3%)
5	270.6	0.344	H-7->LUMO (10%), H-4->LUMO (30%), H-3->LUMO (22%), H-1->LUMO (15%)	H-1->L+1 (2%), HOMO->LUMO (5%), HOMO->L+1 (4%)
6	255.8	0.223	H-5->LUMO (17%), H-1->L+1 (13%), HOMO->L+1 (32%)	H-7->LUMO (6%), H-7->L+2 (3%), H-6->LUMO (5%), H-5->L+2 (3%), H-3->L+1 (7%)
7	250.5	0.307	H-5->LUMO (44%), HOMO->L+1 (17%)	H-8->LUMO (2%), H-6->LUMO (6%), H-4->LUMO (2%), H-3->LUMO (5%), H-3->L+1 (3%), H-1->L+1 (6%)
8	242.3	0.002	H-6->L+1 (27%), H-1->L+3 (11%)	H-7->LUMO (4%), H-7->L+3 (3%), H-6->L+2 (7%), H-5->L+1 (7%), H-3->L+3 (5%), H-1->L+2 (2%), H-1->L+4 (4%), HOMO->L+2 (3%), HOMO->L+3 (8%), HOMO->L+4 (2%)
9	239.7	0.113	H-2->L+1 (19%), H-1->L+1 (39%), HOMO->L+1 (16%)	H-8->LUMO (3%), H-4->L+1 (2%), H-3->L+1 (4%), HOMO->LUMO (3%), HOMO->L+2 (2%)
10	235.0	0.026	H-4->L+1 (10%), H-3->L+1 (34%), H-2->L+1 (25%)	H-1->LUMO (3%), H-1->L+1 (4%), HOMO->L+1 (2%), HOMO->L+6 (3%)
11	232.6	0.005	H-8->LUMO (24%), H-7->LUMO (15%), HOMO->L+1 (16%)	H-6->L+1 (4%), H-5->LUMO (3%), H-5->L+1 (2%), H-5->L+2 (4%), H-3->LUMO (2%), H-1->LUMO (4%), HOMO->L+2 (3%)
12	227.6	0.029	--	H-10->LUMO (3%), H-4->LUMO (8%), H-4->L+4 (7%), H-4->L+5 (9%), H-3->LUMO (3%), H-3->L+4 (3%), H-3->L+7 (3%), H-2->L+1 (4%), H-2->L+5 (7%), H-2->L+6 (4%), H-2->L+7 (8%), H-1->L+3 (2%), H-1->L+5 (5%), H-1->L+6 (5%), H-1->L+7 (5%), HOMO->L+6 (3%)
13	225.0	0.052	--	H-10->LUMO (5%), H-3->L+1 (4%), H-3->L+5 (2%), H-2->L+1 (3%), H-2->L+2 (2%), H-2->L+3 (8%), H-2->L+5 (2%), H-2->L+6 (3%), H-2->L+7 (5%), H-1->L+3 (6%), H-1->L+4 (2%), H-1->L+7 (3%), HOMO->L+1 (5%), HOMO->L+3 (4%), HOMO->L+4 (2%), HOMO->L+5 (5%), HOMO->L+6 (9%), HOMO->L+7 (3%)
14	224.0	0.127	H-10->LUMO (48%)	H-16->LUMO (2%), H-8->LUMO (5%), H-7->LUMO (6%), H-5->LUMO (2%), HOMO->L+5 (2%)
15	223.4	0.119	H-10->LUMO (10%), H-8->LUMO (33%), H-7->LUMO (18%)	H-11->LUMO (2%), H-5->LUMO (8%), H-3->LUMO (2%), H-3->L+1 (3%)

4b (Cl) open

No.	Wave-length (nm)	Osc. Strength (f)	Major contribs	Minor contribs
1	317.4	0.104	**HOMO->LUMO (86%)**	H-10->LUMO (2%), H-2->LUMO (4%)
2	304.4	0.103	H-2->LUMO (14%), H-1->LUMO (72%)	H-8->LUMO (2%), H-5->LUMO (3%)
3	286.2	0.024	H-2->LUMO (61%), H-1->LUMO (10%)	H-4->LUMO (8%), H-3->LUMO (4%), HOMO->LUMO (3%), HOMO->L+6 (2%)
4	276.4	0.030	H-4->LUMO (14%), H-3->LUMO (69%)	H-1->L+7 (2%)
5	268.7	0.481	H-6->LUMO (10%), H-4->LUMO (50%)	H-4->L+1 (3%), H-3->LUMO (7%), H-3->L+1 (3%), H-2->LUMO (7%), H-1->L+1 (3%), HOMO->L+1 (4%)
6	257.5	0.231	H-5->LUMO (12%), H-1->L+1 (17%), HOMO->L+1 (26%)	H-6->LUMO (7%), H-5->L+3 (2%), H-4->LUMO (3%), H-4->L+1 (9%), H-3->L+1 (7%), H-2->L+1 (2%)
7	251.5	0.145	H-5->LUMO (60%), HOMO->L+1 (10%)	H-4->LUMO (7%), H-1->L+1 (2%)
8	246.1	0.107	H-2->L+1 (62%), HOMO->L+1 (24%)	H-4->L+1 (5%)
9	243.7	0.004	H-7->L+1 (28%)	H-6->LUMO (3%), H-6->L+2 (3%), H-6->L+3 (2%), H-4->L+1 (3%), H-4->L+2 (6%), H-4->L+3 (6%), H-3->L+2 (4%), H-3->L+3 (4%), H-2->L+2 (4%), H-2->L+3 (5%), H-1->L+2 (5%), H-1->L+3 (3%), HOMO->L+2 (4%)
10	241.7	0.073	H-4->L+1 (38%), H-2->L+1 (22%), HOMO->L+1 (11%)	H-7->L+1 (2%), H-3->L+1 (9%), H-2->LUMO (4%)
11	232.9	0.053	H-8->LUMO (32%)	H-7->L+1 (2%), H-6->LUMO (8%), H-5->L+1 (3%), H-5->L+3 (2%), H-1->LUMO (5%), HOMO->L+1 (6%), HOMO->L+2 (5%), HOMO->L+6 (2%)
12	228.2	0.021	H-1->L+7 (16%)	H-4->LUMO (2%), H-4->L+5 (5%), H-3->LUMO (7%), H-3->L+1 (2%), H-3->L+4 (6%), H-3->L+5 (6%), H-3->L+7 (3%), H-1->L+1 (7%), H-1->L+3 (4%), H-1->L+4 (2%), H-1->L+5 (8%), H-1->L+6 (2%), HOMO->L+5 (2%), HOMO->L+6 (3%), HOMO->L+7 (3%)
13	226.3	0.044	HOMO->L+6 (13%)	H-10->LUMO (4%), H-8->LUMO (7%), H-4->LUMO (3%), H-2->LUMO (3%), H-2->L+2 (6%), H-2->L+3 (4%), H-2->L+4 (7%), H-2->L+5 (5%), H-2->L+6 (3%), H-2->L+7 (4%), H-1->L+6 (2%), HOMO->L+2 (6%), HOMO->L+4 (4%), HOMO->L+5 (5%)
14	224.3	0.075	H-10->LUMO (45%), H-1->L+1 (11%)	H-9->LUMO (5%), H-8->LUMO (2%), H-4->L+1 (2%), H-1->L+2 (3%), H-1->L+5 (3%)
15	222.2	0.163	H-8->LUMO (24%), H-6->LUMO (27%)	H-11->LUMO (3%), H-5->LUMO (9%), H-5->L+2 (2%), H-4->LUMO (4%), H-3->LUMO (4%)

4c (OMe) open

No.	Wave-length (nm)	Osc. Strength (f)	Major contribs	Minor contribs
1	317.7	0.090	**H-1->LUMO (76%), HOMO->LUMO (14%)**	H-11->LUMO (2%)
2	304.0	0.116	H-2->LUMO (77%)	H-5->LUMO (2%), H-3->LUMO (3%), H-1->LUMO (3%), HOMO->LUMO (4%)
3	287.7	0.024	H-3->LUMO (45%), H-2->LUMO (10%), HOMO->LUMO (27%)	H-4->LUMO (2%), H-1->LUMO (4%)
4	277.6	0.239	H-4->LUMO (12%), H-3->LUMO (36%), HOMO->LUMO (24%)	H-6->LUMO (5%), H-5->LUMO (2%), H-1->LUMO (6%), HOMO->L+1 (6%)
5	274.0	0.153	H-4->LUMO (70%)	H-6->LUMO (3%), H-4->L+4 (2%), HOMO->LUMO (9%), HOMO->L+1 (3%)
6	260.2	0.478	HOMO->L+1 (71%)	H-6->LUMO (5%), H-5->L+2 (3%), HOMO->LUMO (3%), HOMO->L+2 (4%)
7	253.0	0.099	H-6->LUMO (46%), H-5->LUMO (15%), HOMO->L+2 (11%)	--
8	247.7	0.063	H-7->L+1 (11%), H-5->LUMO (16%), HOMO->L+2 (17%), HOMO->L+3 (26%)	H-7->L+2 (3%), HOMO->L+1 (3%), HOMO->L+4 (6%), HOMO->L+5 (2%)
9	239.5	0.039	H-8->LUMO (11%), H-5->LUMO (15%), H-1->L+1 (29%)	H-2->L+1 (5%), HOMO->LUMO (8%), HOMO->L+3 (5%)
10	234.1	0.036	H-5->LUMO (16%), H-2->L+1 (12%), H-1->L+1 (39%)	H-8->LUMO (2%), H-6->LUMO (6%), H-3->L+1 (5%), HOMO->LUMO (4%)
11	231.5	0.015	H-3->L+1 (38%)	H-8->LUMO (5%), H-5->LUMO (2%), H-4->L+1 (4%), H-3->LUMO (4%), H-3->L+5 (3%), H-2->L+1 (9%), H-1->L+1 (3%), H-1->L+6 (5%)
12	227.6	0.047	H-4->LUMO (10%), H-4->L+5 (10%), H-2->L+7 (11%)	H-11->LUMO (2%), H-5->LUMO (2%), H-4->L+4 (7%), H-3->L+7 (3%), H-2->L+1 (5%), H-2->L+3 (3%), H-2->L+5 (9%), H-2->L+6 (5%), H-1->L+5 (4%), H-1->L+6 (3%), H-1->L+7 (5%)
13	226.0	0.136	H-9->LUMO (12%), H-8->LUMO (23%), H-5->LUMO (15%)	H-11->LUMO (6%), H-10->LUMO (3%), H-6->LUMO (3%), H-3->LUMO (3%), H-1->L+1 (6%), H-1->L+6 (2%)
14	224.4	0.097	H-11->LUMO (35%)	H-3->L+1 (5%), H-2->L+1 (6%), H-2->L+2 (4%), H-2->L+5 (2%), H-2->L+7 (2%), H-1->L+1 (3%), H-1->L+2 (3%), H-1->L+3 (5%), H-1->L+4 (5%), H-1->L+6 (3%)
15	223.4	0.009	H-11->LUMO (24%), H-3->L+1 (17%)	H-9->LUMO (4%), H-8->LUMO (2%), H-3->L+5 (3%), H-2->L+3 (3%), H-2->L+6 (3%), H-1->L+5 (4%), H-1->L+6 (6%), HOMO->L+2 (2%)

4d (NO2) open

No.	Wave-length (nm)	Osc. Strength (f)	Major contribs	Minor contribs
1	314.5	0.125	HOMO->L+1 (78%)	H-2->L+1 (3%), H-1->L+1 (2%), HOMO->LUMO (6%), HOMO->L+2 (3%)
2	302.5	0.034	H-15->LUMO (54%)	H-15->L+1 (2%), H-15->L+2 (4%), H-15->L+4 (6%), H-15->L+5 (6%), H-14->LUMO (9%), H-4->LUMO (2%)
3	300.1	0.158	H-2->LUMO (16%), H-2->L+1 (17%), H-1->L+1 (18%)	H-15->LUMO (6%), H-6->LUMO (2%), H-5->L+1 (4%), H-4->LUMO (8%), H-3->LUMO (3%), H-1->LUMO (8%), HOMO->L+1 (4%)
4	286.2	0.630	H-4->LUMO (16%), H-3->LUMO (23%), H-1->L+1 (18%)	H-6->LUMO (5%), H-5->L+1 (4%), H-3->L+1 (6%), H-2->LUMO (7%), H-2->L+1 (5%), HOMO->LUMO (3%)
5	280.8	0.079	H-4->LUMO (16%), H-3->L+1 (14%), H-2->L+1 (28%), H-1->L+1 (10%)	H-4->L+1 (7%), H-2->LUMO (7%)
6	275.6	0.036	H-3->LUMO (18%), H-1->L+1 (12%), HOMO->LUMO (18%)	H-19->LUMO (9%), H-17->LUMO (5%), H-4->LUMO (2%), H-3->L+1 (4%), H-2->LUMO (7%), H-1->LUMO (9%)
7	275.1	0.029	H-19->LUMO (19%), H-17->LUMO (10%), H-2->L+1 (12%), H-1->L+1 (14%)	H-7->LUMO (2%), H-4->LUMO (6%), H-3->LUMO (4%), H-3->L+1 (8%)
8	274.2	0.061	H-19->LUMO (10%), H-3->L+1 (25%), H-1->LUMO (13%), HOMO->LUMO (12%)	H-17->LUMO (5%), H-7->LUMO (3%), H-4->L+1 (4%), H-3->LUMO (4%), H-2->L+1 (3%), H-1->L+1 (3%)
9	272.6	0.067	H-7->LUMO (12%), H-4->LUMO (19%), H-3->L+1 (12%), H-2->LUMO (22%)	H-19->LUMO (7%), H-17->LUMO (3%), H-2->L+1 (8%)
10	264.2	0.031	H-5->L+1 (43%), H-4->L+1 (17%), HOMO->LUMO (11%)	H-5->LUMO (6%), H-3->L+1 (5%)
11	257.1	0.002	H-5->L+1 (11%), H-4->L+1 (37%)	H-7->LUMO (5%), H-6->L+1 (3%), H-5->LUMO (5%), H-5->L+2 (9%), H-3->L+1 (4%), H-2->L+1 (3%), HOMO->LUMO (2%)
12	255.2	0.006	H-3->LUMO (12%), H-1->LUMO (13%), HOMO->LUMO (39%)	H-6->LUMO (2%), H-5->L+1 (2%), H-4->LUMO (5%), H-4->L+1 (5%), H-3->L+1 (4%), H-2->LUMO (5%), HOMO->L+1 (2%), HOMO->L+2 (3%)
13	253.4	0.014	H-7->LUMO (51%)	H-6->LUMO (6%), H-6->L+3 (3%), H-4->LUMO (6%), H-4->L+3 (3%), H-3->LUMO (7%), H-2->LUMO (7%), H-1->LUMO (5%)
14	245.4	0.004	H-3->LUMO (22%), H-2->LUMO (18%), H-1->LUMO (41%)	H-4->LUMO (6%), H-1->L+2 (3%)
15	237.9	0.117	H-5->LUMO (11%), H-5->L+2 (12%), H-4->L+2 (12%)	H-8->L+1 (9%), H-6->LUMO (6%), H-5->L+1 (7%), H-4->L+1 (5%), H-3->L+2 (2%), H-2->L+1 (3%), H-2->L+2 (9%), H-1->L+2 (4%)

4e (mbisCF3) open

No.	Wave-length (nm)	Osc. Strength (f)	Major contribs	Minor contribs
1	317.2	0.111	HOMO->LUMO (72%), HOMO->L+1 (13%)	H-2->LUMO (2%), H-1->LUMO (3%)
2	306.3	0.088	H-1->LUMO (68%), H-1->L+1 (11%)	H-5->LUMO (2%), H-2->LUMO (3%), HOMO->LUMO (3%)
3	286.0	0.023	H-2->LUMO (66%)	H-3->LUMO (7%), H-2->L+1 (9%), H-2->L+4 (3%), H-1->LUMO (3%)
4	277.4	0.023	H-3->LUMO (65%), H-3->L+1 (13%)	H-3->L+5 (2%), H-2->LUMO (5%)
5	268.4	0.438	H-4->LUMO (30%), H-1->L+1 (23%), HOMO->L+1 (23%)	H-6->L+1 (2%), H-3->L+1 (4%), H-1->LUMO (3%), HOMO->LUMO (4%)
6	264.3	0.093	H-4->LUMO (50%), H-1->L+1 (10%), HOMO->L+1 (16%)	H-5->LUMO (3%), H-5->L+3 (3%), H-1->LUMO (2%), HOMO->LUMO (4%)
7	259.7	0.014	H-3->L+1 (15%), H-2->LUMO (11%), H-2->L+1 (66%)	H-3->LUMO (2%)
8	254.8	0.055	H-5->LUMO (48%), H-4->L+1 (17%)	H-5->L+1 (3%), H-5->L+3 (3%), H-4->LUMO (4%), H-4->L+3 (2%), H-1->LUMO (2%), HOMO->L+1 (3%)
9	248.2	0.180	H-5->LUMO (13%), H-4->L+1 (45%)	H-7->L+1 (5%), H-6->L+1 (3%), H-6->L+2 (4%), H-5->L+1 (3%), H-4->L+2 (5%), H-2->L+2 (2%), HOMO->L+1 (4%)
10	244.9	0.067	H-7->L+1 (12%), H-4->L+2 (21%)	H-7->LUMO (4%), H-6->LUMO (4%), H-6->L+2 (7%), H-5->LUMO (6%), H-5->L+1 (2%), H-4->L+1 (7%), H-3->L+2 (5%), H-2->L+2 (5%), H-1->L+2 (7%), HOMO->L+2 (5%)
11	235.9	0.079	H-2->L+2 (17%), H-1->L+2 (17%), HOMO->L+2 (25%)	H-8->LUMO (4%), H-4->L+1 (4%), H-4->L+2 (4%), H-1->L+6 (2%), HOMO->L+1 (3%), HOMO->L+6 (2%)
12	235.3	0.015	H-1->LUMO (11%), H-1->L+1 (38%), HOMO->L+1 (20%)	H-4->L+1 (5%), H-1->L+3 (2%), HOMO->LUMO (7%), HOMO->L+2 (2%), HOMO->L+3 (5%)
13	230.3	0.049	H-8->LUMO (18%), HOMO->L+2 (13%)	H-9->LUMO (4%), H-8->L+1 (4%), H-5->L+3 (2%), H-4->L+1 (3%), H-3->LUMO (4%), H-3->L+5 (3%), H-1->L+2 (6%), H-1->L+7 (5%), HOMO->L+3 (2%), HOMO->L+7 (5%)
14	228.9	0.029	H-3->LUMO (10%)	H-9->LUMO (7%), H-8->LUMO (2%), H-3->L+1 (4%), H-3->L+2 (4%), H-3->L+5 (8%), H-2->LUMO (3%), H-2->L+2 (2%), H-1->L+1 (2%), H-1->L+2 (3%), H-1->L+3 (3%), H-1->L+5 (3%), H-1->L+7 (8%), HOMO->L+1 (2%), HOMO->L+5 (5%), HOMO->L+7 (7%)
15	227.9	0.040	H-2->L+2 (43%)	H-8->LUMO (9%), H-7->L+1 (5%), H-6->L+2 (3%), H-4->L+2 (9%), H-3->L+2 (8%), HOMO->L+2 (3%)
4f (4-Ph) open				

No.	Wave-length (nm)	Osc. Strength (f)	Major contribs	Minor contribs
1	317.6	0.095	H-1->LUMO (68%), HOMO->LUMO (21%)	H-12->LUMO (2%), H-1->L+1 (2%)
2	304.1	0.104	H-2->LUMO (76%)	H-10->LUMO (2%), H-7->LUMO (2%), H-3->LUMO (2%), H-1->LUMO (4%), HOMO->LUMO (3%)
3	286.9	0.018	H-3->LUMO (53%), HOMO->LUMO (18%)	H-4->LUMO (2%), H-3->L+1 (2%), H-2->LUMO (8%), H-1->LUMO (5%)
4	278.7	0.973	H-3->LUMO (17%), HOMO->LUMO (12%), HOMO->L+1 (42%)	H-5->LUMO (6%), H-4->LUMO (5%), H-1->LUMO (5%), H-1->L+1 (2%)
5	275.1	0.230	H-4->LUMO (72%), HOMO->L+1 (10%)	--
6	265.2	0.146	H-5->LUMO (17%), HOMO->LUMO (17%), HOMO->L+1 (31%)	H-7->LUMO (4%), H-7->L+2 (2%), H-4->LUMO (3%), H-3->LUMO (9%), H-1->LUMO (5%)
7	252.8	0.088	H-7->LUMO (65%)	H-2->LUMO (2%), HOMO->L+2 (4%)
8	248.7	0.021	H-8->L+1 (21%), H-2->L+1 (14%), H-1->L+1 (30%), HOMO->L+3 (15%)	--
9	247.9	0.012	H-8->L+1 (17%), H-1->L+1 (31%), HOMO->L+3 (10%)	H-7->LUMO (6%), H-2->L+1 (6%), HOMO->L+2 (5%), HOMO->L+4 (2%)
10	242.6	0.028	H-3->L+1 (60%), H-2->L+1 (12%)	H-4->L+1 (7%), H-3->LUMO (2%), HOMO->L+1 (3%)
11	236.2	0.001	H-6->L+1 (34%), HOMO->L+5 (20%)	H-9->L+5 (3%), H-6->L+2 (4%), H-6->L+7 (6%), H-6->L+9 (5%), H-5->L+5 (9%), H-3->L+5 (2%), H-1->L+5 (3%)
12	235.8	0.004	H-10->LUMO (18%), H-9->LUMO (11%), H-5->LUMO (12%), HOMO->LUMO (10%)	H-8->L+1 (3%), H-7->L+1 (2%), H-7->L+2 (5%), H-1->LUMO (2%), H-1->L+1 (4%), HOMO->L+1 (4%), HOMO->L+2 (3%)
13	228.1	0.071	H-10->LUMO (10%), H-5->LUMO (12%)	H-9->LUMO (3%), H-5->L+1 (6%), H-4->LUMO (8%), H-4->L+4 (2%), H-4->L+6 (5%), H-2->L+6 (3%), H-2->L+7 (4%), H-2->L+9 (4%), H-1->L+7 (3%), H-1->L+8 (3%), HOMO->LUMO (3%), HOMO->L+2 (4%)
14	227.9	0.030	H-5->LUMO (10%)	H-10->LUMO (3%), H-9->LUMO (3%), H-5->L+1 (8%), H-4->L+4 (2%), H-4->L+6 (5%), H-3->LUMO (7%), H-2->L+1 (6%), H-2->L+2 (5%), H-2->L+8 (5%), H-1->L+1 (5%), H-1->L+3 (5%), H-1->L+7 (3%), H-1->L+9 (2%), HOMO->LUMO (2%), HOMO->L+2 (4%)
15	226.2	0.038	H-10->LUMO (10%)	H-3->L+1 (6%), H-3->L+3 (3%), H-3->L+6 (5%), H-3->L+9 (3%), H-2->L+3 (7%), H-2->L+7 (3%), H-2->L+8 (4%), H-1->L+2 (5%), H-1->L+3 (5%), H-1->L+4 (3%), H-1->L+6 (3%), H-1->L+7 (3%), H-1->L+8 (9%), HOMO->L+6 (3%)

4g (tereph) open

No.	Wave-length (nm)	Osc. Strength (f)	Major contribs	Minor contribs
1	319.5	0.085	H-1->L+1 (39%), HOMO->LUMO (30%)	H-3->L+1 (3%), H-2->LUMO (2%), H-2->L+2 (4%), HOMO->L+2 (8%)
2	318.0	0.021	H-2->L+1 (10%), H-1->LUMO (27%), H-1->L+2 (18%), HOMO->L+1 (30%)	H-4->L+1 (3%)
3	308.0	0.339	H-3->L+1 (32%), H-2->LUMO (24%), H-2->L+2 (12%)	H-4->L+2 (4%), H-1->L+1 (5%), HOMO->LUMO (8%)
4	305.8	0.074	H-3->LUMO (24%), H-3->L+2 (19%), H-2->L+1 (29%)	H-4->L+1 (9%), HOMO->L+1 (3%)
5	292.5	1.298	H-6->LUMO (12%), H-4->LUMO (12%), HOMO->LUMO (24%), HOMO->L+2 (20%)	H-8->LUMO (4%), H-3->L+1 (8%), H-2->L+2 (4%)
6	285.9	0.095	H-5->L+1 (33%), H-4->LUMO (18%)	H-8->LUMO (2%), H-7->L+1 (4%), H-6->LUMO (6%), H-6->L+2 (5%), H-5->LUMO (4%), H-5->L+2 (2%), H-4->L+2 (6%), HOMO->L+2 (3%)
7	285.6	0.008	H-6->L+1 (12%), H-5->LUMO (20%), H-5->L+2 (12%), H-4->L+1 (24%)	H-8->L+1 (3%), H-7->LUMO (3%), HOMO->L+1 (3%)
8	276.8	0.044	H-8->L+1 (20%), H-7->LUMO (16%), H-7->L+2 (15%), H-6->L+1 (17%)	H-7->L+1 (7%), H-5->L+2 (2%)
9	276.7	0.034	H-8->LUMO (13%), H-8->L+2 (11%), H-7->L+1 (29%)	H-8->L+1 (4%), H-7->LUMO (3%), H-7->L+2 (3%), H-6->LUMO (6%), H-6->L+2 (7%), H-5->L+1 (5%)
10	266.1	0.004	H-9->LUMO (15%), H-8->L+1 (10%), HOMO->L+1 (11%)	H-12->L+1 (3%), H-11->LUMO (3%), H-9->L+2 (6%), H-6->L+1 (8%), H-4->L+1 (9%), H-3->L+2 (3%), H-2->L+1 (4%), H-1->LUMO (4%), H-1->L+2 (6%)
11	265.6	0.003	H-1->LUMO (28%), H-1->L+2 (21%)	H-9->LUMO (3%), H-9->L+2 (2%), H-8->L+1 (3%), H-6->L+1 (3%), H-3->LUMO (9%), H-3->L+2 (7%), HOMO->L+1 (5%), HOMO->L+3 (3%)
12	265.2	0.037	H-9->L+1 (14%), H-8->LUMO (10%), HOMO->L+2 (27%)	H-6->LUMO (9%), H-4->LUMO (7%), H-2->LUMO (3%), H-1->LUMO (2%), H-1->L+2 (2%)
13	262.3	0.053	H-4->LUMO (20%), H-4->L+2 (36%)	H-13->LUMO (7%), H-13->L+2 (3%), H-9->L+1 (2%), H-2->L+2 (6%), HOMO->LUMO (4%)
14	256.7	0.016	H-8->LUMO (11%), H-8->L+2 (12%), H-6->LUMO (11%), H-6->L+2 (14%)	H-11->L+1 (6%), H-10->LUMO (6%), H-4->LUMO (3%), H-2->L+2 (5%), HOMO->LUMO (9%)
15	256.2	0.001	H-7->LUMO (11%), H-5->LUMO (31%), H-5->L+2 (24%)	H-11->LUMO (3%), H-7->L+2 (8%)

4h (5CF3Oz) open

No.	Wave-length (nm)	Osc. Strength (f)	Major contribs	Minor contribs
1	318.6	0.134	HOMO->LUMO (89%)	H-7->LUMO (2%)
2	305.5	0.103	H-1->LUMO (86%)	H-6->LUMO (3%)
3	285.6	0.036	H-2->LUMO (82%)	H-3->LUMO (5%)
4	278.9	0.030	H-3->LUMO (80%)	H-3->L+1 (2%), H-2->LUMO (5%)
5	255.0	0.052	H-5->LUMO (64%)	H-5->L+1 (4%), H-4->LUMO (9%), H-4->L+1 (4%), H-4->L+2 (6%), H-1->L+1 (3%)
6	248.2	0.072	H-5->LUMO (12%), H-4->LUMO (69%)	H-6->LUMO (3%), H-5->L+1 (2%), H-1->LUMO (4%)
7	240.8	0.126	H-1->L+1 (26%), HOMO->L+1 (43%)	H-6->LUMO (5%), H-4->LUMO (5%), H-2->L+1 (3%), H-1->L+3 (3%)
8	231.8	0.010	H-6->LUMO (10%), H-3->L+1 (10%), H-2->L+1 (34%)	H-4->L+1 (4%), H-2->LUMO (3%), H-2->L+2 (4%), H-1->L+1 (3%), HOMO->L+1 (6%), HOMO->L+3 (3%)
9	228.2	0.042	H-1->L+1 (10%)	H-6->LUMO (8%), H-3->LUMO (6%), H-3->L+1 (4%), H-3->L+3 (4%), H-3->L+4 (9%), H-2->LUMO (2%), H-2->L+3 (5%), H-1->L+4 (3%), H-1->L+5 (8%), H-1->L+6 (5%), HOMO->L+4 (6%), HOMO->L+5 (6%), HOMO->L+6 (6%)
10	227.8	0.075	H-6->LUMO (39%), H-2->L+1 (13%)	H-7->LUMO (9%), H-4->LUMO (4%), HOMO->L+1 (5%), HOMO->L+4 (3%)
11	224.4	0.076	H-7->LUMO (51%)	H-14->LUMO (5%), H-8->LUMO (2%), H-6->LUMO (2%), H-4->L+1 (2%), H-1->L+1 (5%), H-1->L+4 (4%), HOMO->L+1 (7%), HOMO->L+2 (4%), HOMO->L+3 (3%)
12	222.0	0.014	HOMO->L+1 (18%), HOMO->L+3 (10%)	H-7->LUMO (8%), H-3->LUMO (3%), H-2->L+1 (6%), H-2->L+4 (6%), H-1->L+1 (3%), H-1->L+2 (2%), H-1->L+3 (5%), H-1->L+5 (2%), H-1->L+6 (4%), HOMO->L+4 (3%), HOMO->L+5 (6%)
13	217.9	0.183	H-2->L+1 (10%), H-1->L+1 (28%)	H-7->LUMO (2%), H-6->LUMO (6%), H-5->LUMO (3%), H-4->L+1 (4%), H-3->L+1 (9%), H-3->L+4 (2%), H-2->L+4 (2%), H-1->L+3 (3%), H-1->L+5 (3%), HOMO->L+1 (4%), HOMO->L+6 (3%)
14	211.4	0.241	H-4->L+1 (34%), HOMO->L+2 (16%)	H-6->LUMO (4%), H-5->LUMO (7%), H-5->L+1 (5%), H-4->L+2 (2%), H-1->L+1 (6%), H-1->L+2 (5%), HOMO->L+1 (3%)
15	209.8	0.104	HOMO->L+2 (32%)	H-7->LUMO (2%), H-4->L+1 (7%), H-3->L+1 (4%), H-3->L+5 (4%), H-3->L+6 (2%), H-2->L+1 (3%), H-2->L+2 (2%), H-2->L+4 (6%), H-1->L+3 (3%), H-1->L+4 (8%), HOMO->L+3 (7%)

4i (4-NMe2) open

No.	Wave-length (nm)	Osc. Strength (f)	Major contribs	Minor contribs
1	321.5	0.036	H-1->LUMO (55%), HOMO->LUMO (33%)	H-5->LUMO (2%), HOMO->L+1 (2%)
2	309.3	0.251	H-2->LUMO (12%), H-1->LUMO (33%), HOMO->LUMO (35%)	H-5->LUMO (3%), H-3->LUMO (6%), HOMO->L+1 (4%)
3	300.9	0.064	H-2->LUMO (70%), HOMO->LUMO (15%)	H-7->LUMO (2%), H-1->LUMO (3%)
4	287.8	0.827	H-3->LUMO (23%), HOMO->L+1 (55%), HOMO->L+2 (12%)	--
5	283.2	0.059	H-3->LUMO (56%), HOMO->L+1 (15%)	H-2->LUMO (6%), HOMO->LUMO (6%), HOMO->L+2 (5%)
6	273.9	0.028	H-4->LUMO (83%)	H-4->L+1 (2%), H-4->L+4 (4%)
7	271.7	0.045	HOMO->L+2 (14%), HOMO->L+3 (32%), HOMO->L+4 (22%)	H-6->L+1 (4%), HOMO->LUMO (2%), HOMO->L+1 (3%), HOMO->L+5 (9%), HOMO->L+7 (3%)
8	254.5	0.042	H-7->LUMO (48%), H-5->LUMO (11%)	H-8->LUMO (4%), H-7->L+1 (3%), H-7->L+3 (2%), H-6->LUMO (5%), H-5->L+2 (3%), H-5->L+4 (2%)
9	247.1	0.059	H-7->LUMO (23%), H-5->LUMO (53%)	H-9->LUMO (3%), H-8->LUMO (4%), HOMO->LUMO (4%)
10	237.7	0.107	H-1->L+1 (33%), HOMO->L+2 (17%)	H-9->LUMO (7%), H-5->LUMO (5%), H-5->L+1 (3%), H-2->L+1 (4%), HOMO->L+3 (8%)
11	231.6	0.014	H-1->L+1 (26%), HOMO->L+2 (27%)	H-5->L+1 (3%), H-1->L+6 (4%), HOMO->L+1 (8%), HOMO->L+3 (8%)
12	229.2	0.017	H-3->L+1 (25%), H-2->L+1 (11%)	H-9->LUMO (7%), H-3->LUMO (4%), H-3->L+5 (5%), H-2->LUMO (2%), H-2->L+7 (3%), H-1->L+3 (5%), H-1->L+6 (5%), H-1->L+7 (3%), HOMO->L+3 (3%)
13	227.3	0.047	H-4->LUMO (11%), H-4->L+4 (10%), H-2->L+5 (12%)	H-11->LUMO (3%), H-4->L+5 (6%), H-4->L+7 (2%), H-3->L+6 (5%), H-3->L+7 (3%), H-2->L+1 (8%), H-2->L+3 (4%), H-2->L+6 (9%), H-2->L+7 (5%), H-1->L+5 (3%), H-1->L+6 (2%), H-1->L+7 (2%)
14	226.2	0.083	H-11->LUMO (11%), H-10->LUMO (10%), H-9->LUMO (32%), H-1->L+1 (14%)	H-5->LUMO (2%), H-3->L+1 (3%)
15	223.7	0.099	H-11->LUMO (52%)	H-19->LUMO (3%), H-9->LUMO (5%), H-2->L+1 (4%), H-1->L+3 (5%)

Table S 7. Computed electronic transitions for closed-conformers

4a (Me) open				
No.	**Wave-length (nm)**	**Osc. Strength (f)**	**Major contribs**	**Minor contribs**
1	296.4	0.383	**H-4->LUMO (12%), H-1->LUMO (14%), HOMO->LUMO (49%), HOMO->L+1 (10%)**	H-5->LUMO (3%), H-2->LUMO (2%)
2	280.0	0.291	H-4->LUMO (19%), H-1->LUMO (39%), HOMO->LUMO (23%)	H-2->LUMO (3%), H-1->L+1 (3%), HOMO->L+1 (7%)
3	267.6	0.409	H-4->LUMO (47%), H-1->LUMO (30%)	H-2->LUMO (7%), H-1->L+1 (9%)
4	256.8	0.060	H-5->LUMO (49%), H-5->L+1 (15%), H-2->LUMO (12%)	H-4->L+3 (3%), HOMO->LUMO (3%)
5	251.6	0.035	H-5->LUMO (10%), H-2->LUMO (54%)	H-5->L+1 (2%), H-4->LUMO (7%), H-3->LUMO (3%), H-2->L+1 (8%), H-1->L+1 (3%), HOMO->LUMO (3%)
6	247.8	0.017	H-3->LUMO (54%), H-1->L+1 (10%)	H-4->L+1 (4%), H-3->L+1 (7%), H-2->LUMO (7%), H-1->LUMO (2%), HOMO->L+1 (3%)
7	245.9	0.035	H-4->L+1 (13%), H-3->LUMO (20%), H-1->L+1 (14%), HOMO->L+1 (10%)	H-6->LUMO (7%), H-4->LUMO (3%), H-4->L+2 (3%), H-3->L+1 (3%), H-2->LUMO (2%), H-1->LUMO (3%), HOMO->LUMO (4%), HOMO->L+3 (3%)
8	242.9	0.006	H-7->LUMO (24%), H-6->LUMO (10%), H-6->L+1 (12%), H-4->L+2 (17%)	H-7->L+1 (5%), H-7->L+2 (3%), H-6->L+2 (3%), H-1->L+1 (3%), HOMO->LUMO (2%), HOMO->L+1 (5%), HOMO->L+3 (2%)
9	241.7	0.018	H-1->L+1 (25%), HOMO->L+1 (27%)	H-3->LUMO (7%), H-2->L+4 (4%), H-1->L+5 (5%), HOMO->LUMO (8%), HOMO->L+3 (7%)
10	238.7	0.009	HOMO->L+6 (27%)	H-3->LUMO (2%), H-3->L+3 (2%), H-3->L+4 (8%), H-3->L+7 (4%), H-2->LUMO (4%), H-2->L+3 (3%), H-2->L+5 (7%), H-2->L+7 (5%), H-1->L+5 (3%), H-1->L+7 (4%), HOMO->L+1 (4%), HOMO->L+3 (4%), HOMO->L+4 (9%)
11	236.6	0.020	H-2->L+4 (12%), H-1->L+5 (13%), HOMO->L+1 (10%)	H-4->L+1 (4%), H-3->LUMO (4%), H-3->L+4 (4%), H-3->L+5 (4%), H-3->L+7 (2%), H-2->L+6 (2%), H-1->L+1 (6%), H-1->L+4 (5%), H-1->L+7 (7%), HOMO->LUMO (3%), HOMO->L+4 (3%), HOMO->L+6 (3%)
12	234.5	0.169	H-4->L+1 (37%), H-2->L+1 (14%), H-1->L+1 (16%)	H-7->LUMO (8%), H-6->LUMO (3%), H-1->LUMO (2%), HOMO->L+3 (3%)
13	224.9	0.120	HOMO->L+1 (14%), HOMO->L+3 (41%)	H-8->LUMO (4%), H-5->LUMO (2%), H-5->L+3 (4%), H-3->L+1 (4%), H-1->L+3 (4%), HOMO->L+4 (3%), HOMO->L+7 (3%)
14	221.8	0.020	H-4->L+1 (10%), H-2->L+1 (52%)	H-3->L+1 (6%), H-2->LUMO (3%), H-1->L+5 (6%), HOMO->L+3 (3%)
15	218.0	0.016	H-8->LUMO (34%), H-8->L+1 (10%), H-3->L+1 (12%)	H-12->LUMO (3%), H-5->LUMO (4%), H-4->L+3 (4%), HOMO->L+3 (8%)

4b (Cl) closed

No.	Wave-length (nm)	Osc. Strength (f)	Major contribs	Minor contribs
1	299.3	0.372	**H-4->LUMO (12%), H-1->LUMO (14%), HOMO->LUMO (46%), HOMO->L+1 (14%)**	H-5->LUMO (2%), H-5->L+1 (2%), H-1->L+1 (2%)
2	283.7	0.250	H-4->LUMO (15%), H-1->LUMO (43%), HOMO->LUMO (22%)	H-1->L+1 (5%), HOMO->L+1 (8%)
3	270.5	0.513	H-4->LUMO (51%), H-1->LUMO (24%)	H-2->LUMO (7%), H-1->L+1 (8%), HOMO->L+1 (2%)
4	259.1	0.047	H-5->LUMO (34%), H-5->L+1 (17%), H-2->LUMO (25%)	H-6->L+3 (2%), H-4->LUMO (3%), H-4->L+3 (3%), H-2->L+1 (3%), HOMO->LUMO (2%)
5	256.2	0.036	H-5->LUMO (15%), H-2->LUMO (33%)	H-5->L+1 (5%), H-4->LUMO (3%), H-3->LUMO (6%), H-2->L+1 (6%), H-1->LUMO (5%), H-1->L+1 (8%), HOMO->LUMO (7%), HOMO->L+1 (3%)
6	252.3	0.038	H-3->LUMO (21%), H-2->LUMO (20%), H-1->L+1 (23%)	H-5->LUMO (3%), H-4->LUMO (3%), H-4->L+1 (6%), H-3->L+1 (3%), H-1->LUMO (5%), HOMO->L+1 (5%)
7	250.3	0.016	H-3->LUMO (54%)	H-4->L+1 (4%), H-3->L+1 (8%), H-1->LUMO (2%), H-1->L+1 (8%), HOMO->LUMO (5%), HOMO->L+1 (7%)
8	248.5	0.012	H-1->L+1 (26%), HOMO->LUMO (14%), HOMO->L+1 (42%)	H-3->LUMO (3%), H-1->LUMO (3%), HOMO->L+3 (4%)
9	243.9	0.023	H-7->LUMO (30%), H-6->L+2 (10%), H-4->L+2 (23%)	H-8->LUMO (6%), H-7->L+1 (9%), H-4->L+1 (5%), H-1->L+1 (3%)
10	239.9	0.004	H-3->L+4 (10%), H-2->L+1 (17%), HOMO->L+6 (14%)	H-2->LUMO (5%), H-2->L+3 (3%), H-2->L+4 (3%), H-2->L+5 (8%), H-2->L+7 (3%), H-1->L+1 (3%), H-1->L+5 (6%), H-1->L+7 (7%), HOMO->L+3 (3%), HOMO->L+4 (4%)
11	238.9	0.007	H-2->L+4 (10%), HOMO->L+6 (18%)	H-3->LUMO (5%), H-3->L+1 (5%), H-3->L+3 (3%), H-3->L+5 (6%), H-3->L+7 (6%), H-2->L+1 (4%), H-2->L+6 (3%), H-1->L+4 (3%), H-1->L+5 (8%), H-1->L+7 (3%), HOMO->L+3 (4%), HOMO->L+4 (8%)
12	237.2	0.147	H-6->LUMO (13%), H-4->L+1 (44%)	H-7->LUMO (5%), H-4->L+2 (3%), H-2->L+1 (4%), H-1->L+1 (4%), H-1->L+5 (4%), H-1->L+7 (2%)
13	226.9	0.100	H-3->L+1 (11%), H-2->L+1 (28%), HOMO->L+3 (12%)	H-8->LUMO (2%), H-4->L+1 (5%), H-3->L+4 (2%), H-2->L+4 (3%), H-1->L+5 (7%), H-1->L+7 (3%), HOMO->L+1 (3%)
14	226.5	0.049	H-2->L+1 (23%), HOMO->L+3 (37%)	H-6->LUMO (3%), H-5->L+3 (3%), H-4->L+1 (4%), H-2->LUMO (2%), H-1->L+3 (2%), HOMO->L+1 (4%)
15	222.3	0.009	H-3->L+1 (64%)	H-8->LUMO (2%), H-3->LUMO (7%), H-2->L+1 (6%), HOMO->L+4 (3%), HOMO->L+6 (2%)

4C (OMe) closed

No.	Wave-length (nm)	Osc. Strength (f)	Major contribs	Minor contribs
1	297.7	0.567	**H-4->LUMO (11%), H-1->LUMO (17%), HOMO->LUMO (48%)**	H-5->LUMO (4%), H-2->LUMO (6%), HOMO->L+1 (5%)
2	281.0	0.339	H-4->LUMO (20%), H-1->LUMO (26%), HOMO->LUMO (27%)	H-2->LUMO (8%), HOMO->L+1 (9%)
3	269.4	0.244	H-4->LUMO (28%), H-2->LUMO (11%), H-1->LUMO (43%), H-1->L+1 (11%)	--
4	256.1	0.063	H-5->LUMO (54%), H-5->L+1 (11%)	H-8->LUMO (2%), H-6->L+3 (5%), H-4->LUMO (2%), H-2->LUMO (7%), H-1->L+3 (2%), HOMO->LUMO (3%)
5	250.7	0.033	H-4->LUMO (11%), H-2->LUMO (44%), H-2->L+1 (11%)	H-5->LUMO (8%), H-1->L+1 (5%), HOMO->LUMO (2%)
6	248.1	0.044	H-4->L+1 (17%), H-4->L+2 (14%), H-2->LUMO (10%)	H-7->LUMO (6%), H-7->L+1 (5%), H-6->LUMO (5%), H-6->L+2 (3%), H-4->LUMO (9%), H-3->LUMO (3%), H-2->L+2 (5%), H-1->L+1 (7%), HOMO->L+1 (4%)
7	246.1	0.004	H-3->LUMO (67%)	H-4->L+2 (4%), H-3->L+1 (7%), HOMO->L+6 (3%)
8	243.1	0.050	H-4->L+2 (17%)	H-7->LUMO (9%), H-7->L+1 (6%), H-6->LUMO (6%), H-6->L+1 (3%), H-6->L+2 (3%), H-4->LUMO (6%), H-4->L+1 (6%), H-3->LUMO (3%), H-2->L+1 (2%), H-2->L+2 (5%), H-1->L+1 (8%), H-1->L+2 (2%), HOMO->L+1 (8%), HOMO->L+3 (3%)
9	239.5	0.034	H-3->LUMO (14%), H-1->L+1 (11%), HOMO->L+3 (13%), HOMO->L+6 (13%)	H-3->L+5 (3%), H-3->L+7 (5%), H-2->L+4 (6%), H-1->L+5 (5%), HOMO->LUMO (3%), HOMO->L+1 (9%), HOMO->L+4 (5%)
10	238.4	0.017	H-3->L+4 (10%), H-1->L+5 (13%), HOMO->L+6 (12%)	H-4->L+1 (6%), H-4->L+5 (3%), H-2->LUMO (5%), H-2->L+4 (5%), H-2->L+5 (4%), H-2->L+7 (4%), H-1->L+1 (5%), H-1->L+7 (8%), HOMO->L+1 (3%), HOMO->L+4 (3%)
11	235.6	0.125	H-4->L+1 (11%), HOMO->L+1 (28%)	H-6->LUMO (5%), H-3->LUMO (2%), H-3->L+7 (2%), H-2->L+1 (4%), H-1->L+5 (2%), HOMO->LUMO (9%), HOMO->L+3 (7%), HOMO->L+4 (4%), HOMO->L+6 (5%)
12	233.0	0.030	H-2->L+1 (13%), H-1->L+1 (42%)	H-6->LUMO (3%), H-4->L+1 (4%), H-3->L+1 (2%), H-2->L+4 (4%), H-1->LUMO (5%), H-1->L+4 (2%), H-1->L+5 (2%), H-1->L+7 (3%), HOMO->L+1 (2%)
13	223.7	0.094	HOMO->L+1 (22%), HOMO->L+3 (36%)	H-8->LUMO (4%), H-6->LUMO (5%), H-5->LUMO (2%), H-5->L+3 (4%), H-3->L+1 (2%), H-1->L+3 (3%), HOMO->L+4 (3%), HOMO->L+7 (2%)
14	219.6	0.035	H-6->LUMO (10%), H-2->L+1 (39%)	H-8->LUMO (7%), H-4->LUMO (2%), H-4->L+1 (8%), H-3->L+1 (4%), H-2->L+3 (2%), H-1->L+5 (6%), HOMO->L+3 (3%)
15	217.2	0.040	H-8->LUMO (32%)	H-13->LUMO (2%), H-8->L+1 (7%), H-6->LUMO (7%), H-5->LUMO (3%), H-3->L+1 (7%), H-2->L+1 (7%), HOMO->L+3 (9%)

4d (NO2) closed

No.	Wave-length (nm)	Osc. Strength (f)	Major contribs	Minor contribs
1	317.7	0.346	H-4->LUMO (10%), H-1->LUMO (23%), HOMO->LUMO (43%), HOMO->L+1 (12%)	H-4->L+1 (2%), H-1->L+1 (4%)
2	309.5	0.032	H-1->LUMO (56%), HOMO->LUMO (32%)	H-1->L+1 (3%), HOMO->L+1 (5%)
3	301.8	0.000	H-16->LUMO (33%), H-15->LUMO (32%)	H-16->L+1 (5%), H-16->L+2 (3%), H-16->L+3 (7%), H-15->L+1 (4%), H-15->L+2 (3%), H-15->L+3 (7%)
4	291.9	0.411	H-4->LUMO (25%), H-2->LUMO (41%), H-1->LUMO (10%)	H-5->LUMO (2%), H-4->L+1 (3%), H-3->LUMO (7%), HOMO->LUMO (3%)
5	282.6	0.306	H-4->LUMO (36%), H-2->LUMO (35%)	H-5->LUMO (3%), H-4->L+1 (4%), H-3->LUMO (9%), H-1->LUMO (2%), HOMO->L+1 (3%)
6	281.3	0.021	HOMO->LUMO (17%), HOMO->L+1 (46%)	H-5->LUMO (3%), H-5->L+1 (4%), H-4->L+1 (4%), H-2->LUMO (3%), H-1->LUMO (2%), H-1->L+1 (7%), HOMO->L+3 (6%)
7	276.1	0.004	H-3->LUMO (76%), H-2->LUMO (13%)	H-3->L+1 (4%)
8	275.6	0.000	H-19->LUMO (22%), H-18->LUMO (39%)	H-19->L+1 (3%), H-19->L+3 (4%), H-18->L+1 (5%), H-18->L+2 (3%), H-18->L+3 (7%), H-17->LUMO (6%)
9	269.3	0.040	H-1->L+1 (66%), HOMO->L+1 (12%)	H-1->LUMO (3%), H-1->L+3 (5%)
10	263.6	0.056	H-5->LUMO (41%), H-5->L+1 (32%)	H-4->L+1 (2%), H-4->L+4 (3%), H-1->L+1 (4%), HOMO->L+1 (6%)
11	261.2	0.041	H-7->LUMO (80%)	H-9->L+2 (2%), H-8->LUMO (3%), H-8->L+2 (2%), H-4->L+2 (4%)
12	249.7	0.015	H-4->L+1 (13%), H-2->L+1 (56%)	H-3->L+1 (4%), H-2->L+3 (4%), H-1->L+1 (4%)
13	244.4	0.057	H-4->L+1 (44%), H-2->L+1 (14%)	H-9->LUMO (2%), H-8->LUMO (4%), H-5->L+1 (4%), H-4->LUMO (3%), H-3->L+1 (4%), HOMO->L+7 (4%)
14	243.6	0.007	H-3->L+1 (49%)	H-4->L+1 (6%), H-3->L+3 (5%), H-3->L+6 (2%), H-3->L+8 (3%), H-2->L+5 (4%), H-1->L+6 (4%), HOMO->L+5 (3%), HOMO->L+7 (6%)
15	238.6	0.033	H-5->LUMO (39%), H-5->L+1 (26%)	H-6->LUMO (3%), H-5->L+3 (6%), H-4->LUMO (7%), H-4->L+4 (4%)

4e (mbisCF3) closed

No.	Wave-length (nm)	Osc. Strength (f)	Major contribs	Minor contribs
1	305.5	0.234	H-1->LUMO (14%), HOMO->LUMO (47%)	H-4->LUMO (8%), HOMO->L+1 (9%), HOMO->L+2 (9%)
2	293.0	0.094	H-1->LUMO (60%), HOMO->LUMO (20%)	H-4->LUMO (4%), H-1->L+1 (3%), H-1->L+2 (3%), HOMO->L+1 (3%), HOMO->L+2 (3%)
3	273.9	0.449	H-4->LUMO (37%), H-2->LUMO (29%), H-1->LUMO (13%)	H-5->LUMO (4%), H-3->LUMO (4%)
4	267.0	0.140	H-4->LUMO (29%), H-2->LUMO (47%)	H-4->L+1 (2%), H-4->L+2 (2%), H-3->LUMO (5%)
5	265.7	0.027	H-5->LUMO (16%), HOMO->LUMO (19%), HOMO->L+1 (15%)	H-5->L+1 (3%), H-5->L+2 (4%), H-4->L+1 (3%), H-3->LUMO (4%), H-1->LUMO (4%), H-1->L+1 (8%), H-1->L+2 (5%), HOMO->L+2 (9%)
6	260.9	0.040	H-3->LUMO (31%), H-2->LUMO (11%), H-1->L+1 (19%), H-1->L+2 (10%)	H-5->LUMO (4%), H-5->L+1 (2%), H-5->L+2 (2%), H-3->L+1 (2%), H-3->L+2 (2%), HOMO->LUMO (5%), HOMO->L+1 (3%)
7	259.6	0.034	H-3->LUMO (46%), H-1->L+1 (24%), H-1->L+2 (12%)	H-1->LUMO (4%)
8	258.6	0.058	H-5->LUMO (31%), HOMO->L+1 (21%), HOMO->L+2 (11%)	H-5->L+1 (8%), H-5->L+2 (7%), H-4->L+3 (2%), H-2->LUMO (3%), HOMO->LUMO (6%), HOMO->L+3 (3%)
9	244.6	0.016	H-2->L+1 (33%), H-2->L+2 (11%)	H-9->LUMO (4%), H-4->L+1 (7%), H-3->L+1 (6%), H-3->L+2 (2%), H-3->L+4 (4%), H-2->LUMO (2%), H-2->L+4 (3%), H-2->L+5 (3%), H-1->L+5 (4%), H-1->L+7 (3%)
10	243.1	0.005	H-9->LUMO (25%), H-4->L+1 (14%)	H-9->L+1 (2%), H-8->L+1 (6%), H-8->L+2 (4%), H-7->L+1 (3%), H-7->L+2 (2%), H-5->L+1 (3%), H-4->L+2 (6%), H-2->L+2 (6%), H-1->L+2 (3%)
11	240.4	0.001	HOMO->L+6 (26%)	H-3->LUMO (3%), H-3->L+1 (8%), H-3->L+2 (5%), H-3->L+3 (4%), H-3->L+5 (5%), H-3->L+7 (7%), H-2->L+3 (3%), H-2->L+4 (4%), H-2->L+6 (3%), H-2->L+7 (4%), H-1->L+5 (2%), HOMO->L+3 (6%), HOMO->L+4 (9%)
12	235.9	0.086	H-4->L+1 (16%), H-4->L+2 (20%)	H-9->LUMO (3%), H-8->LUMO (2%), H-7->LUMO (3%), H-5->L+2 (3%), H-4->LUMO (2%), H-3->L+4 (4%), H-2->L+1 (4%), H-2->L+2 (3%), H-2->L+4 (3%), H-2->L+5 (2%), H-1->L+1 (2%), H-1->L+4 (3%), H-1->L+5 (7%), H-1->L+7 (5%), HOMO->L+6 (2%)
13	231.9	0.007	H-3->L+1 (17%), H-2->L+1 (20%)	H-4->L+1 (7%), H-4->L+2 (5%), H-3->LUMO (3%), H-3->L+2 (8%), H-3->L+4 (3%), H-2->LUMO (3%), H-2->L+2 (8%), HOMO->L+3 (7%), HOMO->L+6 (5%)
14	230.6	0.058	H-3->L+1 (25%), H-3->L+2 (10%), H-1->L+5 (10%)	H-4->L+1 (6%), H-4->L+2 (5%), H-3->L+4 (3%), H-2->L+1 (4%), H-2->L+4 (6%), H-1->L+7 (4%), HOMO->L+3 (4%)
15	227.5	0.058	HOMO->L+1 (18%), HOMO->L+3 (27%)	H-6->LUMO (6%), H-6->L+1 (2%), H-6->L+2 (3%), H-4->L+3 (2%), H-3->L+1 (4%), H-3->L+2 (2%), H-1->L+3 (4%), HOMO->L+2 (5%), HOMO->L+4 (4%), HOMO->L+7 (3%)
4f (4-Ph) closed				

No.	Wave-length (nm)	Osc. Strength (f)	Major contribs	Minor contribs
1	302.1	0.904	H-4->LUMO (21%), H-1->LUMO (15%), HOMO->LUMO (32%), HOMO->L+1 (11%)	H-5->L+1 (2%), H-2->LUMO (6%)
2	286.0	0.460	H-4->LUMO (25%), H-1->LUMO (13%), HOMO->LUMO (26%), HOMO->L+1 (21%)	H-2->LUMO (5%)
3	275.5	0.257	H-4->LUMO (23%), H-1->LUMO (45%), H-1->L+1 (20%)	H-2->LUMO (4%), HOMO->LUMO (2%)
4	258.1	0.050	H-5->LUMO (34%), H-5->L+1 (24%), H-2->LUMO (15%)	H-6->L+3 (3%), H-4->LUMO (4%), H-2->L+1 (3%), HOMO->LUMO (3%)
5	257.2	0.014	H-2->LUMO (24%), H-2->L+1 (12%), H-1->LUMO (10%)	H-6->LUMO (4%), H-5->LUMO (7%), H-5->L+1 (3%), H-4->L+1 (5%), H-3->LUMO (4%), H-1->L+1 (9%), HOMO->LUMO (6%), HOMO->L+1 (3%)
6	252.5	0.071	H-4->LUMO (10%), H-4->L+1 (11%), H-2->LUMO (28%), H-1->L+1 (10%)	H-8->LUMO (6%), H-6->LUMO (5%), H-6->L+1 (3%), H-5->LUMO (4%), H-5->L+1 (3%), H-4->L+2 (3%), H-1->LUMO (3%), HOMO->L+1 (3%)
7	250.2	0.004	H-8->LUMO (10%), H-3->LUMO (56%), H-3->L+1 (12%)	H-4->L+2 (5%), H-2->L+1 (3%)
8	249.2	0.027	H-8->LUMO (12%), HOMO->LUMO (20%), HOMO->L+1 (35%)	H-8->L+1 (2%), H-4->LUMO (3%), H-4->L+2 (6%), HOMO->L+3 (7%)
9	248.6	0.008	H-8->LUMO (17%), H-3->LUMO (16%), H-1->L+1 (22%)	H-8->L+1 (3%), H-4->L+2 (8%), H-1->LUMO (6%), HOMO->LUMO (3%), HOMO->L+1 (9%)
10	245.3	0.073	H-6->LUMO (22%), H-4->L+1 (24%), H-1->L+1 (22%)	H-8->LUMO (5%), H-6->L+1 (3%), H-4->L+2 (2%), H-2->L+1 (5%), H-1->LUMO (3%)
11	239.8	0.004	HOMO->L+8 (19%)	H-3->L+6 (9%), H-3->L+9 (3%), H-2->LUMO (5%), H-2->L+1 (8%), H-2->L+3 (4%), H-2->L+7 (5%), H-2->L+9 (4%), H-1->L+7 (5%), H-1->L+9 (5%), HOMO->L+3 (4%), HOMO->L+6 (6%)
12	238.9	0.003	H-2->L+6 (13%), H-1->L+7 (13%), HOMO->L+8 (11%)	H-3->LUMO (6%), H-3->L+1 (4%), H-3->L+3 (3%), H-3->L+7 (4%), H-3->L+9 (5%), H-2->L+1 (5%), H-2->L+8 (3%), H-1->L+6 (2%), H-1->L+9 (5%), HOMO->L+3 (2%), HOMO->L+6 (6%)
13	238.0	0.004	H-7->LUMO (36%), H-7->L+1 (12%), H-7->L+5 (13%), H-6->L+4 (10%), H-4->L+4 (18%)	H-7->L+3 (2%)
14	228.6	0.007	H-6->LUMO (14%), H-2->L+1 (45%)	H-3->L+1 (3%), H-3->L+6 (3%), H-2->LUMO (4%), H-2->L+6 (3%), H-1->L+7 (7%), H-1->L+9 (3%), HOMO->L+3 (4%)
15	227.2	0.126	HOMO->L+3 (42%)	H-9->LUMO (2%), H-9->L+1 (3%), H-5->L+3 (4%), H-3->L+1 (9%), H-1->L+3 (3%), HOMO->L+1 (6%), HOMO->L+5 (2%), HOMO->L+6 (2%), HOMO->L+7 (2%), HOMO->L+9 (3%)

4g (tereph) closed

No.	Wave-length (nm)	Osc. Strength (f)	Major contribs	Minor contribs
1	320.7	1.532	H-8->LUMO (34%), H-2->LUMO (19%), HOMO->LUMO (23%)	H-11->L+1 (3%), H-4->LUMO (6%), H-3->L+1 (2%), H-1->L+1 (4%)
2	304.7	0.000	H-1->LUMO (51%), HOMO->L+1 (20%)	H-3->LUMO (8%), H-2->L+1 (2%), H-1->L+2 (8%)
3	298.9	0.132	H-2->LUMO (26%), H-1->L+1 (14%), HOMO->LUMO (41%)	H-8->LUMO (6%), HOMO->L+2 (6%)
4	295.9	0.000	H-3->LUMO (71%), H-1->LUMO (14%)	H-2->L+1 (9%)
5	289.1	0.366	H-8->LUMO (29%), H-2->LUMO (40%)	H-4->LUMO (9%), H-3->L+1 (7%), H-1->L+1 (3%), HOMO->L+2 (2%)
6	275.7	0.000	H-7->LUMO (12%), H-5->LUMO (47%)	H-4->L+1 (5%), H-3->LUMO (7%), H-3->L+2 (3%), H-2->L+1 (3%), H-1->LUMO (7%), H-1->L+2 (2%), HOMO->L+1 (2%)
7	274.1	0.017	H-6->LUMO (10%), H-4->LUMO (30%), HOMO->LUMO (13%), HOMO->L+2 (13%)	H-8->LUMO (3%), H-5->L+1 (3%), H-3->L+1 (4%), H-2->L+2 (4%), H-1->L+1 (8%)
8	272.7	0.000	H-5->LUMO (28%), H-1->LUMO (19%), H-1->L+2 (14%), HOMO->L+1 (13%)	H-10->L+1 (4%), H-9->LUMO (4%), H-9->L+2 (3%), H-3->LUMO (3%), H-3->L+2 (2%)
9	272.1	0.063	H-8->LUMO (14%), H-4->LUMO (35%), HOMO->LUMO (14%)	H-10->LUMO (3%), H-10->L+2 (2%), H-9->L+1 (5%), H-2->LUMO (3%), H-1->L+1 (6%), HOMO->L+2 (9%)
10	266.5	0.000	H-3->L+2 (11%), H-2->L+1 (15%), H-1->L+2 (13%)	H-11->LUMO (8%), H-11->L+2 (2%), H-9->LUMO (3%), H-8->L+1 (8%), H-7->LUMO (3%), H-5->LUMO (9%), H-3->LUMO (4%), H-1->LUMO (6%), HOMO->L+1 (9%)
11	265.5	0.037	H-6->LUMO (44%), H-3->L+1 (11%), H-2->L+2 (13%)	H-7->L+1 (5%), H-4->LUMO (9%), H-1->L+1 (5%), HOMO->LUMO (4%), HOMO->L+2 (4%)
12	264.7	0.000	H-7->LUMO (74%)	H-6->L+1 (6%), H-5->LUMO (6%), H-4->L+1 (2%)
13	264.1	0.057	H-6->LUMO (34%), H-3->L+1 (18%), H-2->L+2 (23%)	H-7->L+1 (2%), H-2->LUMO (4%), H-1->L+1 (5%), HOMO->L+2 (2%)
14	261.1	0.000	H-10->L+1 (15%), H-9->LUMO (25%), H-3->L+2 (15%), H-2->L+1 (13%)	H-9->L+2 (8%), H-8->L+1 (3%), H-2->L+4 (2%)
15	260.2	0.125	H-10->LUMO (34%), H-10->L+2 (12%), H-9->L+1 (22%)	H-11->L+1 (2%), H-1->L+1 (4%), HOMO->L+2 (5%)

4h (5CF3Oz) closed

No.	Wave-length (nm)	Osc. Strength (f)	Major contribs	Minor contribs
1	304.2	0.069	H-1->LUMO (10%), HOMO->LUMO (75%)	H-4->LUMO (5%), HOMO->L+1 (3%)
2	288.8	0.057	H-1->LUMO (78%), HOMO->LUMO (14%)	H-5->LUMO (2%)
3	264.8	0.046	H-4->LUMO (45%), H-2->LUMO (43%)	H-5->L+2 (3%)
4	263.0	0.057	H-4->LUMO (32%), H-2->LUMO (45%)	H-5->LUMO (5%), H-3->LUMO (3%), H-1->LUMO (6%), HOMO->LUMO (2%)
5	257.7	0.010	H-3->LUMO (89%)	H-2->LUMO (4%)
6	251.3	0.340	H-5->LUMO (84%)	H-3->LUMO (3%), H-2->LUMO (2%)
7	239.6	0.014	HOMO->L+1 (15%), HOMO->L+2 (11%), HOMO->L+5 (25%)	H-3->L+1 (3%), H-3->L+4 (6%), H-3->L+6 (6%), H-2->L+3 (4%), H-2->L+4 (2%), H-2->L+6 (3%), HOMO->L+3 (7%)
8	239.3	0.004	H-3->L+3 (11%), H-2->L+3 (10%), H-1->L+1 (23%), H-1->L+4 (14%), H-1->L+6 (13%)	H-2->L+1 (6%), H-2->L+4 (6%), HOMO->L+5 (2%)
9	235.8	0.053	H-1->L+1 (13%), HOMO->L+1 (40%)	H-6->LUMO (3%), H-2->L+4 (3%), HOMO->LUMO (3%), HOMO->L+2 (3%), HOMO->L+3 (4%), HOMO->L+5 (9%)
10	230.8	0.013	H-1->L+1 (53%), HOMO->L+1 (12%)	H-3->L+1 (3%), H-3->L+4 (2%), H-2->L+3 (3%), H-1->L+3 (6%), H-1->L+6 (3%)
11	222.9	0.016	H-6->LUMO (58%), HOMO->L+1 (11%)	H-12->LUMO (3%), H-11->LUMO (4%), H-7->LUMO (3%), H-6->L+1 (2%), H-4->LUMO (3%)
12	217.6	0.106	HOMO->L+1 (12%), HOMO->L+2 (48%)	H-7->LUMO (3%), H-6->LUMO (3%), H-3->L+1 (6%), H-1->L+2 (5%), HOMO->L+4 (2%), HOMO->L+6 (2%)
13	216.2	0.049	H-2->L+1 (48%)	H-7->LUMO (3%), H-5->L+1 (3%), H-3->L+1 (9%), H-1->L+2 (3%), H-1->L+3 (4%), H-1->L+4 (8%), HOMO->L+2 (4%)
14	213.3	0.294	H-2->L+1 (18%), H-1->L+3 (36%), HOMO->L+3 (10%)	H-7->LUMO (3%), H-4->L+2 (2%), H-3->L+1 (3%), H-2->L+6 (3%), H-1->L+6 (2%), HOMO->L+4 (4%)
15	210.0	0.100	H-7->LUMO (11%), HOMO->L+2 (12%), HOMO->L+4 (12%)	H-5->L+1 (5%), H-5->L+2 (6%), H-3->L+1 (7%), H-3->L+3 (3%), H-3->L+5 (2%), H-2->L+5 (3%), H-1->L+2 (8%), HOMO->L+3 (4%), HOMO->L+6 (7%)

4i (4-NMe2) closed

No.	Wave-length (nm)	Osc. Strength (f)	Major contribs	Minor contribs
1	318.0	1.209	HOMO->LUMO (78%), HOMO->L+1 (10%)	H-6->LUMO (3%)
2	285.1	0.076	H-1->LUMO (62%), HOMO->L+1 (11%)	H-5->LUMO (4%), H-2->LUMO (6%), H-1->L+1 (7%)
3	274.7	0.039	HOMO->L+1 (30%), HOMO->L+2 (19%), HOMO->L+3 (24%)	H-7->L+1 (3%), H-2->LUMO (5%), H-1->LUMO (8%), HOMO->LUMO (2%)
4	269.4	0.060	H-2->LUMO (59%), HOMO->L+3 (11%)	H-2->L+1 (5%), H-1->LUMO (8%), HOMO->L+2 (7%)
5	258.0	0.136	H-2->LUMO (13%), HOMO->L+1 (35%), HOMO->L+2 (10%), HOMO->L+3 (12%)	H-6->LUMO (9%), H-6->L+1 (3%), HOMO->LUMO (5%)
6	254.3	0.028	H-5->LUMO (57%)	H-8->LUMO (3%), H-6->L+2 (4%), H-5->L+1 (7%), H-3->LUMO (3%), H-2->LUMO (4%), H-1->LUMO (3%), HOMO->L+3 (4%)
7	246.9	0.013	H-3->LUMO (73%)	H-5->LUMO (2%), H-3->L+1 (6%)
8	243.5	0.002	H-4->LUMO (59%)	H-4->L+1 (7%), H-4->L+7 (3%), H-3->L+4 (3%), H-2->L+5 (3%), H-1->L+4 (4%), H-1->L+6 (7%)
9	238.5	0.019	H-4->LUMO (15%), H-1->L+2 (10%), H-1->L+6 (20%)	H-4->L+4 (4%), H-4->L+5 (2%), H-4->L+7 (4%), H-3->LUMO (8%), H-3->L+5 (4%), H-3->L+7 (3%), H-1->L+1 (3%), H-1->L+3 (5%), H-1->L+4 (6%)
10	237.2	0.003	H-4->LUMO (14%), H-3->L+4 (11%), H-2->L+5 (17%), H-2->L+7 (10%)	H-6->LUMO (3%), H-4->L+4 (6%), H-3->LUMO (7%), H-3->L+5 (5%), H-2->L+1 (8%), H-2->L+4 (4%), H-1->L+1 (2%)
11	233.8	0.121	H-6->LUMO (13%), H-1->L+1 (27%)	H-2->L+1 (7%), H-1->LUMO (9%), H-1->L+2 (8%), H-1->L+3 (3%), H-1->L+4 (4%), H-1->L+6 (3%), H-1->L+7 (2%)
12	232.6	0.103	H-6->LUMO (52%)	H-5->LUMO (2%), H-4->LUMO (4%), H-1->L+1 (2%), H-1->L+2 (2%), HOMO->LUMO (9%), HOMO->L+1 (4%), HOMO->L+3 (3%)
13	228.3	0.017	H-2->L+1 (62%), H-1->L+1 (10%)	H-2->LUMO (6%), H-2->L+4 (4%)
14	220.8	0.178	H-1->L+1 (29%), HOMO->L+2 (10%)	H-8->LUMO (7%), H-6->LUMO (4%), H-5->LUMO (5%), H-5->L+2 (2%), H-2->L+1 (2%), H-2->L+2 (3%), H-2->L+4 (3%), H-1->L+2 (3%), H-1->L+3 (3%), HOMO->L+3 (5%)
15	217.7	0.009	H-8->LUMO (10%), H-3->L+1 (10%), H-1->L+2 (21%), H-1->L+3 (12%)	H-6->L+1 (4%), H-6->L+2 (2%), H-5->LUMO (3%), H-2->L+5 (2%), H-1->L+1 (8%), H-1->L+4 (2%), HOMO->L+2 (2%)

3. References

(1) Brown, H. C.; Dodson, V. H. Studies in Stereochemistry. XXII. The Preparation and Reactions of Trimesitylborane. Evidence for the Non-Localized Nature of the Odd Electron in Triarylborane Radical Ions and Related Free Radicals 1. *J. Am. Chem. Soc.* **1957**, *79* (9), 2302–2306. https://doi.org/10.1021/ja01566a076.

(2) Schepper, J. D. W.; Orthaber, A.; Pammer, F. Preparation of Structurally and Electronically Diverse N → B-Ladder Boranes by [2 + 2 + 2] Cycloaddition. *J. Org. Chem.* **2021**, *86* (21), 14767–14776. https://doi.org/10.1021/acs.joc.1c01402.

(3) Schepper, J.; Orthaber, A.; Pammer, F. Tetrazole-Functionalized Organoboranes Exhibiting Dynamic Intramolecular N→B-Coordination and Cyanide-Selective Anion Binding. *Chem. – A Eur. J.* **2024**, *30* (37), e202401466. https://doi.org/10.1002/chem.202401466.

(4) Armarego, W. L. .; Perrin, D. D. *Purification of Laboratory Chemicals*, 4th ed.; Butterworth-Heinemann: Oxford, 1997.

(5) Fulmer, G. R.; Miller, A. J. M.; Sherden, N. H.; Gottlieb, H. E.; Nudelman, A.; Stoltz, B. M.; Bercaw, J. E.; Goldberg, K. I. NMR Chemical Shifts of Trace Impurities: Common Laboratory Solvents, Organics, and Gases in Deuterated Solvents Relevant to the Organometallic Chemist. *Organometallics* **2010**, *29* (9), 2176–2179. https://doi.org/10.1021/om100106e.

(6) Ando, S.; Matsuura, T. Substituent Shielding Parameters of Fluorine-19 NMR on Polyfluoroaromatic Compounds Dissolved in Dimethyl Sulphoxide- d 6. *Magn. Reson. Chem.* **1995**, *33* (8), 639–645. https://doi.org/10.1002/mrc.1260330805.

(7) Altomare, A.; Cascarano, G.; Giacovazzo, C.; Guagliardi, A.; Burla, M. C.; Polidori, G.; Camalli, M. SIR 92 – a Program for Automatic Solution of Crystal Structures by Direct Methods. *J. Appl. Crystallogr.* **1994**, *27* (3), 435–435. https://doi.org/10.1107/S002188989400021X.

(8) Sheldrick, G. M. A Short History of SHELX. *Acta Crystallogr. Sect. A Found. Crystallogr.* **2008**, *64* (1), 112–122. https://doi.org/10.1107/S0108767307043930.

(9) Frisch, M. J.; Trucks, G. W.; Schlegel, H. B.; Scuseria, G. E.; Robb, M. A.; Cheeseman, J. R.; Scalmani, G.; Barone, V.; Petersson, G. A.; Nakatsuji, H.; Li, X.; Caricato, M.; Marenich, A. V; Bloino, J.; Janesko, B. G.; Gomperts, R.; Mennucci, B.; Hratchian, H. P.; Ortiz, J. V; Izmaylov, A. F.; Sonnenberg, J. L.; Williams-Young, D.; Ding, F.; Lipparini, F.; Egidi, F.; Goings, J.; Peng, B.; Petrone, A.; Henderson, T.; Ranasinghe, D.; Zakrzewski, V. G.; Gao, J.; Rega, N.; Zheng, G.; Liang, W.; Hada, M.; Ehara, M.; Toyota, K.; Fukuda, R.; Hasegawa, J.; Ishida, M.; Nakajima, T.; Honda, Y.; Kitao, O.; Nakai, H.; Vreven, T.; Throssell, K.; Montgomery Jr., J. A.; Peralta, J. E.; Ogliaro, F.; Bearpark, M. J.; Heyd, J. J.; Brothers, E. N.; Kudin, K. N.; Staroverov, V. N.; Keith, T. A.; Kobayashi, R.; Normand, J.; Raghavachari, K.; Rendell, A. P.; Burant, J. C.; Iyengar, S. S.; Tomasi, J.; Cossi, M.; Millam, J. M.; Klene, M.; Adamo, C.; Cammi, R.; Ochterski, J. W.; Martin, R. L.; Morokuma, K.; Farkas, O.; Foresman, J. B.; Fox, D. J. Gaussian 16 {R}evision {C}.01. 2019.

(10) Friebolin, H.; Thiele, C. M. *Ein- Und Zweidimensionale NMR-Spektroskopie*, 5th ed.; Wiley-VCH, Weinheim, 2013.

(11) Koch, R.; Sun, Y.; Orthaber, A.; Pierik, A. J.; Pammer, F. Turn-on Fluorescence Sensors Based on Dynamic Intramolecular N→B-Coordination. *Org. Chem. Front.* **2020**, *7* (12), 1437–1452. https://doi.org/10.1039/d0qo00267d.